SYNTHETIC APERTURE SONAR FOR SUB BOTTOM IMAGING

BY

MAREK KAROL DUTKIEWICZ

SUBMITTED IN PARTIAL FULFILMENT OF
THE REQUIREMENTS FOR THE DEGREE OF
MASTER OF SCIENCE IN ENGINEERING

UNIVERSITY OF CAPE TOWN
SEPTEMBER 1986

ABSTRACT

The major problems associated with implementing synthetic apertures in sonar may be overcome by applying the technique to sub-bottom imaging. The use of a low frequency aids both penetration of the sediment and the attainment of long coherent apertures. The implementation of synthetic apertures realises a narrow fan beam. By directing this beam out sideways, a more rapid survey rate is possible than that achieved by the normal echo-sounding mode used in sub-bottom profiling. The synthetic aperture technique appears to offer significant advantages over that of parametric arrays, for high resolution sub-bottom imaging.

Synthetic apertures have been implemented in a laboratory tank, under controlled conditions at a fresh water reservoir, and under realistic operational conditions at sea. Encouraging results have been obtained.

ACKNOWLEDGEMENTS

I would like to thank the following people and organisations for their support:

Prof. P.N.Denbigh, my supervisor.

Institute for Maritime Technology (IMT) for the use of their facilities at the fresh water reservoir and the use of the research boat the 'Shirley T'.

National Research Institute for Oceanology (NRIO), Stellenbosch for the loan of the transducer used.

Mr. G.Rosenthal of the Civil Engineering Department (U.C.T.) for the loan of the A/D unit used.

The various members of the Central Acoustics Laboratory, U.C.T.

Financial support was received from the C.S.I.R. during the course of this project.

CONTENTS

CHAPTER 1 INTRODUCTION

It is common practice in radar and sonar imaging to use an array of many receiving elements in order to achieve fine resolution. A technique of realising such fine resolution using a single element is that of synthetic apertures. This is achieved by moving the single element in space, and carrying out transmission and reception of signals at various positions. In this way a long aperture, with resultant narrow beam, may be realised. The advantages are:

1) The use of a single element greatly reduces the mechanical complexity and expense of the system.

2) It is possible to create longer apertures than may be mechanically constructed.

The technique relies on the storage of a large amount of information and complex processing. Optical and digital methods are commonly used for storage and image reconstruction.

Two classes of synthetic apertures may be distinguished, namely unfocused and focused apertures. Unfocused apertures require the targets to lie in the far-field of the aperture, thus restricting the usable length of aperture. If the aperture is focused, it is possible to image targets in the near-field of the aperture, and a resolution of one half the radiating element size is achievable. This spectacular result is independent of both range and wavelength, although longer apertures are necessary at greater ranges.

The technique of synthetic aperture imaging is well established in radar, having been developed in the 1960's[1]. The extension of the technique to sonar was first mentioned in 1973[2]. Since then a number of attempts at building synthetic aperture systems have been made[3,4]. These attempts have met with success under controlled conditions using 'good' targets. Attempts to extend the technique to use in sidescan sea-bed

mapping applications are believed to have been largely unsuccessful. This is because of two major problems which do not occur in radar.

1) In spite of the lesser operating ranges the low propagation velocity of sound causes the two-way propagation times to be much larger for a sideways looking sonar than for an equivalent radar. This is liable to cause a severe undersampling of the synthetic aperture at typical towing speeds.

2) The inertia of a boat or towed body is much less than that of an aircraft or satellite. This together with the influence of swell and waves can result in deviations of the sampling positions from a straight line path. The deviations may constitute an unacceptably large fraction of a wavelength.

If a low operating frequency is used, the straight line path requirement will be less severe because of the larger wavelength being used. Further, the requirement for the avoidance of undersampling, which is that aperture samples must be spaced a distance of less than one half wavelength apart, means that a greater boat velocity is possible when using a lower operating frequency.

Sub-bottom imaging is carried out at low operating frequencies, as the attenuation of the acoustic signal within the sub-bottom is proportional to the frequency of the signal. Thus the use of a low operating frequency aids penetration of sediments. The transducer is usually towed close to the sea floor, thus operating ranges are fairly short. This means that a higher prf is possible than for an equivalent sidescan sonar operating at greater range. This aids the avoidance of undersampling of the aperture. A well developed technique for high-resolution sub-bottom imaging does not exist. A technique that is receiving a lot of attention in this regard is that of parametric arrays. These are capable of generating narrow

low-frequency pencil beams. The use of synthetic apertures appears to be another possibility.

The purpose of this thesis is to investigate the feasibility of using synthetic apertures for high resolution sub-bottom imaging.

References

1. L.J.Cutrona, Synthetic Aperture Radar, Chap. 23 of "Radar Handbook", M.I.Skolnik(ed.) McGraw-Hill, New York, 1970.

2. Sato, Ueda, Fukuda, "Synthetic aperture sonar", J. Acoust. Soc. Am., 54(2), 799-802(1973)..

3. Sato, Ikeda, "Sequential synthetic aperture sonar system-a prototype of a synthetic aperture sonar system",IEEE Trans. on Sonics and Ultrasonics, Vol SU-24, No.4, July 1977.

4. Loggins et al., "Results from rail synthetic aperture experiments", J. Acoust. Soc. Am., 71(S1), S85(1982).

CHAPTER 2 SYNTHETIC APERTURES : THEORY AND BACKGROUND

Synthetic apertures have been in use for fine resolution radar terrain mapping since the 1960's. The idea was originally conceived by Sherwin and Cutrona [1], and separately by Carl Wiley[2]. The attraction of the technique is the ability to achieve along track resolution significantly finer than the beamwidth of the radiating element being used. The synthetic aperture may be thought of in terms of creating a synthetic array, or in terms of doppler filtering. The difference between the two treatments is that in the former the co-ordinate system is fixed in space, whereas in a doppler treatment the co-ordinate system moves with the radar.

For the purposes of this thesis, the synthetic aperture will be treated as the creation of an array, as this simplifies the visualization of the procedure. The doppler treatment may be found in Brown[3].

2.1 THEORY

The difference between conventional and synthetic means of beamforming with arrays is illustrated in Figure 2.1. In the case of a conventional array, a single transmitter is used together with an array of many receiving elements. The signals received by each of these elements are combined to form a narrow beam. In a synthetic aperture a single receiving element is physically moved along the aperture length, with signals received at each aperture position being stored for later use in beamforming. In practice it is easier to move both transmitter and receiver together, but the principle of operation is unchanged. An effect of moving both transmitter and receiver is to improve the resolution realisable, by a given length of aperture, by a factor of two. The reason for this will become discussed later in this section. This case of a moving transmitter and receiver (which may in fact be the same element) will be used in the derivations carried out in this chapter.

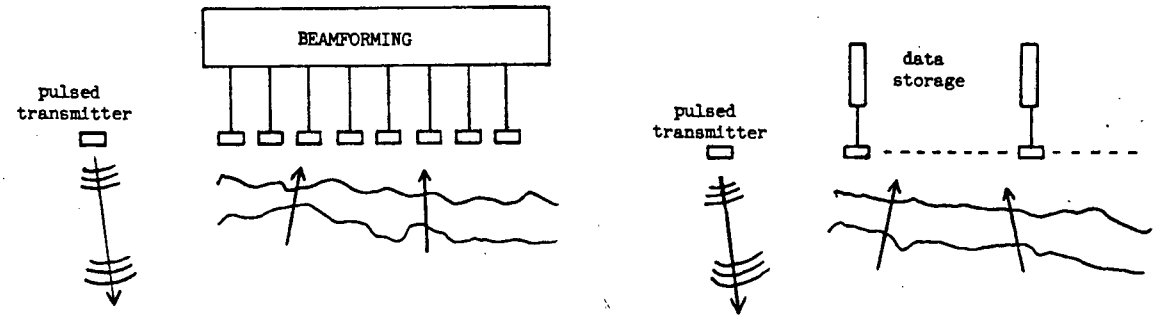

Figure 2.1 Beamforming by (a) conventional array (b) synthetic aperture.

Consider the synthetic aperture as a line of N point elements, spaced a distance d_e apart. At each position transmission and reception of signals is carried out.

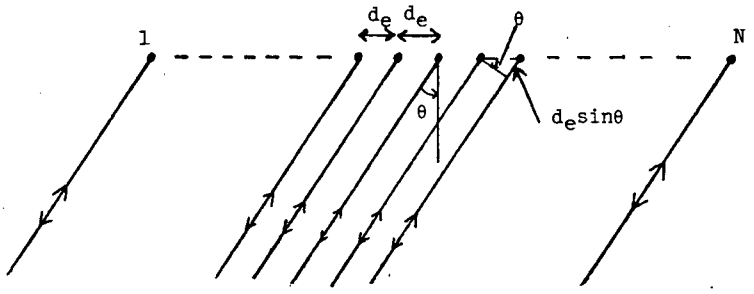

Figure 2.2 Signals arriving at aperture from a target at angle θ.

Let the incident wave at the centre of the aperture from a target at an angle θ be $Ae^{j\omega_o t}$ .The phase difference of the signal arriving at the n'th element will be $2(nkd_e\sin\theta)$; $k=2\pi/\lambda$. Thus the signal received by this element is

$$Ae^{j(\omega_o t+2nkd_e\sin\theta)}$$

The signal $G(\theta)$ received by the aperture is then the sum of all these signals.

$$G(\theta) = \sum_{n=-\frac{N-1}{2}}^{\frac{N-1}{2}} A_n e^{j(\omega_o t+2nkd_e\sin\theta)}$$

If the aperture is uniformly weighted i.e. $A_n=1$ then

$$G(\theta) = e^{j\omega_o t} \sum_{n=-\frac{N-1}{2}}^{\frac{N-1}{2}} e^{j2nkd_e\sin\theta}$$

$$|G(\theta)| = \sum_{n=-\frac{N-1}{2}}^{\frac{N-1}{2}} e^{j2nkd_e\sin\theta}$$

$$= e^{-j(N-1)kd_e\sin\theta}\{1+e^{j2kd_e\sin\theta}+ \ldots + e^{j2(N-1)kd_e\sin\theta}\}$$

$$= e^{-j(N-1)kd_e\sin\theta}\{\frac{e^{j2Nkd_e\sin\theta} - 1}{e^{-j2kd_e\sin\theta} - 1}\}$$

$$= \frac{e^{jNkd_e\sin\theta} - e^{-jNkd_e\sin\theta}}{e^{jkd_e\sin\theta} - e^{-jkd_e\sin\theta}}$$

$$= \frac{\sin(Nkd_e\sin\theta)}{\sin(kd_e\sin\theta)}$$

Normalising gives:

$$|G(\theta)| = \frac{\sin(Nkd_e\sin\theta)}{N\sin(kd_e\sin\theta)} \qquad \ldots (2.1)$$

It will be noticed that this is identical to the radiation pattern obtained for a conventional linear array of point receivers having 2N elements[4]. This factor of two arises due to the element being used for both transmission and reception of signals at each position in the synthetic aperture. Thus the phase change between adjacent aperture positions is twice that which it would be in the case of reception only. A sketch of the amplitude of $G(\theta)$ is shown in Figure 2.3

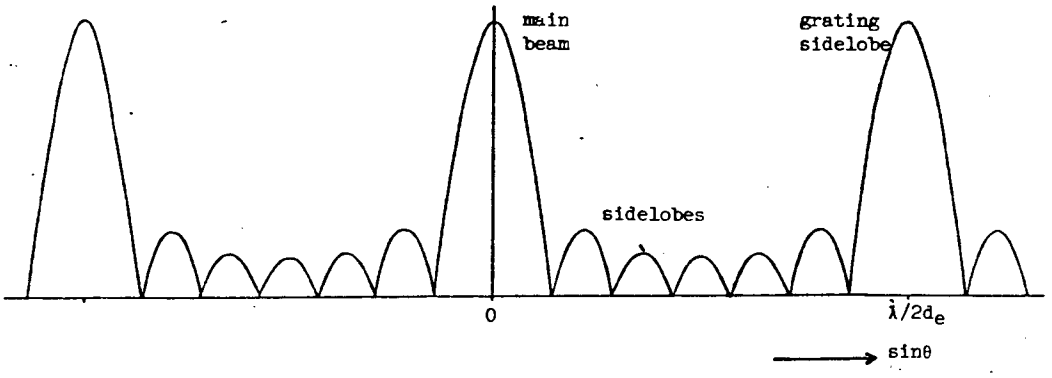

Figure 2.3 Radiation pattern of synthetic aperture.

2.1.1 RESOLUTION

Strictly the angular resolution is defined as the angle between the -3dB points of the radiation pattern. ie. the resolution of the aperture is found by setting

$$|G(\theta)| = \frac{\sin(Nkd_e\sin\theta)}{N\sin(kd_e\sin\theta)} = \frac{1}{\sqrt{2}}$$

For small angles and apertures long in terms of wavelengths

$$\sin(kd_e\sin\theta) \simeq kd_e\sin\theta$$

$$\Rightarrow \quad \frac{\sin(Nkd_e\sin\ )}{Nkd_e\sin} = \frac{1}{\sqrt{2}}$$

which occurs for $Nkd_e\sin\theta \simeq 0.44\pi$

$$\Rightarrow \qquad \theta_{3dB} = \frac{0.44\pi}{Nkd_e}$$

$$= \frac{0.22\lambda}{Nd_e}$$

The resolution is twice this $\delta_a = \frac{0.44\lambda}{Nd_e}$

Substituting the aperture length $L_e = (N-1)d_e \simeq Nd_e$ for N large, gives an angular resolution

$$\delta_a = \frac{\lambda}{2.3L_e}$$

This is finer by a factor of two than the resolution achievable by a conventional array of the same length. The reason for this is mentioned earlier in this chapter.

The along track resolution at range R is given by $\delta = R\delta_a$

$$\delta = \frac{R\lambda}{2.3L_e}$$

For simplicity, the 4dB beamwidth is often considered, which gives the normal form for the resolution at range R:

$$\delta = \frac{R\lambda}{2Le} \qquad \ldots (2.2)$$

Depending upon whether the aperture is focused or not limitations are placed on the length of aperture Le that may be realised.

(a) unfocused

In the case of an unfocused aperture, only targets in the far field of the aperture may be imaged. A target is considered to be in the far field of the aperture if the wave front arriving from the target may be considered as a plane wave. The requirement for this is[5] that the difference between the minimum and maximum two-way path lengths over the full aperture must be less than $\lambda/4$. By considering Figure 2.4, the limitation on the aperture length may be determined.

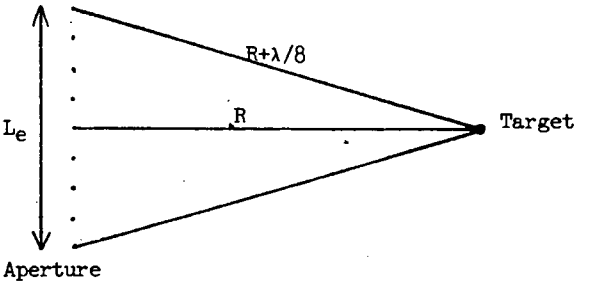

Figure 2.4 Length of unfocused synthetic aperture.

L_e is restricted by requiring $R \geq L_e^2/\lambda$ ie.

$L_e \leq \sqrt{R\lambda}$ and hence the resolution is

$$\delta \geq \frac{\sqrt{R\lambda}}{2}$$

(b) focused

If the aperture is focused, targets in the near-field of the aperture may be imaged. The focusing is achieved by allowing for a spherical wavefront arriving at the aperture. In this case all element positions for which the target is insonified may be used in the aperture (Figure 2.5). If omni-directional elements were used, it would be possible to realise an infinitely long aperture, giving infinitely fine resolution. Real elements however have a finite width of the main beam. This width is normally defined as the angle between the -3dB points. For an element of length D this is given by $\theta=\lambda/D$. Hence at a range R an aperture of length

$$Le = R\lambda/D \qquad \ldots (2.3)$$

is realisable.

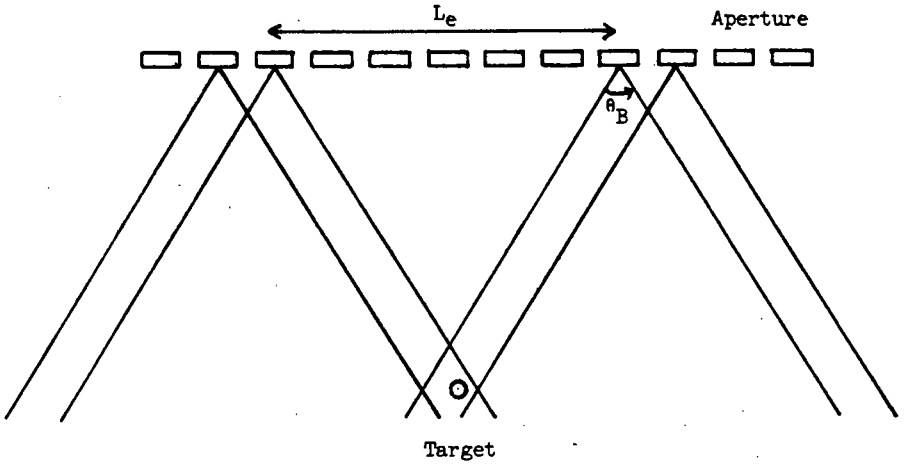

Figure 2.5 Length of focused synthetic aperture.

Substituting this length of aperture (eq 2.3) into eq (2.2) yields a resolution for a full focused aperture of

$$\delta = \frac{D}{2}$$

This has the useful property of being independent of both range and wavelength. However from eq 2.3 it is evident that for a given transducer size, the aperture length necessary to achieve the same resolution increases for greater range and longer wavelength.

The derivation has assumed that the amplitude response of the main lobe of the aperture element is flat. In practice this is not the case. In particular if the same element is used for both transmission and reception of signals, the edge of the lobe will be 6dB down on the centre. This causes amplitude shading for long apertures. The effect of this is a slignt degradation of the resolution, but is beneficial in reducing sidelobe levels (See 2.1.2).

In practise it is not normally possible to realise a full length focused aperture, and focusing is applied to a shorter aperture. In this case the resolution is given by $\delta = D/2\gamma$, where γ is the fraction of the maximum aperture used.

A graphical comparison of the resolution achievable

using similar elements by (i) a conventional array; (ii) an unfocused synthetic aperture; and (iii) a focused synthetic aperture is shown in Fig. 2.6. The case considered in this figure is that of an X-band antenna with dimension D=3m.

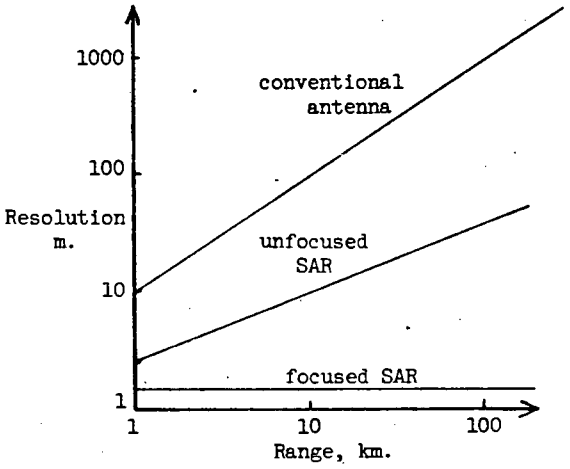

Figure 2.6 Resolution achievable by conventional and synthetic means using an X-band antenna of dimension 3m.

2.1.2 SIDELOBES

Reference to figure 2.3 will show the occurence of sidelobes, caused by the non-infinite length of the aperture, and grating sidelobes caused by the sampled nature of the aperture.

Grating sidelobes occur when the denominator of eq.2.1 is zero ie. $kd_e \sin\theta = \pm n\pi \qquad n=1,2,3,\ldots$

In these cases $G(\theta) = 1$. The first grating sidelobe occurs at $kd_e \sin\theta = \pi$

$$\Rightarrow \quad \sin\theta = \frac{\pi}{kd_e} = \frac{\lambda}{2d_e}$$

This will be outside real space if we set $\lambda/2d_e > 1$ ie. $d_e < \lambda/2$. In other words if the aperture samples are less

than half a wavelength apart, grating sidelobes will not occur. This requirement is analagous to the Nyquist criterion for a sampled system. Careful choice of sample spacing in relation to the transducer size may allow a less stringent requirement in certain cases[5].

Ordinary sidelobes occur at maxima of the numerator of eq.2.1

ie.
$$Nkd_e\sin\theta = \frac{2n+1}{2}\pi \qquad n=1,2,3,\ldots$$

$$\Rightarrow \qquad \sin\theta = \frac{(2n+1)\lambda}{4L_e}$$

The first sidelobe is 13.2dB down on the main lobe, which might be unacceptably large. The sidelobe levels can be reduced by aperture shading. This may be naturally achieved in a long aperture by the tapered nature of the beam (See 2.1.1), or may be artificially applied[6]. The penalty is a slight broadening of the beam. Examples of aperture shadings may be found in most radar textbooks[6].

2.1.3 BEAM STEERING

It may be advantageous to use a beam steered to an angle other than orthogonal to the aperture. This steering is achieved by applying the appropriate phase adjustment to the signal arriving at each aperture position.

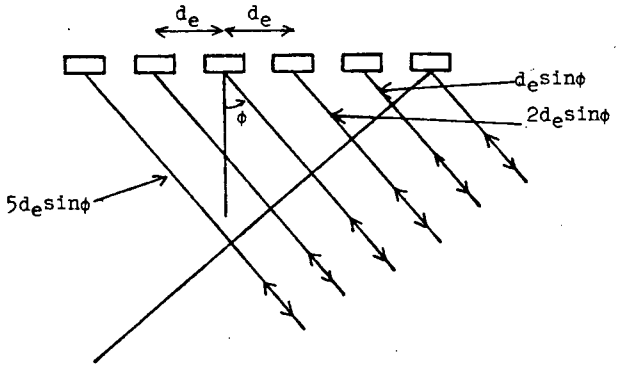

Figure 2.7 Aperture steered to angle ϕ.

By applying a phase shift of $2nkd_e\sin\phi$ to the signal at the n'th aperture position the beam is steered to an angle ϕ away from broadside. The effect on the array pattern[7] is to alter it to

$$|G(\theta)| = \frac{\sin(Nkd_e(\sin\theta-\sin\phi))}{N\sin(kd_e(\sin\theta-\sin\phi))}$$

There is an increase in the beamwidth as the beam is steered to an angle ϕ of $1/\cos\phi$. There is further a more stringent requirement for the avoidance of grating sidelobes. Grating sidelobes occur for:

$$kd_e(\sin\theta-\sin\phi) = \pm n\pi \qquad n=1,2,3,\ldots$$

$$\Rightarrow \qquad \sin\theta-\sin\phi = \pm\frac{n\lambda}{2d_e}$$

In the worst case, of a beam steered to 90°, a grating sidelobe will occur at -90° if $d_e \geq \lambda/4$. However this degree of steering is seldom used, and at a more normal angle of steer of 45°, spacing d_e of less than $\lambda/2.8$ is sufficient to avoid grating sidelobes.

2.1.4 PHASE PERTURBATIONS

The major problem of synthetic apertures is that the samples may not be accurately positioned. Further, each sample is taken at a different instant in time, and media and path imperfections may lead to the formation of an imperfect beam. Both these problems are not evident in conventional arrays, where the elements are locked in space and each receives the signal at much the same instant in time. The effect of these imperfections is to introduce phase perturbations to the received signals. A theoretical treatment of this problem is available[3]. The effect on the beam pattern is illustrated in fig 2.8. The major effect is a broadening of the beam with resultant loss of resolution. The effect may be alleviated if the nature of the imperfections are known, by applying an appropriate weighting function. In Chapter 3 an experimental examination of the chief sources of phase errors is made.

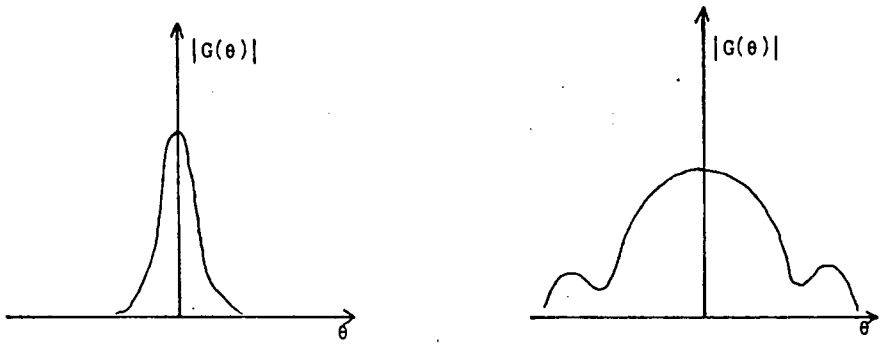

Figure 2.8 Effect of phase perturbations on the beam pattern a) ideal beam; b) perturbed beam

2.2 IMPLEMENTATION OF SYNTHETIC APERTURES

The use of synthetic apertures requires a large amount of data storage. Information needs to be stored over a period of time before it can be processed. Each separate received signal is used in a number of different beams, and thus clearly needs to be stored before being utilised.

Unfocused apertures need little manipulation in order to synthesize a beam, as the operation is purely one of summation. The realisation of long focused apertures is however a complicated process. Manipulation of the data is necessary to allow for a spherical wavefront arriving at the aperture. The larger the range, the longer the aperture that must be realised in order to obtain the same resolution. Two forms of storage and processing are typically used. These are optical and digital techniques. Early implementations used optical processing almost exclusively, but with the increase in availability of computing power, the latter techniques are becoming more widely used.

2.2.1 OPTICAL PROCESSING[1]

In optical processing the received signals are stored as light intensities on photographic film. The deflection over the width of the film corresponds to the range dimension,

whereas the length corresponds to along track distance. A sketch of an optical arrangement to realise focused synthetic apertures is shown below

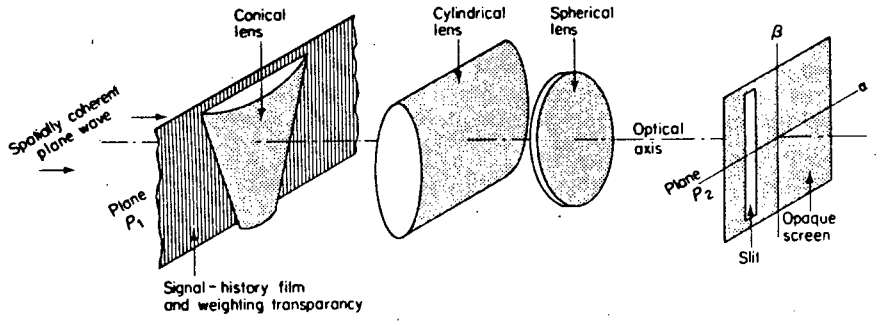

Figure 2.9 Focused synthetic aperture radar using optical processing. (Skolnik[5])

The signal received from a single point target will appear as a hyperbolic curve on the film, with varying doppler nature of the light as the aperture element moves past the target. The exact nature of the target record depends upon its range. The image recorded on film will be a superposition of many such targets. This may be regarded as a one dimensional hologram of the targets and is extracted by illuminating the film with coherent light and passing the image through a conical lens. The purpose of the conical lens is twofold. Firstly it is used to focus the aperture for a spherical wavefront, and secondly it realises a longer aperture for greater ranges in order to maintain constant resolution. Shading of the aperture may be achieved by using a shaded transparency. The foregoing process is used to focus the aperture in the along track dimension. Focussing in the range dimension is achieved by means of a cylindrical lens. The final image is focussed on a screen by means of a spherical lens. The end result is a photographic image of the area being surveyed.

This technique is relatively easily realised, but cannot be carried out in real time.

2.2.2 DIGITAL PROCESSING

With digital processing methods, the amplitude and phase of the received signals are numerically stored, typically by extracting the in-phase and quadrature components of the signal. The focussing procedure is carried out numerically, and the display may take a number of forms. It is possible to carry out processing in real-time. A great deal of versatility in shading and steering of the beam is readily available. The generation of long apertures however requires a large amount of storage capability.

The system detailed in chapter 3 utilises digital processing, and hence no more will be said about it here.

2.3 SYNTHETIC APERTURES IN SONAR

The logical extension of synthetic aperture techniques to use in sonar was a long time coming, for reasons that will become apparent. First mention of the use of synthetic apertures in sonar was made in 1973[8]. A simple laboratory model of a one dimensional synthetic aperture sonar system operating at 1 MHz was used to image a long steel wire, with good success. The same researchers subsequently constructed a two dimensional sonar system[9] and again encouraging results were achieved using spherical targets. Further work[10,11] conducted has described and demonstrated techniques for overcoming phase effects caused by turbulence in the propagating media. However all the experimental work has been carried out under controlled laboratory conditions.

Two papers published by Cutrona in 1975[12] and 1977[13] have compared synthetic aperture techniques to conventional techniques for sidescan sonar applications. He comes to the conclusion that by using multiple radiating beams it is possible to use synthetic apertures for such applications, with improved performance over conventional systems.

The following differences between the use of synthetic apertures in sonar and radar as outlined by Cutrona[12] show the major problems faced by the sonar designer in attempting to use synthetic aperture techniques.

1. "A major difference in parameter values between sonar and radar is in the signal propagation speeds, 1500 m/s for sonar and $3*10^8$m/s for radar. The result is a much more severe range ambiguity problem for sonar than for radar." Range ambiguities occur when return signals from one transmit pulse arrive after the next pulse has been transmitted. The return time to the target is thus not unambiguously known. Because of the lower propagation speed in sonar, typical return times are greater than those occuring in radar. This range ambiguity is more serious for high prf. A high prf is necesssary to avoid undersampling of a synthetic aperture at typical towing velocities in sonar. Cutrona outlines a method using multiple beams to achieve a desired unambiguous range.

2. "This same difference in propagation speeds makes achievement of range resolution more difficult in radar than for sonar, specifically with respect to signal bandwidth required." The range resolution is given by $c\tau/2$ where τ is the pulse length. In order to achieve a given range resolution τ may be significantly longer in sonar applications, thus requiring less signal bandwidth. At typical operating frequencies this turns out to require less fractional bandwidth in sonar than in radar.

3. "In radar the noise which competes with signals is internally generated. In sonar, noise is present in the environment." Thus noise is more of a problem in sonar applications.

4. "Multipath, path stability and refraction are more severe for sonar than radar." The ocean is not an ideal propagation medium. Reflections occur from both bottom and

surface, thus leading to multipath effects. Temperature variations lead to velocity profiles, which cause ray bending. This may be severe in the case of large operating range.

5. "A problem plaguing radar designers is that of dynamic range. Radar signals have a dynamic range in excess of 80dB. Sonar dynamic range is apparently much less." This is primarily due to the lesser operating ranges.

6. "In radar one has a spreading loss (inverse fourth power). In sonar one has both this spreading loss and in addition a signal attenuation which depends on both frequency and range."

7. "Finally, and perhaps most important, the motion compensation is much more severe for sonar than for radar." This is as a result of the inertia of the sonar vessel being less than that of an aircraft, coupled with the effect of swell and waves. This is likely to cause the aperture to deviate from a straight line.

Another examination of the use of synthetic apertures in sonar[14] comes to similar conclusions. "The proper compensation of transducer stray motion is considered to be a crucial factor in obtaining high quality maps using synthetic array processing." A technique using two transducers, to determine the azimuth angle of the target echoes, as well as the phase and return time, has been implemented in the laboratory as a test system[15]. Improved immunity to path fluctuations was reported.

Nevertheless there are a few reports of attempts to realise synthetic apertures. Good results have been reported[16] using an apparatus mounted on rails to image spherical targets. Experiments conducted at sea[17] using a low frequency moving source and stationary receiver have shown that signal coherence lengths of a few nautical miles may be achieved. It

is however believed that attempts to use synthetic apertures for sidescan mapping have not met with a great deal of success.

References

1. L.J.Cutrona, Synthetic Aperture Radar, Chap. 23 of "Radar Handbook", M.I.Skolnik (ed.) McGraw-Hill, New York, 1970.

2. C.Wiley, Goodyear aircraft corporation, 1951

3. W.Brown, "Synthetic aperture radar", IEEE Trans. on Aerospace and Electronic Systems, Vol. AES-3, No.2, March 1967.

4. M.I.Skolnik, "Introduction to Radar Systems", McGraw-Hill International Student Edition(1981), Chap. 8

5. M.I.Skolnik, "Introduction to Radar Systems", McGraw-Hill International Student Edition(1981), Chap. 14

6. M.I.Skolnik, "Introduction to Radar Systems", McGraw-Hill International Student Edition(1981), Chap. 7 p. 232

7. M.I.Skolnik, "Introduction to Radar Systems", McGraw-Hill International Student Edition(1981), Chap. 8 p. 282

8. Sato, Ueda, Ikeda, "Synthetic Aperture Sonar", J.Acoust. Soc. Am. Vol.54 799-802(1973).

9. T.Sato, O.Ikeda, "Sequential synthetic aperture sonar system-a prototype of a synthetic aperture sonar system", IEEE Trans. on Sonics and Ultrasonics, Vol SU-24, No. 4, July 1977.

10. Ikeda, Sato, "Further examination of synthetic aperture sonar in a turbulent medium", J.Acoust. Soc. Am. 68(2) 516-522(1980).

11. Ikeda et al., "Image reconstruction from disturbed synthetic aperture sonar data using aperture division", J.Acoust. Soc. Am. 78(1) 112-119(1985).

12. L.J.Cutrona, "Comparison of sonar system performance achievable using synthetic-aperture techniques with the performance achievable by more conventional means", J.Acoust. Soc. Am., 58(2), 336-348(1975).

13. L.J.Cutrona, "Additonal characteristics of synthetic aperture sonar systems and a further comparison with nonsynthetic aperture sonar systems", J.Acoust. Soc. Am., Vol 61, No. 5 1213-1217(1977).

14. H.Lee, "Extension of synthetic aperture radar(SAR) technique to undersea applications", IEEE Journal on Oceanic Engineering, Vol. OE-4, No. 2, 60-63(1979).

15. P.Gough, "Side looking sonar or radar using phase difference monopulse techniques, coherent and non-coherent applications", IEE Proc., 130(5) 392-398(1983).

16. Loggins et al., "Results from rail synthetic aperture experiments", J.Acoust. Soc. Am., 71(S1), S85(1982).

17. R.Williams, "Creating an acoustic synthetic aperture in the ocean", J.Acoust. Soc. Am., 60(1), 60-73(1976).

CHAPTER 3 EXPERIMENTAL WORK WITH SYNTHETIC APERTURES

Earlier work on synthetic apertures had been carried out by Littlewort[1,2] . Successful imaging of mid-water targets in a laboratory tank was achieved. A system capable of extracting quadrature and in-phase components of a received signal was inherited from the project. Based upon this design, a system to realise focused synthetic apertures in a laboratory tank was constructed. The operation of this system will be described, and imaging of mid-water targets using the system will be demonstrated.

3.1 EXPERIMENTAL SYSTEM

The sonar used separate transmit and receive transducers mounted adjacent to one another. The positioning of these transducers in a laboratory tank was achieved by use of stepper motors. The position of the transducer pair could be controlled and monitored to an accuracy of 0.1mm under control of an HP86 computer. In this way the transducer pair could be moved along an accurate straight line path, with transmission and reception of signals being carried out at fixed distance intervals. The in-phase and quadrature components of the signal received at each position were sampled and stored by means of a BIOMATION data acquisition unit controlled by the HP86 computer. A block diagram of the sonar system is shown in Fig 3.1

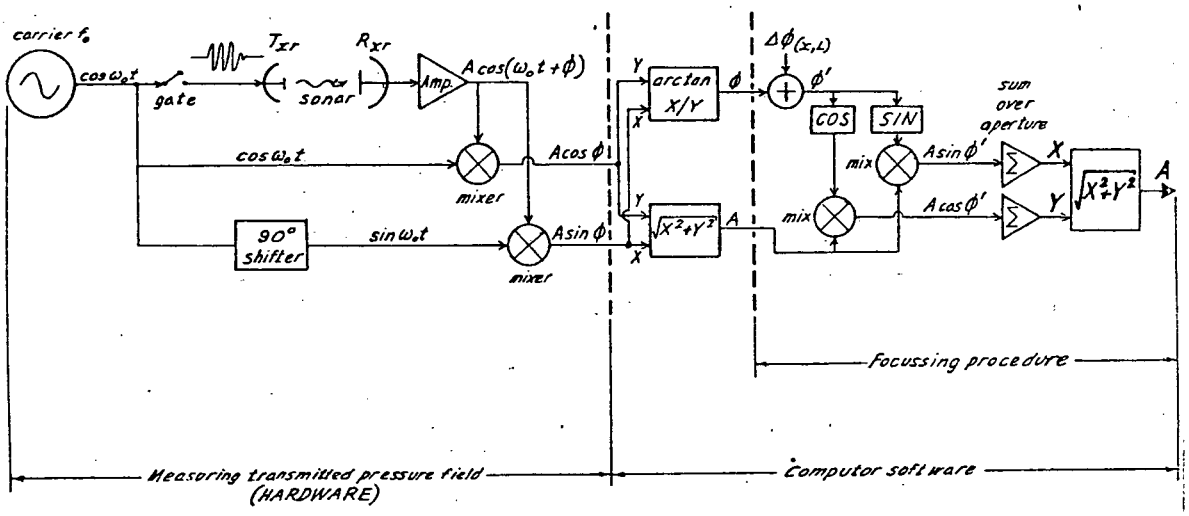

Figure 3.1 Block diagram of a focused synthetic aperture sonar system.(Littlewort[2])

The design of the various blocks is detailed in Appendix A.

The in-phase and quadrature components of the received signal enabled the amplitude and phase of the signal to be calculated. This information was then transferred by serial link to the U.C.T. UNIVAC computer. The processing to create synthetic apertures was carried out on the UNIVAC computer.

3.2 PROCESSING ALGORITHM

The process of realising a focused synthetic aperture may be thought of as creating a curved aperture centred about the point on which the aperture is being focused. The processing for each image point begins by calculating the two way propagation distance to each of the sampling positions in the aperture. On the basis of this, the phase correction needed to make all received signals co-phasal is calculated. This correction is then applied to the contents (amplitude and phase) of the range bin corresponding most closely to the two way propagation distance. The corrected signals for each of the aperture positions is then vectorially summed to yield the target strength for that image point. This process is carried out for each of the image points in turn. Details of the software developed to realise this focusing, together with an example of its operation may be found in Appendix B.

3.3 IMAGES OF MID-WATER TARGETS IN LABORATORY TANK

In order to test the system constructed, and to verify the operation of synthetic apertures, initial tests were carried out using two ping-pong balls mounted in a laboratory water tank. The arrangement used is illustrated in Figure 3.2 The transducers used were 8mm square and operated at a frequency of 200 kHz. The pulse length used was 80μs, corresponding to a range resolution of 6cm. The transducer pair was moved along a staight line path of 39cm., with transmission and reception of signals being carried out with the transducers stationary at intervals of 5mm . At each

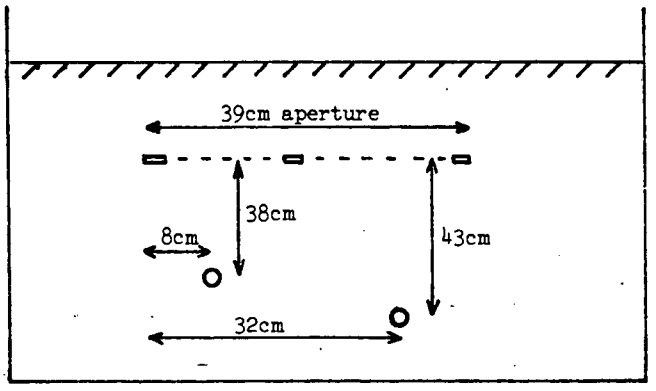

Figure 3.2 Experimental arrangement of two mid-water targets.

sample position the in phase and quadrature components of the returned signal were sampled and stored. A range interval of 250μs-700μs was sampled at a frequency of 100kHz, and stored on floppy disk. The amplitude and phase of all the stored samples was later calculated and transferred to mainframe computer.

Three different synthetic apertures were used to image the scanned space. These were:

a. An unfocused aperture of length 5cm.

b. A focused aperture of length 10cm.

c. A focused aperture of length 39cm.

The unfocused aperture corresponds to the maximum length of aperture which may be used if the targets are to be maintained in the far-field of the aperture. For the 39cm aperture, the complete aperture data is used for all the points in the image, i.e. the beam is focused and steered to each point in the image plane. For the case of the 10cm aperture where 39cm of data is available, the section of the data is moved(Fig. 3.3). The central 29cm of the image is obtained by selecting the appropriate section of the data and using focusing but no deflection. The outer 5cm of the image are obtained by

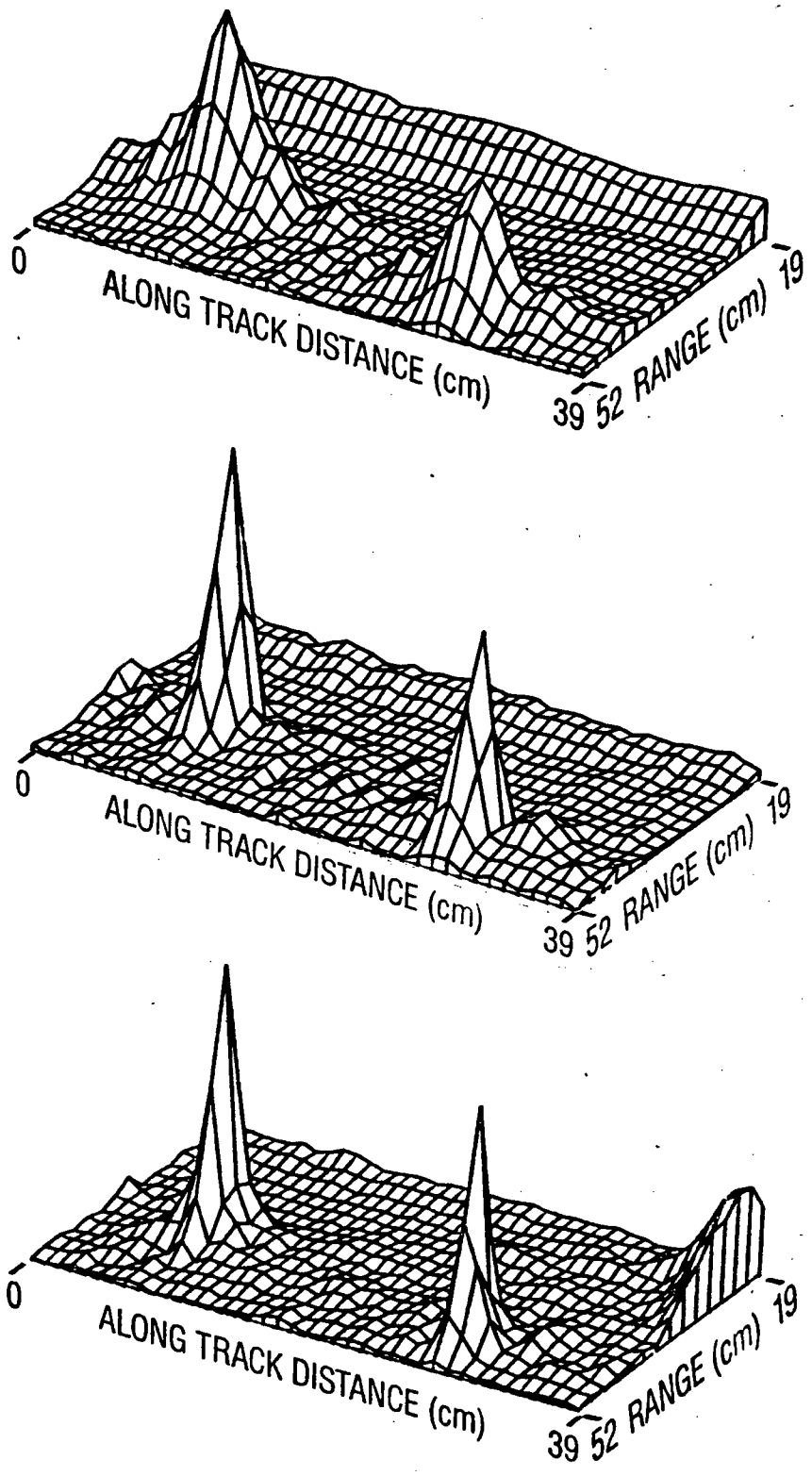

Figure 3.4 Images of two mid-water targets: (a) 5cm. unfocused aperture; (b) 10cm. focused aperture; (c) 39cm. focused aperture.

deflecting the beam.

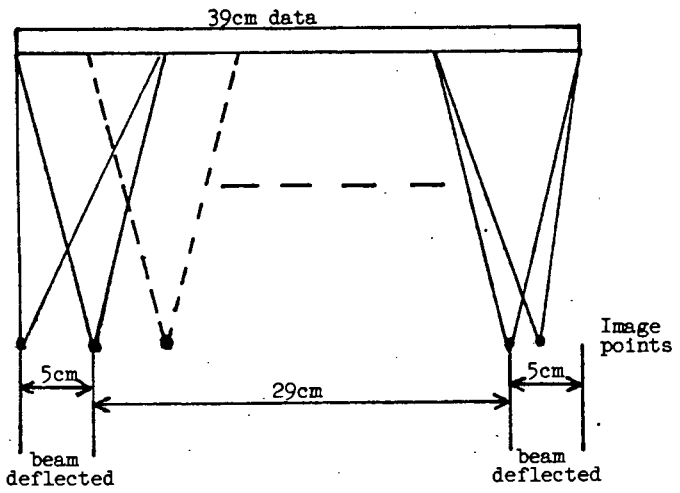

Figure 3.3 Use of data for 10cm synthetic aperture.

The results achieved using these apertures are displayed in fig 3.4 using a SACLANT 3-D graphics package which is available on the U.C.T. UNIVAC computer. The displays are of range versus along track distance, with the vertical axis being a measure of the target intensity. The improvement in resolution as the aperture is lengthened is clear. The along track resolution is in good agreement with that predicted. By using equation 2.3 the expected along-track resolutions for the three apertures are 3.2cm,1.6cm,0.4cm respectively. Two further points regarding the reconstructions are of note:

1. No artificial amplitude shading was employed, yet in the case of the long apertures the sidelobes are well below those predicted. This is caused by a natural shading of the aperture created by the shape of the transducer beam. The signals received at the edges of the aperture are 6 dB weaker than those received at the centre of the aperture for the case of a target directly below the aperture. (2.1.5)

2. The spurious peak noticeable at range 20cm and along track 39cm is part of a grating sidelobe. This grating lobe occurs because the sample spacing of 5mm is greater than half a wavelength(3.75mm). It occurs at a different range to the

main lobe because of the effect of focusing the aperture.

These experiments were carried out under very controlled conditions; conditions which are unlikely to be evident in the field. To illustrate the sort of effects that are likely to occur in the field, two types of perturbations were applied to the data:

1. By assuming an aperture sample spacing of 4.5mm as opposed to 5mm, the reconstruction using a 39cm aperture shown in figure 3.5a was obtained.

2. A random phase perturbation of up to 70^{o} was applied to each received signal. The reconstructed image using a 39cm aperture on the perturbed data is shown in figure 3.5b. This phase perturbation would be caused by unwanted transducer motion or media turbulence.

A 39cm aperture reconstructed image using unperturbed data is included (Figure 3.5c) for comparative purposes.

It will be noticed that the phase perturbation has the effect of reducing the target to background ratio, but with no great degradation of resolution. The use of an incorrect sample spacing on the other hand leads to a serious degradation of the image.

3.4 SUMMARY

The results presented in this chapter have demonstrated the operation of the focused synthetic aperture system. The results achieved under controlled conditions, using point-like targets are in good agreement with those predicted. The effect of two typical perturbations has illustrated that it is important to accurately know the aperture spacing. The effect of random phase perturbations, as are likely to result from small scale deviations from a straight line aperture, does not seriously degrade the image.

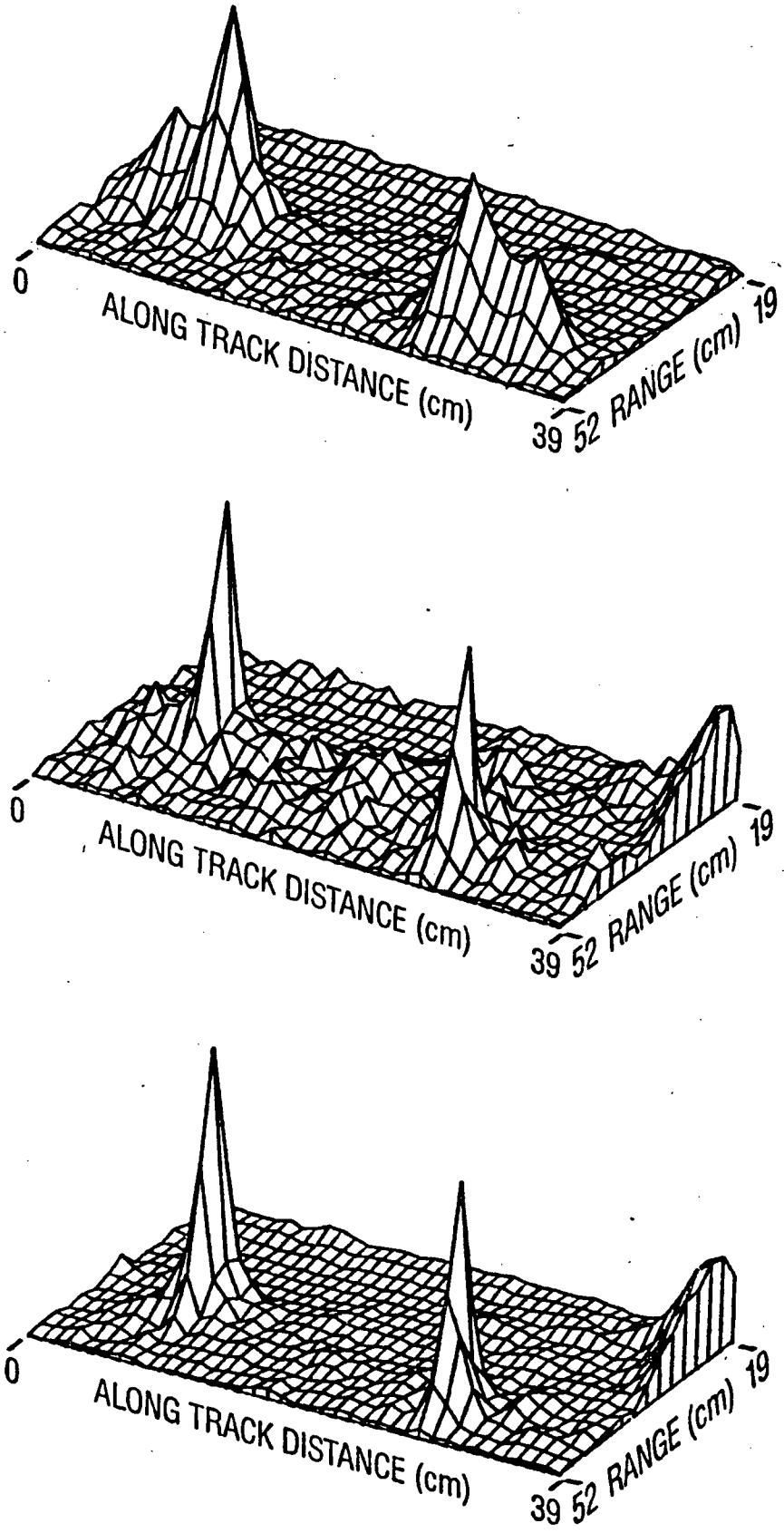

Figure 3.5 Effect of phase perturbations: (a) 10% position error; (b) random phase error; (c) unperturbed aperture.

References

1. G.Littlewort, "Wavefront distortion and synthetic aperture imaging." B.Sc(Eng) Thesis, U.C.T.(1982).

2. G.Littlewort, "Sub-bottom profiling and synthetic aperture imaging in sonar." B.Sc(Hons) Project, U.C.T.(1983).

CHAPTER 4: A REVIEW OF SUB-BOTTOM IMAGING

Acoustic methods are used to image objects and layers beneath the sea bed and may fall into one of two broad categories, namely seismic profiling and sub-bottom profiling. Seismic profiling usually uses a single explosive or explosive type source and multiple omnidirectional receive hydrophones. Penetration depths are considerable and the signal processing is aimed particularly at emphasizing strata using reflective or refractive methods. On the other hand, sub-bottom profiling usually combines a boomer, air gun or tone burst source with a single hydrophone receiver, both commonly mounted in a 'fish' towed close to the sea bed. The maximum penetration is modest compared with seismic systems and, depending upon the type of sediment and the frequency range in which most of the transmit energy is contained, might be between 1m and 100m.

Before outlining the commonly used seismic and sub-bottom profiling techniques, it is instructive to examine the acoustic characteristics of sub-bottom sediments.

4.1 ACOUSTIC PROPERTIES OF SEDIMENTS

Extensive literature exists on the acoustic properties of sub-bottom sediments. Both laboratory and in-situ measurements of acoustic attenuation and velocity in a variety of sediments have been carried out. One of the chief contributors has been E.L.Hamilton and his paper[1] gives a good summary of the results.

A series of papers published by Biot[2] gives the general theory for transmission of sound in fluid-filled porous media. He models a saturated sediment as a frame of particles separated by the fluid. The theory describes propagation of two compressional waves and a shear wave. The shear wave propagates due to the rigidity of the frame. One compressional wave is transmitted through the fluid and the

other through the frame of solid particles. These two waves are coupled. This theory predicts an attenuation asymptotically proportional to the square of frequency at low frequencies and the square root of frequency at high frequencies.

Empirical measurements as summarized by Hamilton[1] show the attenuation (in dB/m) to be directly proportional to frequency. This is at variance with Biot's theory, which bases loss mechanisms on the viscosity of the fluid. It is thought that the major loss mechanism is in fact inter-granular friction[1]. A graphical representation of the relationship between attenuation and frequency is shown in figure 4.1.

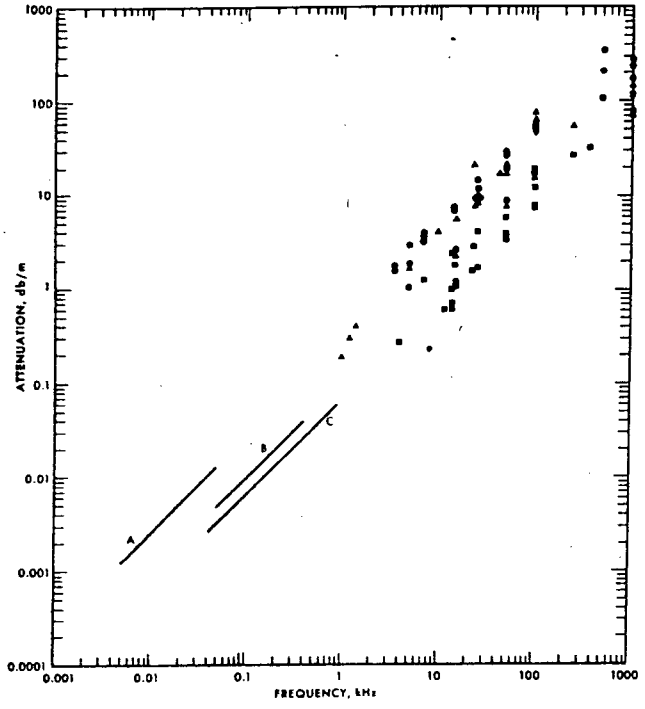

Figure 4.1 Attenuation versus frequency for various sediment types (Hamilton[1])

A further observation is that the attenuation varies widely with sediment type. Based on the theory of inter-granular friction, we expect the attenuation to be larger when the rigidity of the frame of sediment particles is larger. Comparison of figures 4.2a and 4.2b relating rigidity to porosity and attenuation to porosity confirms this.

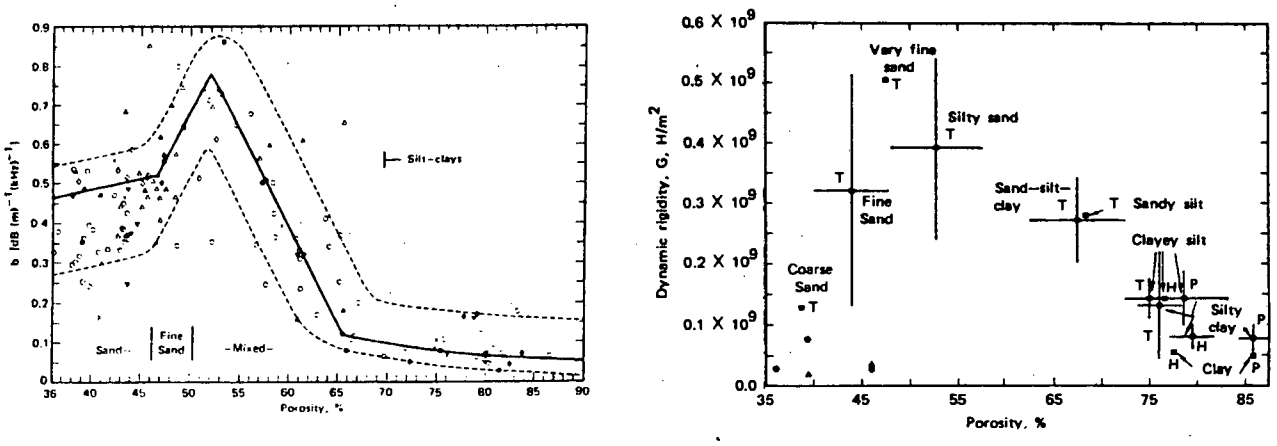

Figure 4.2 (a) attenuation; (b) dynamic rigidity as a function of porosity.[1]

It is thus evident that the penetration achievable will vary with sediment type. This has in fact been used as a technique for determining sediment type[3].

The second acoustic property of interest is that of velocity. It is found that the acoustic velocity is greater in sediments than in water. It is dependent on sediment type, in general being greater for higher density sediments. Acoustic properties of some typical sediments are shown in Table 4.1.

Table 4.1 Acoustic properties of various sediments

Sediment Type	Density g/cm³	Sound Speed m/s	Impedance 1.5MRayls
Coarse sand	2.03	1836	2.48
Fine sand	1.98	1742	2.30
Silty sand	1.83	1677	2.05
Sand-silt-clay	1.58	1578	1.66
Silty Clay	1.42	1519	1.44

4.2 SEISMIC PROFILING[5]

Seismic profiling is principally aimed at detecting rock strata. The application that led to the development of the

technique was the search for oil. Penetration depths are normally large, and in sea-bound applications, go far beyond the saturated sediment sub-bottom. Since high penetration is desired, very low frequency sound (eg.40Hz) is used, and a large amount of power transmitted. Devices used for sound generation are explosive in nature[5]. Examples are:dynamite, air guns, sparkers. Omnidirectional receive hydrophones are used to detect returning acoustic signals.

A number of different receiver/transmitter geometries are used, and by analysis of the results, information about the depth and angle of tilt of rock layers can be determined. Two methods of operation may be distinguished. These are refractive and reflective techniques.

4.2.1 Refractive techniques

Experiments carried out by Ewing and Worzel (1948)[6] measuring the first arrival of seismic signals for a variety of transmitter-receiver distances yielded a rather unexpected result. (Fig.4.3). It would be expected that the time of arrival would vary linearly with distance of separation, but this is not the case.

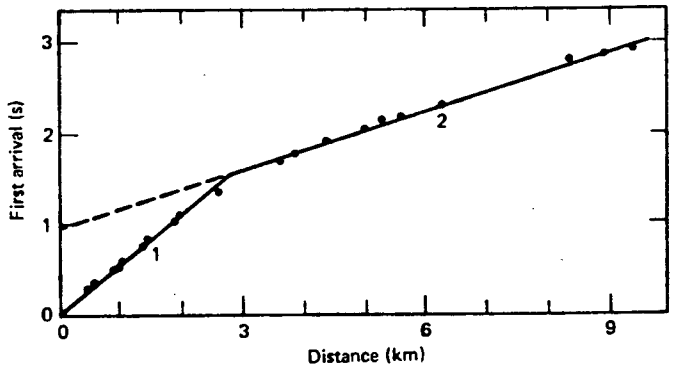

Figure 4.3 Seismic data, T versus distance (Ewing and Worzel)[4]

This unexpected curve may be explained (Fig.4.4) as follows. The upper layer(water) has a lesser acoustic velocity than the rock layer underlying it. The acoustic

signal travelling from the transmitter, through the water into the sediment, then along the boundary, and finally back to the receiver will arrive before the direct signal for receiver to transmitter distances greater than a critical distance. This critical distance will depend upon the depth of the layer and the acoustic velocity in the lower medium.

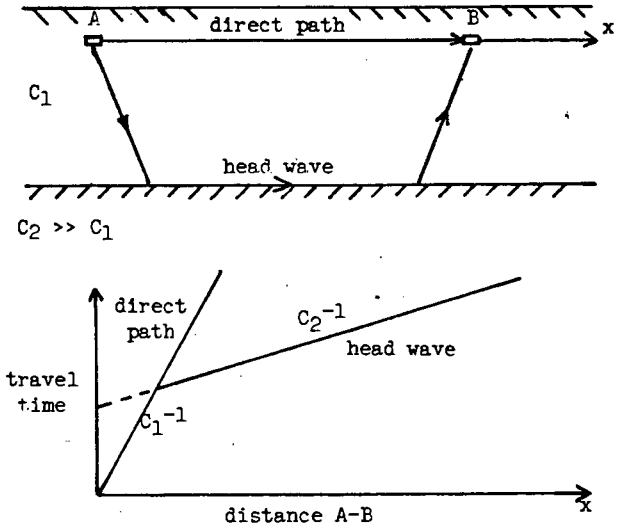

Figure 4.4 Direct path and head wave path for seismic refraction profiling. a) ray paths
b) return signal times

By careful analysis of the curve measured (Fig.4.3), information regarding the depth and type of rock may be deduced, without prior knowledge of the rock type[5].

If, however, the layer is at an angle other than horizontal, erroneous information will be extracted. By taking two such profiles, 180 degrees apart, information regarding the angle of the layer may also be deduced[5]. Two methods of generating these profiles are chiefly used.

(i) A stationary receiver is mounted on a sono-buoy, whilst a ship carrying a transmitter is moved past the sono-buoy, with transmissions being carried out at various distances of separation. Information received at the sono-buoy is either stored, or transmitted by radio link to the mother ship.

(ii) Two vessels, each carrying a transmitter and receiver are used. Signals are alternately transmitted from A to B and then from B to A.

This technique may be extended to detect multiple layers provided that the sound velocity increases with layer depth (as is usual). The distance of ship track needed to generate the required curve may be large for deep layers.

4.2.2 REFLECTION TECHNIQUES

Reflection techniques make use of the reflection of acoustic signals from sub-bottom strata to determine the depth of the boundary layer. Many measurements with different transmitter/receiver distances are used (Fig.4.5) thus enabling depth of sediments to be determined without prior knowledge of sound velocity in the sediments.

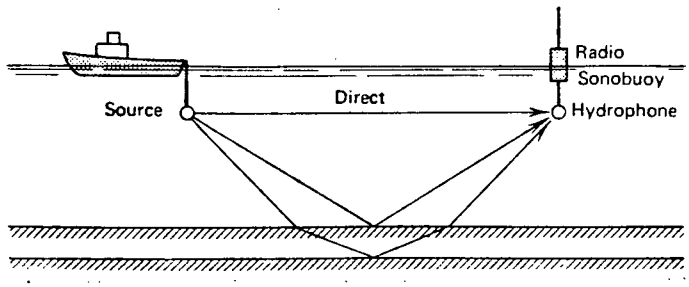

Figure 4.5 Seismic reflection profiling[4]

Measurements need not be taken over as large a range of distances as is necessary for the refractive technique. Two methods are commonly used

(i) A sonobuoy is dropped in the sea, and the ship carrying the transmitter moves away from the buoy. Signals are transmitted at known distances, and signals received by the sonobuoy either radioed to the mother ship or stored for later use.

(ii) An easier and more continuous form of operation is to string a streamer of hydrophones behind the mother ship. Each hydrophone is a different distance from the transmitter. Signals received at each hydrophone are used to construct the profile.

4.3 SUB-BOTTOM PROFILING

The aim of sub-bottom profiling is to map the layers of sediment beneath the sea floor. Penetration is less than that achieved in seismic profiling. Because the depth of penetration is less, more portable systems than equivalent seismic systems are realizable. Typically, a single transducer or array of transducers is used to direct a beam downwards. Signals are reflected from layers and targets on the sea bottom and below and are received by a hydrophone. The amount of penetration depends upon sediment type and frequency. Most systems operate at frequencies between 1kHz and 10kHz. An example of such a sub-bottom profile is shown (Fig.4.6). The occurrence of a tilting layer is evident.

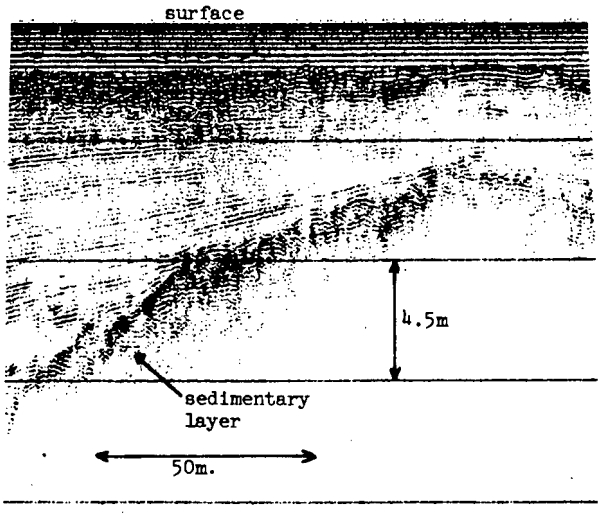

Figure 4.6 Sub-bottom profile[3]

The resolution of this type of system is clearly restricted. This limitation is a result of the low frequencies used. The beamwidth radiated by a typical transducer is very wide. For

example, at a typical operating frequency of 4kHz, a transducer 0,5m in diameter will have a beamwidth of 49 degrees. For reflecting strata this is not particularly disadvantageous. The return from a layer shows up clearly as a sharp transition between white and black on a chart recording and the only effect is to cause a broadening of the black bands corresponding to strata. For regions containing thin stratification, this may cause a problem as the returns from seperate strata may merge into one another[7]. A technique to separate such strata, based upon deconvolution has been developed[7].

Difficulty occurs when we try to separate objects spaced closely in the along-track dimension. Clearly, two objects spaced closer than the width of the beam cannot be distinguished. For the 0,5m transducer mentioned earlier, at a range of 15m, this resolution is 11,25m. In order to realise the best resolution, the transducer and hydrophone are normally towed close to the sea floor. Further, the detection of a point-like target is characterised by a 'crescent' on the chart recording. This occurs because the target is insonified for a large range of transducer positions (Fig.4.7).

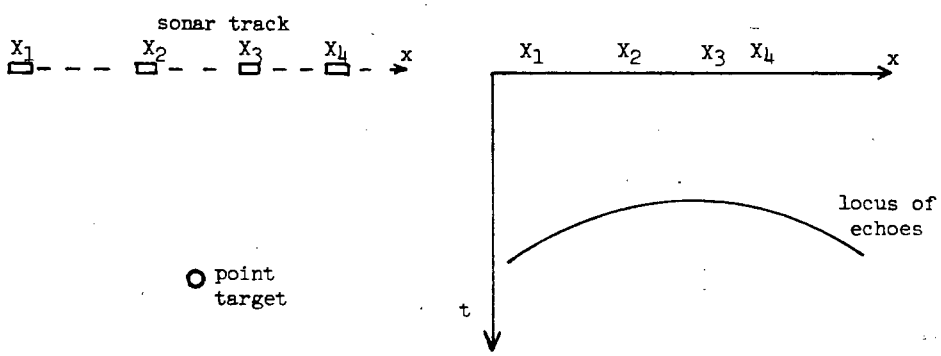

Figure 4.7 Detection of point target by wide-beam sonar (a) physical picture; (b) sonar returns.

A trained eye will be able to pick out point-like targets from their crescents, but clearly such a system is not acceptable for detecting small objects.

4.4 HIGH RESOLUTION TECHNIQUES

The techniques mentioned above are aimed at the detection of rock or sediment layers. For this purpose, there is little need for fine resolution in the along track or cross-track dimensions. Thus the use of a wide beam is not a serious problem. In fact in the case of seismic reflection and refraction profiling, the use of a wide beam is necessary.

There exists a need for a system to detect small buried objects. Examples of uses are: locating buried mines in military applications, searching for buried wrecks, checking buried pipelines. As yet there does not exist a well developed technique for such applications. Three approaches will be considered.

4.4.1 CONVENTIONAL ARRAYS

By either using a long physical transducer, or array of transducers, a fine beam may be created. At frequencies suitable for sediment penetration, the length of array necessary to achieve a narrow beam is great. For example consider the well known 'GLORIA" sidescan sonar[8], used for long range sea-floor mapping. Because of the long ranges of operation, attenuation of the acoustic signal within the water is a problem, hence a relatively low frequency of operation was chosen (6.5kHz). A $2{,}5^{o}$ beam is created using a 5,3m array of transducers. Although the frequency used is suitable for sub-bottom penetration, the system has not been used for such applications. A consideration of the implications of using a long unfocused aperture, shows that the system is only suitable for imaging objects at ranges of 100m (the far-field distance) and beyond. The along-track resolution at 100m range is 5m. Thus due to the large minimum operating range and coarse resolution the system is not suitable for use in sub-bottom imaging.

By using focusing on a long array, objects in the

near-field of the array may be imaged. This focusing may be either electronically or mechanically realised. The construction of such a mechanically focused array has been reported[9]. The transducers are mounted in a curved rather than linear array. The intention was to use the system to detect buried objects in a potential harbour site. The array is focused for a particular range, and thus may only be used in very specific applications.

Thus it would appear that the achievement of fine resolution sub-bottom imaging using conventional techniques is unlikely.

4.4.2 PARAMETRIC ARRAYS

A parametric array utilises the interference between two high frequency signals to create an end-fire array of low frequency sources. The effect is to generate a narrow, low-frequency pencil beam. The achievement of short pulses is aided by the use of the high-frequency sources, and thus good range resolution is possible. A problem is that the conversion efficiency of the high frequency energy to lower frequency is low. A large primary signal power is necessary to achieve a reasonable source level. Improvement is possible using pulse compression techniques[10].

A few parametric sub-bottom imaging systems have been built[10,11]. Typically they have large power requirements (>10kW). Resolutions in the order of metres have been reported. Penetrations of 50m have been achieved using high power systems. The systems have been successfully used to detect buried rocks, pipelines and sediment layers. The use of a narrow pencil beam, although giving an easily interpretable return, places a severe limitation on the area that may be surveyed using a single beam. The use of a narrow fan beam on the other hand would allow the imaging of a significantly larger area to the side of the

survey vessel, as is the case in a sidescan sonar. This difference is illustrated in Figure 4.8

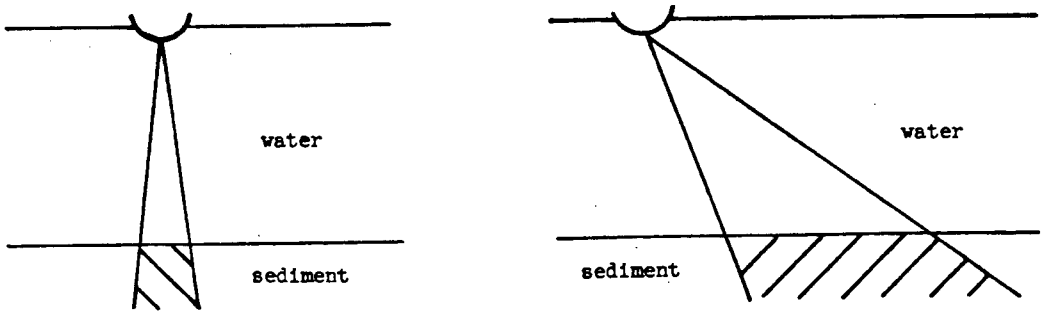

Figure 4.8 Cross sectional view of area insonified by (a) pencil beam; (b) fan beam

4.4.3 SYNTHETIC APERTURES

It has been established in an earlier chapter that the effective achievement of synthetic apertures is aided by short range and low frequency operation. Both of these are present in sub-bottom imaging applications.

By using a linear synthetic aperture a narrow fan beam is realised. By using this fan beam in a sideways looking mode, it is possible to realise a sub-bottom sidescan imaging system. In this way it would be possible to construct a map of sub-bottom objects for a large area of sea floor.

References

1. E.L.Hamilton, "Compressional wave attenuation in marine sediments", Geophysics, 37, 620-646(1972).

2. M.Biot, "Theory of propagation of elastic waves in a fluid saturated porous solid. I Low frequency range, II higher frequency range.", J.Acoust. Soc. Am. vol. 28, 168-191(1956).

3. Ivor Pretorius, NRIO(Stellenbosch), Private Communication.

4. C.Clay, H.Medwin, Acoustical Oceanography: principles and applications, J.Wiley, 1977, Chap. 8.

5. M.Dobrin, Introduction to Geophysical Prospecting, McGraw-Hill, New York, 1976, Chap. 5

6. Ewing, Worzel, "Long-range sound transmission", in Propagation of sound in the ocean, Memoir 27, Geological Society of America, New York, 1948.

7. Bolus, Sivaprasad, Frost, "A theoretical vertical and lateral model for the analysis of acoustic subbottom data through simulation", J.Acoust. Soc. Am., 67(5), 1512-1522(1980).

8. A.S.Laughton, "The first decade of GLORIA", J.Geophys. Res., 86(B12),11511-11534(1981).

9. Ohgaki, Shimizu, Miyazawa, "Acoustical imaging of an object buried in seafloor sediment by using a focused ultrasonic transducer.", J.Acoust. Soc. Am., 67(5),1603-1607(1980).

10. H.O.Berktray, et al., "Sub-bottom profiling using parametric sources", Proceedings of the Institute of Acoustics Conference on Underwater Applications of Non-Linear Acoustics, Bath, Sept. 1979.

11 W.L.Konrad, "Applications of the parametric acoustic source", Proceedings of the Institute of Acoustics Conference on Underwater Applications of Non-Linear Acoustics, Bath, Sept. 1979.

CHAPTER 5 WAVEFRONT DISTORTION BY SEDIMENTS

Investigative work into the effects of a sand-water interface on the implementation of synthetic apertures has been carried out by Littlewort.[1] By simulation of a single point target, it was shown that imaging of buried targets by means of synthetic apertures is feasible. Attempts to image targets buried beneath sand in a laboratory tank were, however, not successful. It was thought that the problems may have been a result of the box within which the targets were buried, or of reverberation within the sand volume.

In this chapter an investigation into the effect of a sediment-water interface on synthetic apertures is made. The problem is investigated theoretically, by computer simulation and experimentally.

5.1 THEORETICAL INVESTIGATION

Waves travelling from one medium to another, undergo two major effects. Firstly, a certain fraction of the incident energy is reflected at the interface; and secondly, rays incident at angles other than normal to the interface undergo refraction at the interface. In the case of acoustic waves at a water-sediment interface, the sediment almost always has a greater propagation speed than the water, which causes the waves to be refracted away from the normal to the interface (Fig. 5.2). A further effect is that the sound undergoes a greater attenuation in the sediment volume than in the water. The reason for this has been discussed in chapter 4.

The effect of these three features on the imaging of buried targets by means of synthetic apertures, will be examined.

(a) Refraction

Referring to Figure 5.1, a transducer positioned directly

overhead the target (for a horizontal interface) will see the target in the correct along-track position, but it will appear closer than it actually is, because of the disparity of velocities. For transducers positioned away from directly overhead, the target will appear to be horizontally displaced from its true position.

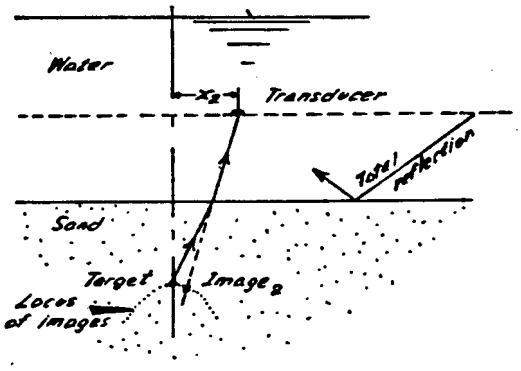

Figure 5.1 Apparent position of buried target for various transducer positions (Littlewort[1])

This displacement is greater the further the transducer is moved from directly above the target. The effect of this displacement of the apparent echo position is to cause the wavefront arriving at the synthetic aperture to be not spherical, but in fact a slightly flattened curve. This will cause a degradation of the image of the target if a spherical wavefront is assumed, as is the case in a focused synthetic aperture system. The amount of degradation will depend upon the range and depth of burial of the target. An experimental examination of this effect is undertaken later in this chapter.

(b) Attenuation

It is clear, referring again to Figure 5.1, that signals received by transducer positions towards the edges of a synthetic aperture imaging a buried target, will undergo greater attenuation than those in the centre. This is because the rays coming from and returning to these positions travel greater distances in the sediment. The

effect of this is to apply a natural amplitude shading of the aperture. This causes a slight degradation of the main beam, but has the advantage of suppressing sidelobes(2.1.2).

(c) Transmission coefficient

The transmission and reflection coefficients for waves travelling between two homogeneous media will be derived[2].

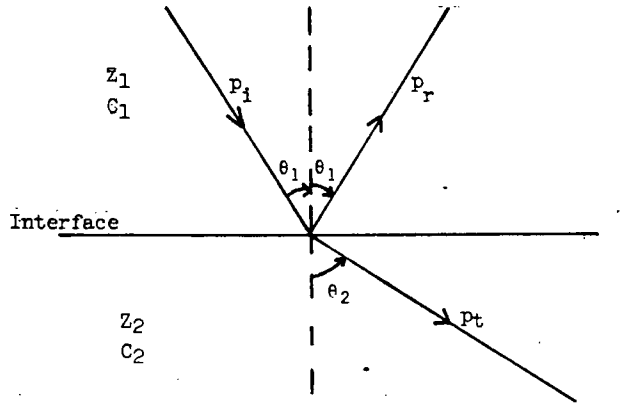

Figure 5.2 Reflected and transmitted waves at water-sediment interface.

The pressures on either side of the boundary must be equal

$$p_i + p_r = p_t \qquad \ldots (5.1)$$

The normal components of the velocity must be equal at the boundary

$$u_i\cos\theta_1 - u_r\cos\theta_1 = u_t\cos\theta_2 \qquad \ldots (5.2)$$

The relation between pressure and velocity is $\frac{p}{u} = Z \Rightarrow u = \frac{p}{Z}$

Thus (5.2) becomes

$$\frac{p_i\cos\theta_1}{Z_1} - \frac{p_r\cos\theta_1}{Z_1} = \frac{p_t\cos\theta_2}{Z_2} \qquad \ldots (5.3)$$

(5.1) and (5.3) can be combined to give

$$\frac{p_r}{p_i} = \frac{Z_2\cos\theta_1 - Z_1\cos\theta_2}{Z_2\cos\theta_1 + Z_1\cos\theta_2}$$

and

$$\frac{p_t}{p_i} = \frac{Z_2\cos\theta_1}{Z_2\cos\theta_1 + Z_1\cos\theta_2}$$

where θ_1 and θ_2 are related by Snell's law: $\frac{\sin\theta_1}{C_1} = \frac{\sin\theta_2}{C_2}$

The relations of interest are, however, the intensity ratios: $R = \frac{I_r}{I_i}$ and $T = \frac{I_t}{I_i}$ where $I = \frac{p^2}{Z}$

Therefore, the reflection coefficient is $R = \frac{p_r^2/Z_1}{p_i^2/Z_1} = \frac{p_r^2}{p_i^2}$

$$\Rightarrow R = \frac{(Z_2\cos\theta_1 - Z_1\cos\theta_2)^2}{(Z_2\cos\theta_1 + Z_1\cos\theta_2)^2}$$

and the transmission coefficient is easiest to derive from: $T = 1 - R$

$$\Rightarrow T = \frac{4Z_1Z_2\cos\theta_1\cos\theta_2}{(Z_2\cos\theta_1 + Z_1\cos\theta_2)^2} \quad \ldots (5.4)$$

These equations apply only for θ_1 less than the critical grazing angle, as θ_2 is not defined beyond this angle. The critical grazing angle is the angle for which the refracted angle is 90 degrees, ie no energy is transmitted to the second medium.

In the case of synthetic apertures we are interested in T_{12} and T_{21} , the transmission coefficient from medium 1 to 2 and that for waves travelling from 2 to 1. From (5.4) it is evident that $T_{12} = T_{21}$, ie the 'two way' transmission coefficient is T^2.

Equation (5.4) can be rewritten as

$$T = \frac{4\ Z_2/Z_1\ \cos\theta_1\cos\theta_2}{(Z_2/Z_1\ \cos\theta_1 + \cos\theta_2)^2} \quad \ldots (5.5)$$

In a typical sub-bottom application, medium 1 is water and medium 2 is sand. Based on values used by other researchers , the following parameters were used.

$$\frac{C_2}{C_1} = \frac{1675}{1500} = 1.12 \ ; \ \frac{\rho_2}{\rho_1} = 1.96 \Rightarrow \frac{Z_2}{Z_1} = 2.2$$

Plotting T^2 against θ_1 as determined from eq 5.5, we obtain the curve below (Figure 5.3)

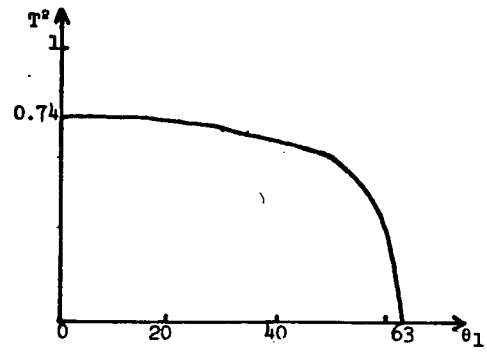

Figure 5.3 Transmission coefficient as a function of angle of incidence for two way travel.

It must be noted that although there is an angle beyond which all the energy is reflected (the critical grazing angle), there is no position for which a buried target will not be visible. This is because the rays entering the sediment are refracted away from the normal. Provided that care is taken to limit the aperture such that angles of incidence of less than about 50 degrees are used, the effect of the transmission loss on the creation of a synthetic aperture will not be great.

It is apparent from the theoretical examination that the major problem in imaging buried targets might be the degradation caused by refraction. It was necessary to carry out some experimental examination to find out how serious the effect is.

5.2 SIMULATION OF A BURIED TARGET

In order to qualitatively examine the effect of both refraction and attenuation on the imaging of buried targets, computer simulation was employed. The computer simulation generated return signals that would have been received by a transducer traversed over a buried target. The sediment

simulated was a coarse sand having a propagation velocity of 1860m/s and an attenuation of 100dB/m, at a frequency of 200kHz. This was intended to correspond to conditions used in the laboratory tank. The simulation generated return signals at 5mm intervals over a total aperture length of 39cm (as in the mid-water results described in chapter 3).The return signals at each aperture position were calculated as follows. The time of the return echo from the target was calculated by allowing for refraction at the sand-water interface and thus determining the travel times in each of the media. A pulse length of 90μs with a cosine squared shaping was assumed, starting at the two-way travel time from the target. This was done in order to simulate a real pulse. The amplitude of the received pulse was calculated by allowing for attenuation during the travel time in the sediment and for spherical spreading during both the out and back travel times. An arbitrary maximum pulse height for the directly overhead case was assumed, and all other signals were calculated relative to this amplitude. The phase was determined from the two-waytravel time to the target, and was assumed constant over the full pulse length. At all other points in time the signal was assumed to have zero amplitude. Simulated return signals at 10μs intervals were stored for use in the synthetic aperture algorithm. The implementation of this procedure is described in Appendix C.

In this manner a simulation was carried out for a point target buried 5cm below a flat sand surface which was in turn 30cm below the transducer path. The beam of the transducer was assumed to be omnidirectional. No account was taken of transmission loss at the sediment interface, which should have no effect on the creation of the synthetic aperture for aperture lengths used in the simulation (See Section 5.1c).

The reconstructed image using processing incorporating correction for the effect of refraction, is shown in Figure 5.4(a). The algorithm calculated the time of arrival and phase correction necessary to make all signals arriving at the

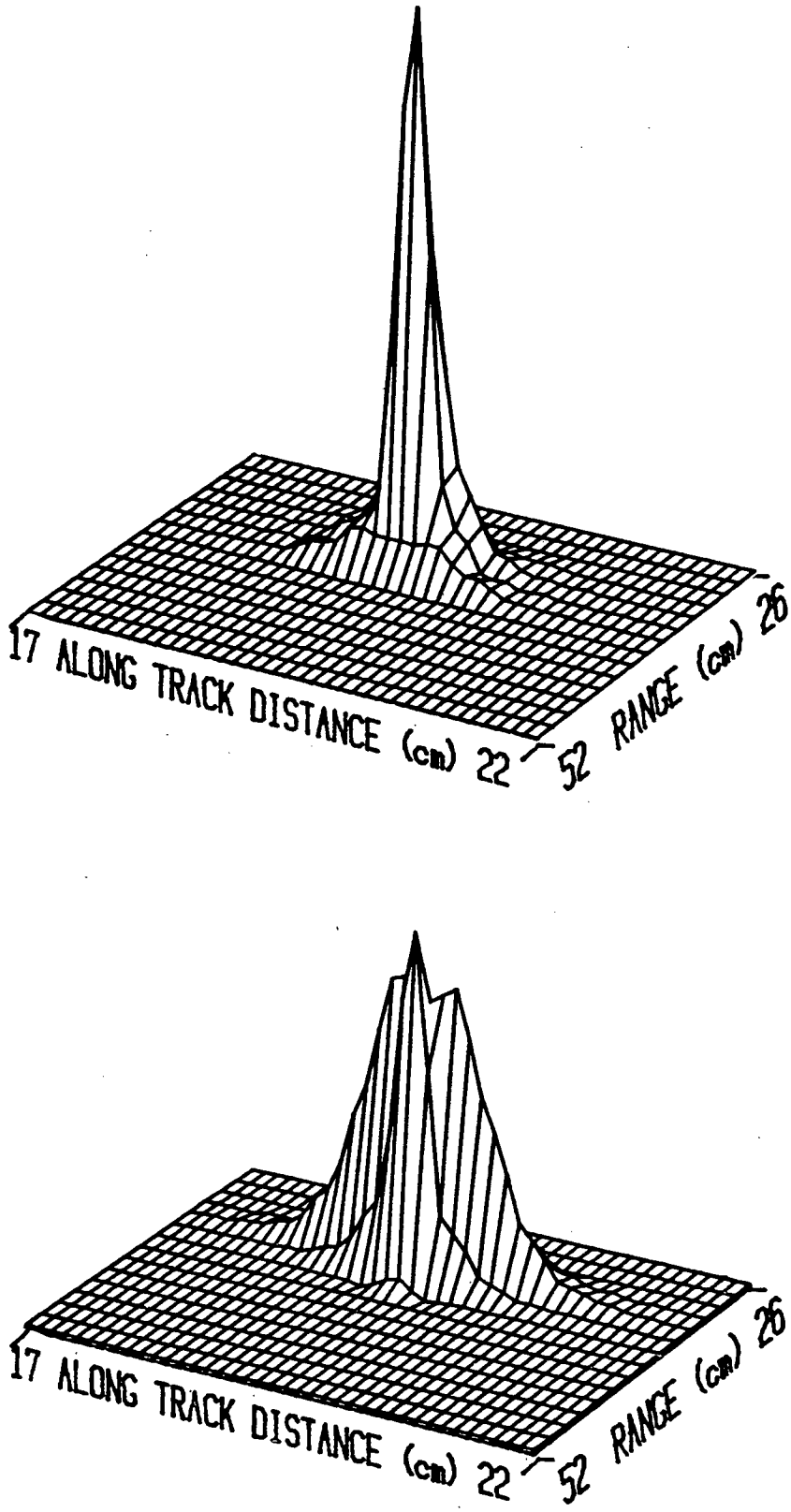

Figure 5.4 39cm. focused aperture reconstruction of simulated buried target: (a) corrected for refraction;
(b) refraction ignored.

aperture from the target co-phasal in the same manner as these were determined in the simulation. In processing, it was necessary to allow for the fact that the pulse had a non-zero width in order to obtain the sharpest image. This image occurs if all signals are timed relative to one half the pulse length rather than the start of transmission. This is as expected. Processing in a similar fashion, but ignoring the effect of refraction yielded the image shown in Figure 5.4(b). The scale of the vertical axis (representing target strength) has been increased by a factor of two relative to Fig 5.4(a) in order for the resolution to be more easily compared. The target is degraded in strength and resolution. The resolution of the corrected image (Fig. 5.4(a)) is approximately 0.3cm and the uncorrected (Fig. 5.4(b)) approximately 1cm. The latter corresponds to the resolution expected from an aperture of 13cm length.

Figures 5.5(a) and 5.5(b) were produced using apertures of length 15cm using corrected and uncorrected processing respectively. Aperture shading was necessary in order to reduce sidelobe levels. A Hamming weighting function ($W(z)=0.54+0.46 \cos (2\pi z/L_e)$) was used. Now the two images are similar in amplitude and along track resolution, having a resolution of approximately 0.8cm. This resolution is in fact better than that achieved using a 39cm uncorrected aperture. It is thought that this improvement is related to the use of a long pulse. From the above, it is clear that if the refractive effect is ignored, the coherency of the return echoes is limited, and thus the optimum along-track resolution cannot be achieved. The degree of limitation is more severe the greater the range and depth of burial. In sub-bottom profiling application, the length of aperture is likely to be limited by transducer beamwidth and transducer motion anyway, so this further limitation is unlikely to be severe. In applications where it is, and finer resolution is required, it is possible to achieve optimal resolution. It is, however, a lengthy process and requires knowledge of the depth of the sediment and the relative velocities in the sediment and water.

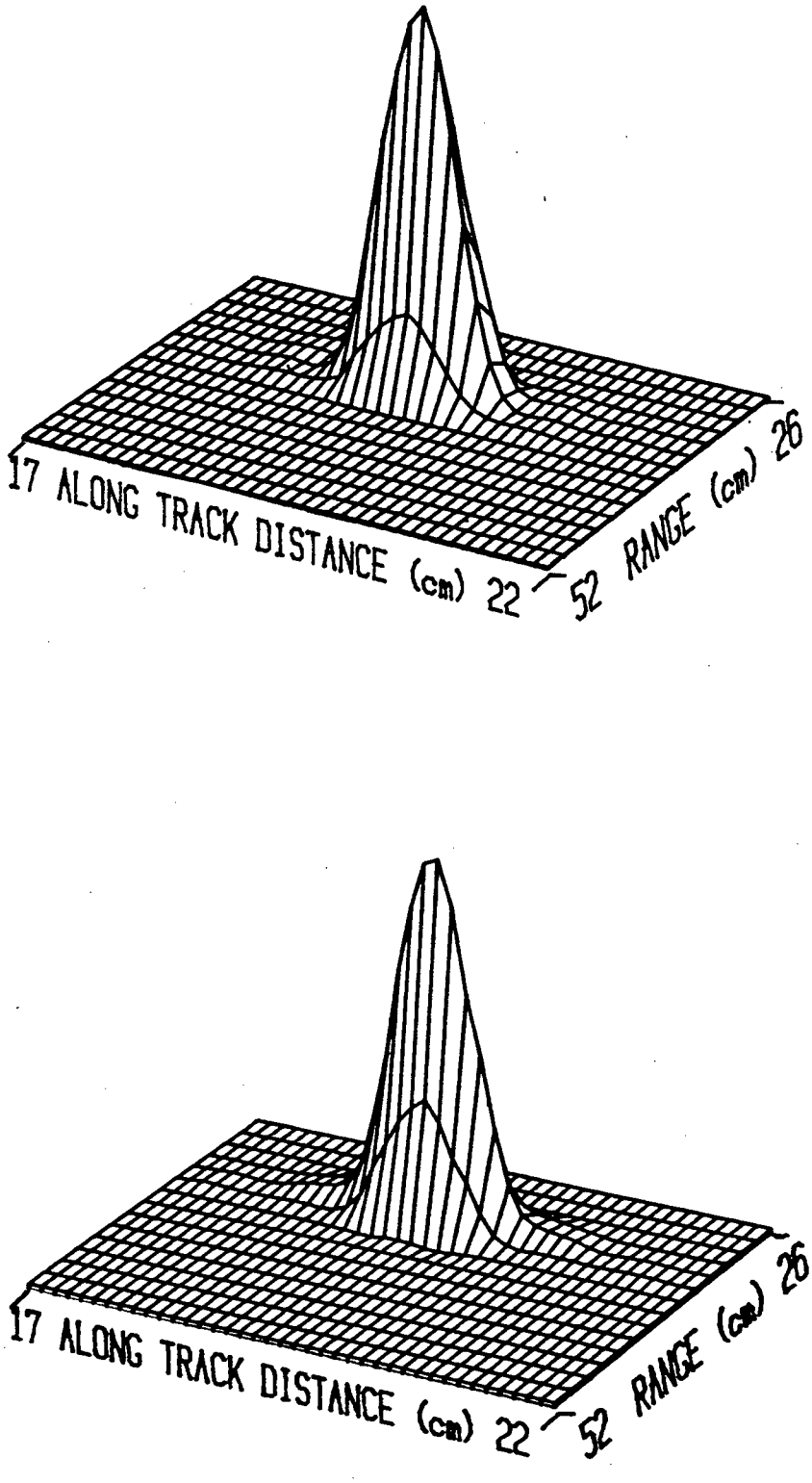

Figure 5.5 15cm. focused aperture reconstruction of simulated buried target: (a) corrected for refraction; (b) refraction ignored.

The simulation applied here is equivalent to a 5kHz system, working at 12m above a sand surface imaging a target buried 2m deep. The resolution is limited to that achievable by a 6m aperture, which is 0,35m. This would be quite acceptable for most applications.

The simulation carried out here has assumed the use of a worst case sediment. For typical sands encountered in sub-bottom applications[3,4] the ratio C_2/C_1 is 1.1 and not 1.2 as used in the simulation. Thus the restriction on the aperture length would in practice be less severe than that occuring for the simulated conditions.

5.3 EXPERIMENTS WITH BURIED TARGETS

In order to attempt to image a buried target in a laboratory tank, a box filled with sand was placed in the tank. Initial attempts to image buried ping-pong ball targets were unsuccessful. An iron rod was then pushed through the sand at a depth of 7cm below the surface. This rod also extended out of the side of the box to act as a mid-water target (Fig. 5.6). This enabled a comparison of buried and mid-water images to be made. The box was filled to the top with sand to attempt to lessen the effect of the box edges. The sand was shaken and stirred to remove as many air bubbles as possible. It was then left to settle for a couple of days before experiments were carried out. The water was still cloudy when experiments were carried out, and it was not noticed that sand had come out at a few places near the box edges, thus exposing parts of the box edges, which acted as targets.

Synthetic apertures were implemented using the same procedures as detailed in chapter 3. Apertures of 35cm length with 5mm spacing between samples were realised. The transducer was moved at a distance of 20cm above the sand surface in the case of the buried target, and at the same height (ie 27cm above rod) in the case of the mid-water target. In this way, a reconstruction of the mid-water target and the buried target could be independently achieved. It was hoped that an

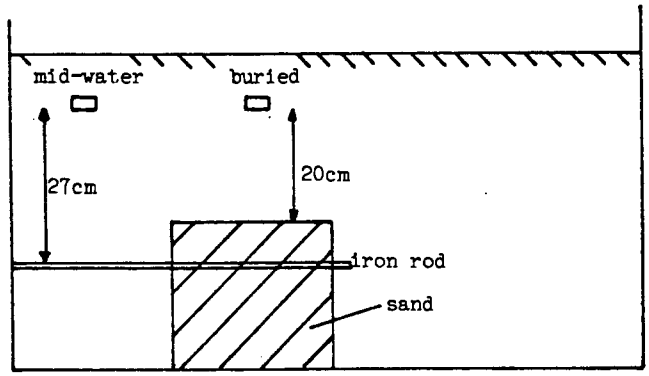

Figure 5.6 Experimental arrangement for tests with buried target. Transducer moves away from viewer to generate apertures.

attenuated version of the mid-water target would be visible at the same position in the buried reconstruction. The results are portrayed using the same vertical scale in Figure. 5.7.

The target is clearly visible in the mid-water reconstruction, but is undetectable in the reconstruction of the buried target. This latter reconstruction shows a large and extensive reflection from the sand surface. The expected target strength of the rod, assuming an attenuation of 100dB/m of sediment put the rod's image strength below the background level. Individual targets much stronger than this are visible. Investigation in the laboratory showed that there were echoes coming from the box edges, and these are thought to have led to these images. On the basis of these investigations, it seems very likely that the 'reflecting layer' observed by Littlewort[1] is in fact caused by the box/sand edge.

It was clear that there were large difficulties with laboratory work due to the necessity to contain targets and sand within a box. The use of 200kHz as an operating frequency was not ideal for the achievement of penetration. It was thus decided that it would be beneficial to experiment under more real conditions using a lower frequency.

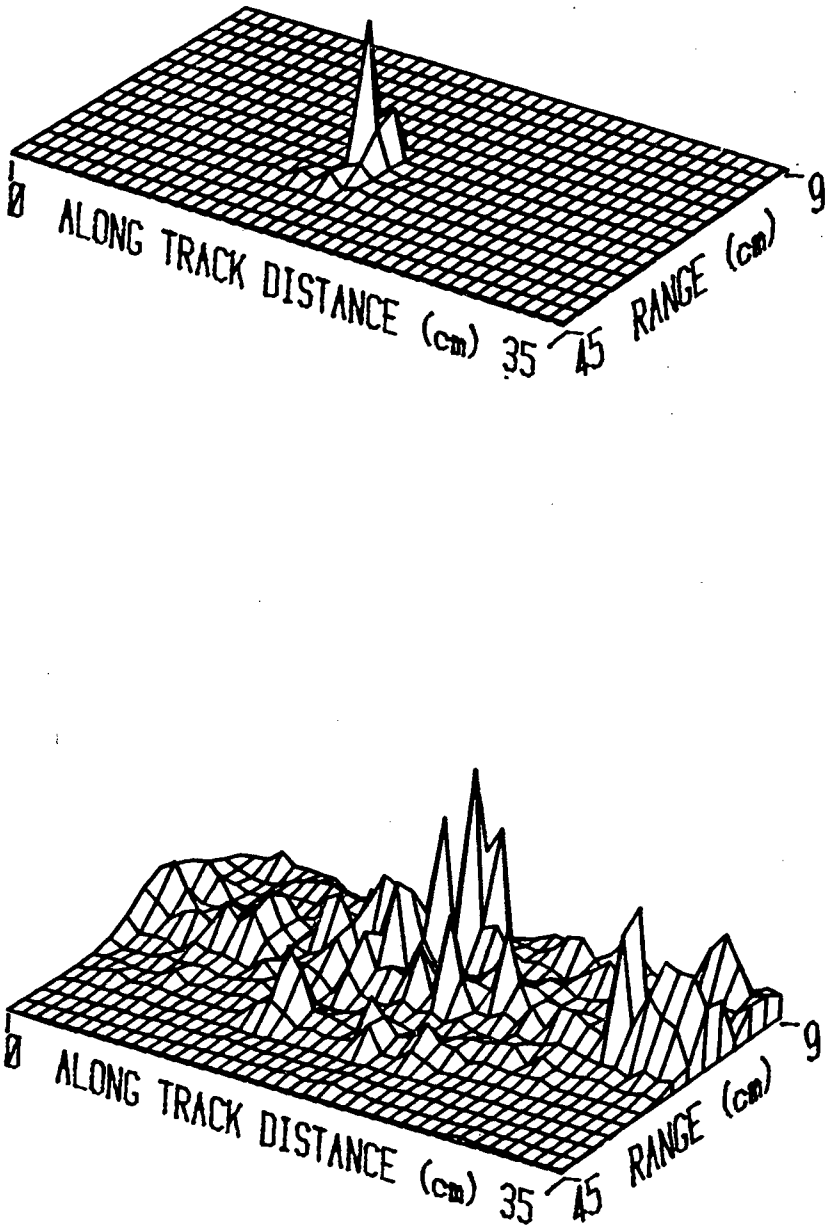

Figure 5.7 35cm. focused aperture reconstructions:
(a) mid-water target; (b) buried target.

5.4 EXPERIMENTS WITH BURIED SOURCE

The problem of surface echoes experienced in attempting to image buried targets does not occur if a buried source is imaged using a moving receiver. In this case the resolution expected is twice that achievable by using a moving transmitter and receiver (eq 2.2). This arrangement does, however, enable the effect of refraction to be studied.

Measurements carried out on the sand used showed that the attenuation was 100dB/m and the speed of propagation relative to that in water was 1.1. This corresponded to literature figures for silty sand (Table 4.1). The transmitter was an 8mm square transducer, and was buried 5cm beneath a smoothed sand surface. The receiver, a similar transducer, was traversed along a 39cm aperture 30cm above the sand surface. A pulse length of 120μs of 200kHz signal was transmitted, and signals were recorded at aperture positions 5mm apart.

Examination of the recorded waveforms indicated that the transmitted signal was visible over 15cm of aperture but not beyond this. This is caused by the limited width of the physical beam of the transducer used and attenuation of the signal in the sand. Reconstructions of the 'target' were made using a 15cm aperture. These are portrayed in Figure 5.8. Figure 5.8(a) is a reconstruction which takes account of refraction, and Figure 5.8(b) is achieved by ignoring refraction. The former image is slightly sharper, but the 3dB resolution of each is the same (approximately 2cm). This is similar to that predicted by eq 2.2

There is little degradation caused by ignoring refraction. This is because the aperture used is fairly short. (See 5.2).

5.5 SUMMARY

The results of this chapter have demonstrated that there may be a broadening of the beam of a synthetic aperture due to the effect of refraction. Provided that care is taken not to use

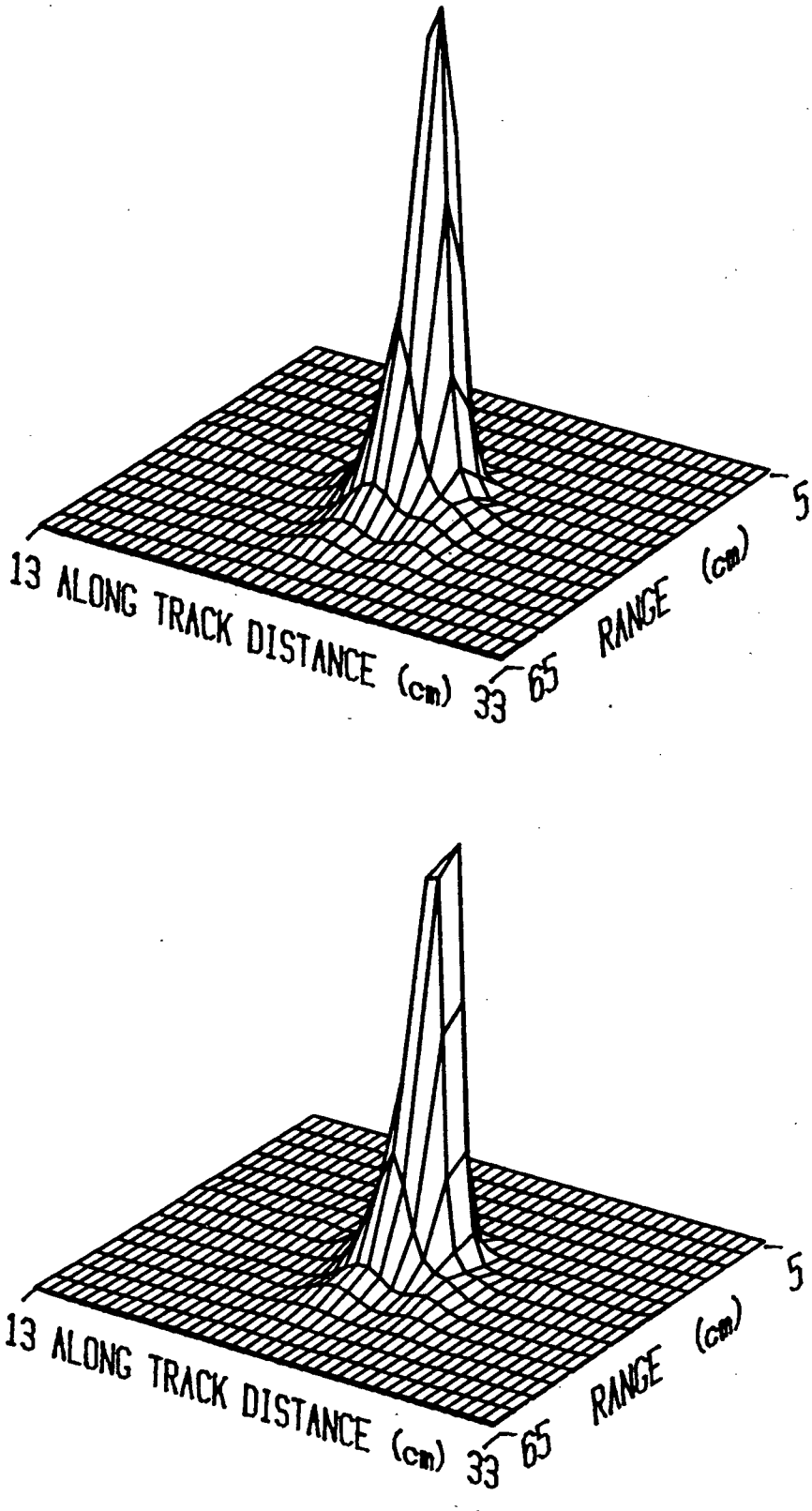

Figure 5.8 15cm. focused aperture reconstructions of buried source: (a) corrected for refraction; (b) refraction ignored.

very long apertures, this effect is small enough to be neglected. In cases where very fine resolution is required, it is possible to sharpen the image by correcting for refraction. This is a time-consuming operation and relies on accurate knowledge of the transducer-sand distance and the relative velocities in the two media.

Attempts to image buried targets have shown the problem of surface reflections, which limit the minimum depth of burial at which targets may be detected. It was felt that operation at lower frequencies, over a more extensive sediment area would be more beneficial than the continution of laboratory experimentation.

References

1. G.Littlewort, "Sub-bottom profiling and synthetic aperture imaging in sonar.", B.Sc(Hons) Project, U.C.T.(1983).

2. Kinsler et al., Fundamentals of Acoustics, 3rd edition, Wiley(1982), Chap. 6.

3. Muir, Horton, Thompson, "The penetration of highly directional acoustic beams into sediments", Jour. of Sound and Vibration, 64(4), 539-551(1979).

4. R.Ceen, N.Pace, "Acoustic signals in marine sediments due to water-borne parametric arrays.", Proceedings of the Institute of Acoustics Conference on Underwater Applications of Non-Linear Acoustics, Bath, Sept. 1979.

CHAPTER 6 RESERVOIR TESTS

A fresh water reservoir with a floating laboratory was available for use in experimentation. The reservoir floor was known to contain scattered rocks lying in a bed of silt. The laboratory had a 4,5m long rectangular hole cut in the floor. The transducer was suspended in the water from a trolley which could run along rails down the length of the hole. Photographs of the laboratory and the trolley can be seen in Figure 6.1.

These facilities enabled synthetic apertures to be realised under fairly controlled conditions. A transducer, taken from a conventional sub-bottom profiling array was loaned from the National Research Institute for Oceanology (NRIO). It was operated at a resonant frequency of 4,5kHz (as determined from a circle diagram) and radiated a conical beam of 100 degrees (as specified by the manufacturers). These properties made it suitable for use as a synthetic aperture element, and for penetration of the sediment.

The experimental arrangement necessitated a few changes to the sonar system used in the laboratory tank. These changes are outlined in the first part of this chapter, thereafter experiments carried out using the system are described.

6.1 SONAR SYSTEM MODIFICATIONS

There were two major differences in the experimental arrangement to that used in the laboratory tank. Firstly, only one transducer was available and hence it was necessary to use this both as transmitter and receiver. For this purpose, a duplexer was designed. The details of this can be found in Appendix A.

Secondly accurate, stationary positioning of the transducer whilst measurements were being taken, as done in the tank, was not possible. Hence, it was necessary to record signals whilst the transducer was in motion. For this purpose, a digital

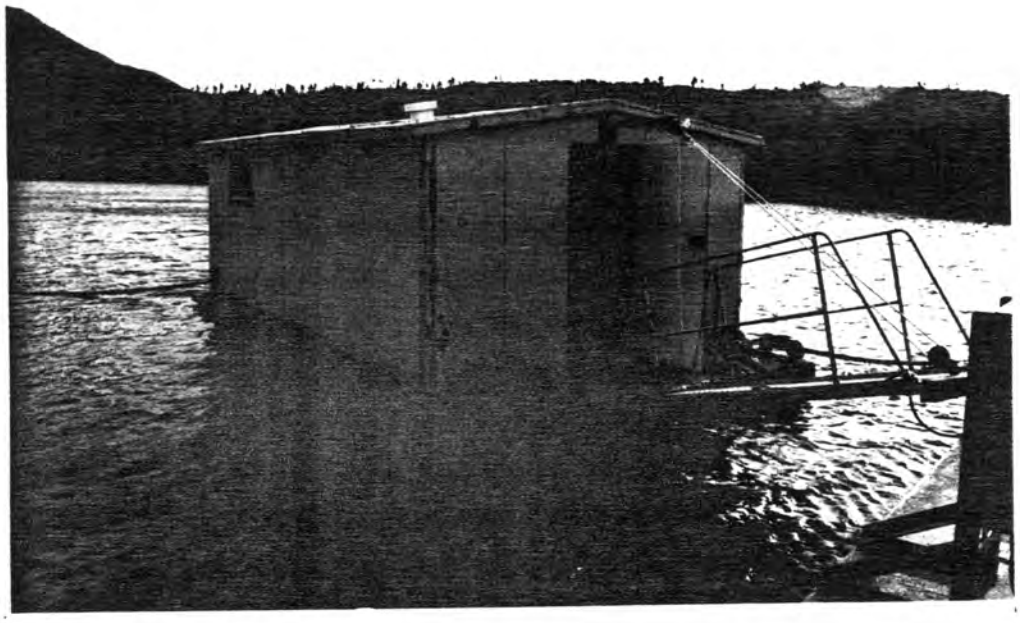

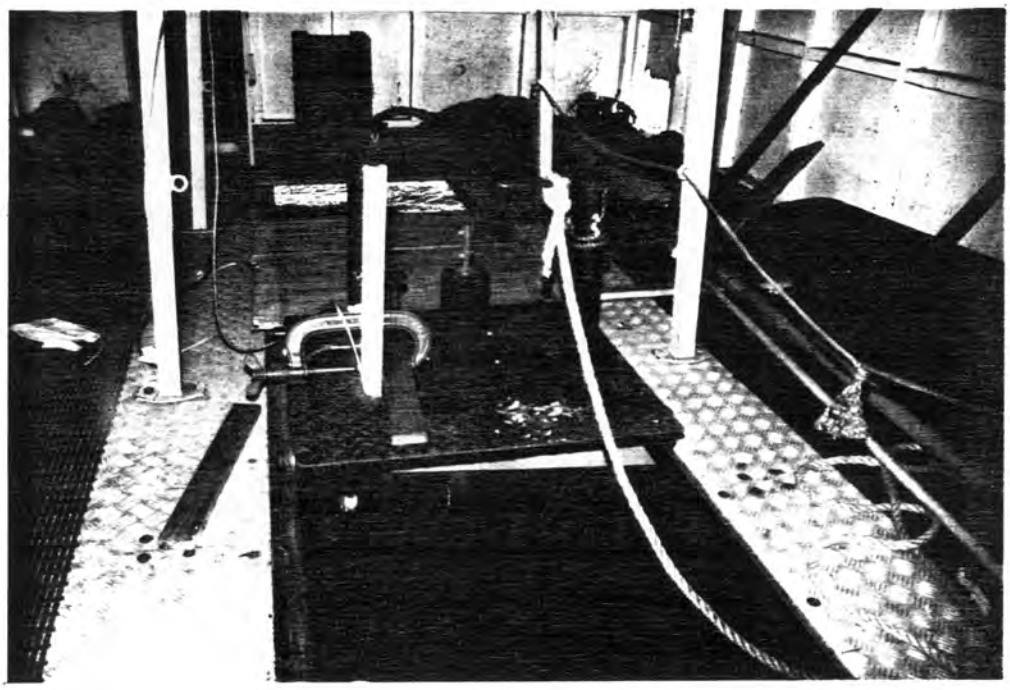

Figure 6.1 Photographs of (a) floating laboratory;
(b) trolley used to move transducer.

oscilloscope capable of storing four kilobytes of information, was used. This severely limited the amount of information that could be stored, since it was necessary to store the in-phase and quadrature components of the return signals from all aperture positions within this memory. For this purpose, a selectable range interval of each return signal was sampled using a sampling interval of 160μs. This was sufficient to adequately sample the return signals as the transducer bandwidth limited the pulse length to 1ms. Initially, a two metre range gate was felt to be sufficient. This necessitated storing 16 samples of the in-phase and quadrature components at each aperture position, making 32 samples per aperture position. Using the full memory capacity, this enabled 128 aperture positions to be stored for one run. Utilising the full track length of 4,5m meant that a sample spacing of 4cm was realised. This is less than $\lambda/2$ (16cm), as is required to avoid the occurrence of grating sidelobes.

The pulse repetition interval was fixed at 116ms, and based on this, it was necessary to pull the trolley at 0,7m/s. The towing was done by hand and started on a 'beep' signal from the controlling computer (HP86), which also 'beeped' at this end of the sampling, by which time it was ensured that the trolley had just reached the end of its run. A short time was allowed before the start of the sampling, to allow for the reaction time of the person pulling the trolley. In this way, it was possible to determine the average velocity at which the trolley was moved. As shown in Chapter 3, providing the average velocity is well known, a slightly inconsistent velocity over the aperture can be tolerated.

A block diagram of the modified system is shown in Figure 6.2. Circuit and software detail may be found in the Appendices.

6.2 ECHO-SOUNDING MODE

It is usual in sub-bottom profiling to work with the transducer directed downwards. This configuration was adopted for initial tests. Two experiments were carried out. First,

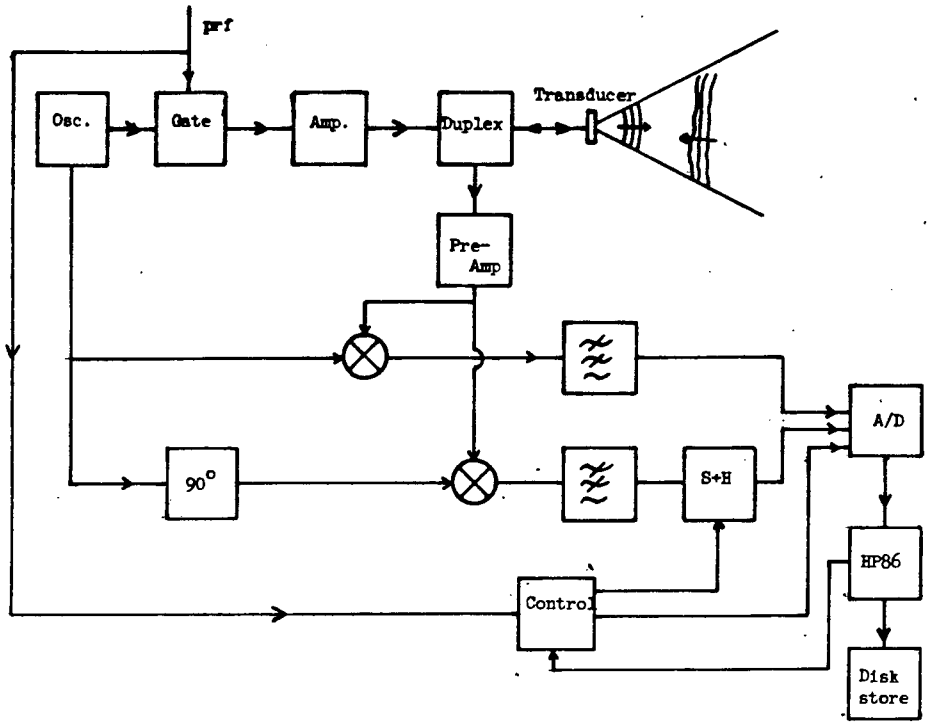

Figure 6.2 Block diagram of sonar system.

signals from the sediment directly below the laboratory were stored for later processing. Then, a long concrete pipe was lowered onto the reservoir bed below the laboratory, perpendicular to the line of motion of the transducer and similar synthetic aperture data was stored. The aim was to see whether penetration was being achieved, and secondly to see whether the pipe on the reservoir floor could be detected. The images achieved using a 4m aperture are shown in Figure 6.3. Only 4m of data was available for the reconstruction and hence a beam was focused and steered to each point in the image plane.

The images are dominated by a large signal off the reservoir bottom. There is no obvious target where the pipe ought to be (at along track 1,5m) in figure 6.3b. The variation in intensity with along-track distance is thought to be due to the type of bottom. A rocky bottom will give a strong echo whereas a muddy bottom will be a weaker reflector.

Specular reflectors, an example of which is the reservoir

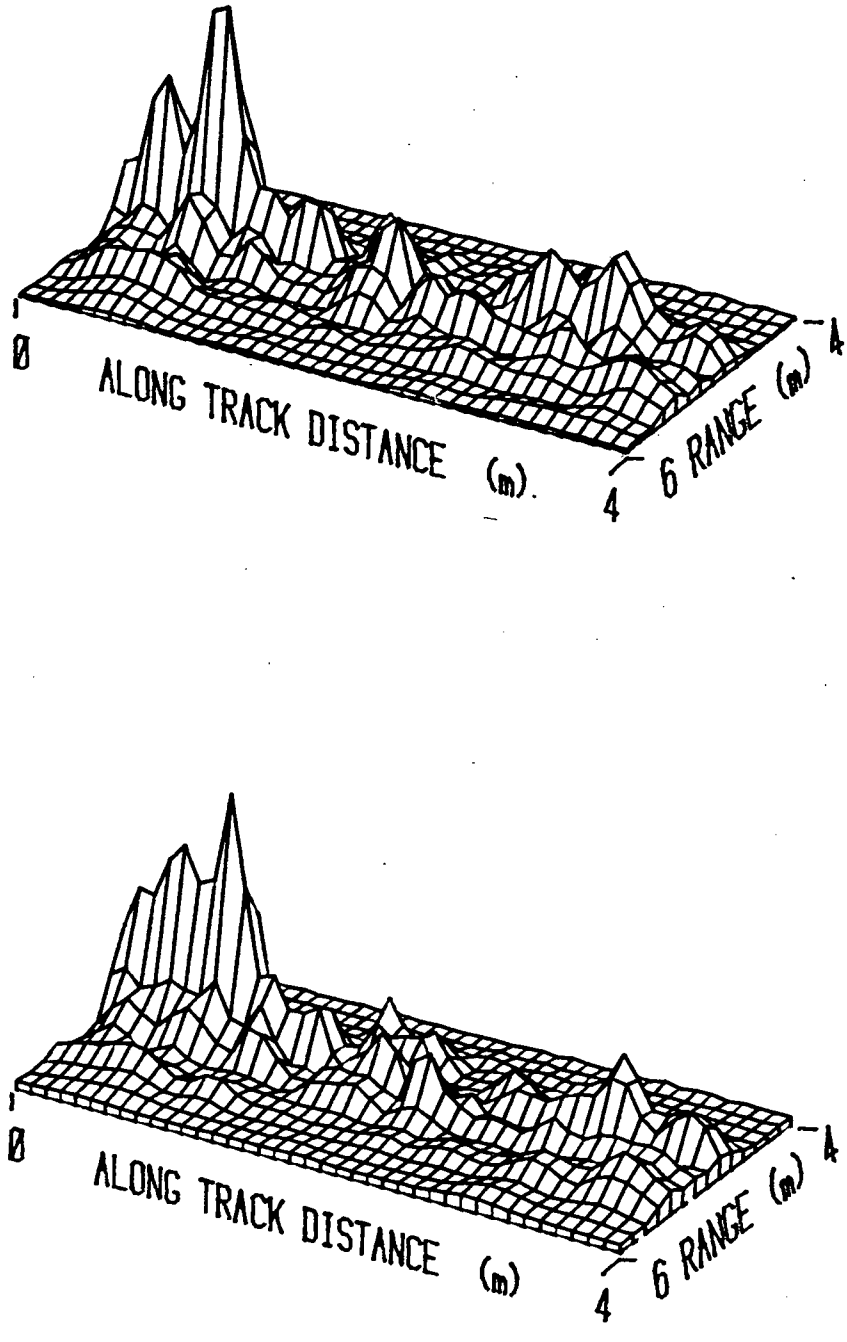

Figure 6.5 Images of area below laboratory: (a) no pipe present; (b) pipe present.

bottom when viewed at 4,5kHz, will be characterised by a constant phase of return echo as the transducer is moved over them. Figure 6.4 shows a phasor display of the return echoes as recorded at each transducer position. The vertical axis represents the range or depth and the horizontal, the along-track distance. The length of each line in the plot represents the amplitude of the echo, and its orientation depicts the phase.

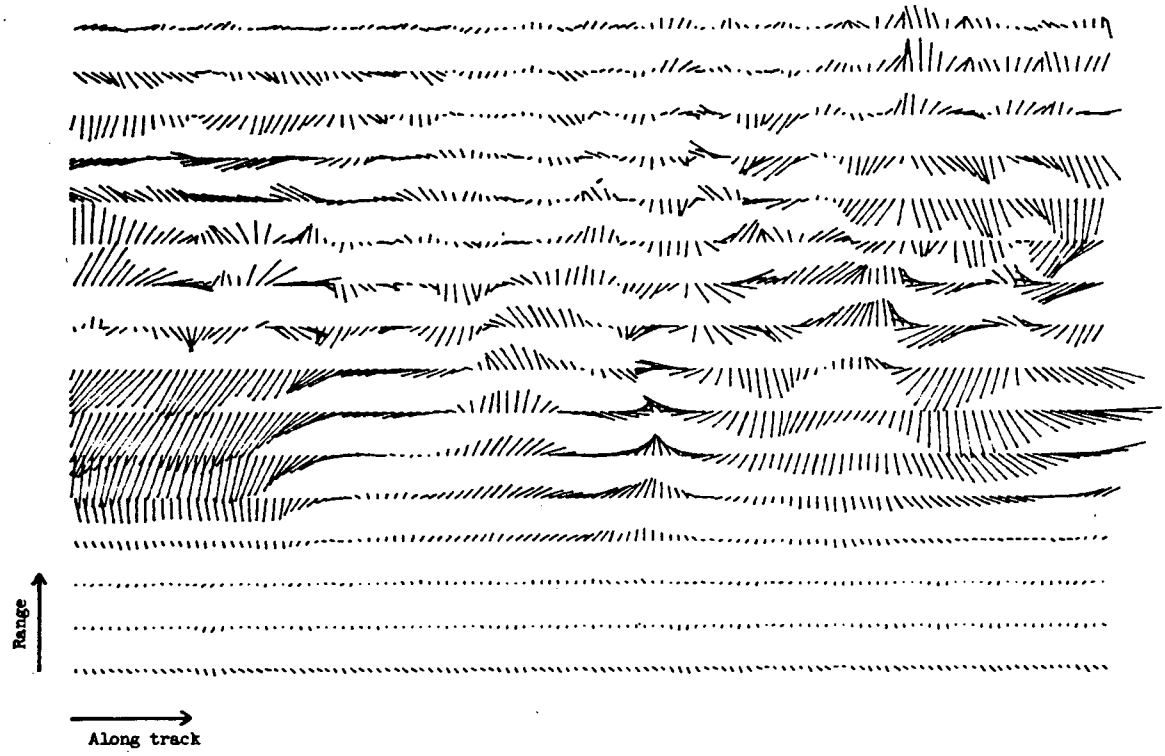

Figure 6.4 Phasor display of return signals at each aperture position.

An example of a specular target is the reflector seen in the fifth row. This is the echo off the reservoir floor. The slow variation of phase is a result of the changing depth of the bottom. A point-like target will be characterised by a phasor which rotates in a different manner (see Appendix C). The phase of the echo will vary slowly when the transducer is overhead the target, but more rapidly as the transducer moves away. This type of target is not obvious in the raw data, but there is evidence of some rotation at greater ranges. The synthetic aperture processing used in a focused system is

aimed at imaging point-like targets. Specular targets will thus only add coherently for a short range of aperture positions, corresponding to when the transducer is directly overhead. Specular targets are, however, in general stronger reflectors than point targets, the result being that even with this short coherence length, the reconstruction from specular targets may dominate those from point targets. This is the same problem that was encountered in the tank (Chapter 5).

A method of de-emphasizing horizontal specular reflectors is to not use portions of the aperture directly overhead the image point. In this way a squint beam is realised. If the same area is viewed from two different squint angles, the same point features can be expected to be evident. Unfortunately, the amount of data gathered did not enable this procedure to be carried out. Instead, different 2m sets of data were used to focus and steer beams over the entire 4m image plane. Firstly, the set of data 0 to 2m was used, then 1m to 3m and then 2m to 4m. The resultant images showed a concentration of energy directly beneath the set of data used. This is in agreement with the idea that most of the feature is specular in nature.

This seems reasonable for the bottom, but not for the feature at ranges greater than the bottom. The first assumption would be that these occur from sub-bottom reflections. It, however, seems unlikely that in an area which has a strong bottom backscatter (eg first 1m of image), suggesting a rocky bottom, penetration would be achieved. A second, and more likely explanation is that the targets at greater range are also bottom feature but at an angle to the side of the area directly below the laboratory. The occurrence of this feature highlights a problem with the use of synthetic apertures in this mode. Although the processing of the synthetic aperture leads to a good along-track resolution, the lateral resolution remains unchanged, and is poor. A perspective view of the geometry is shown in Figure 6.5.

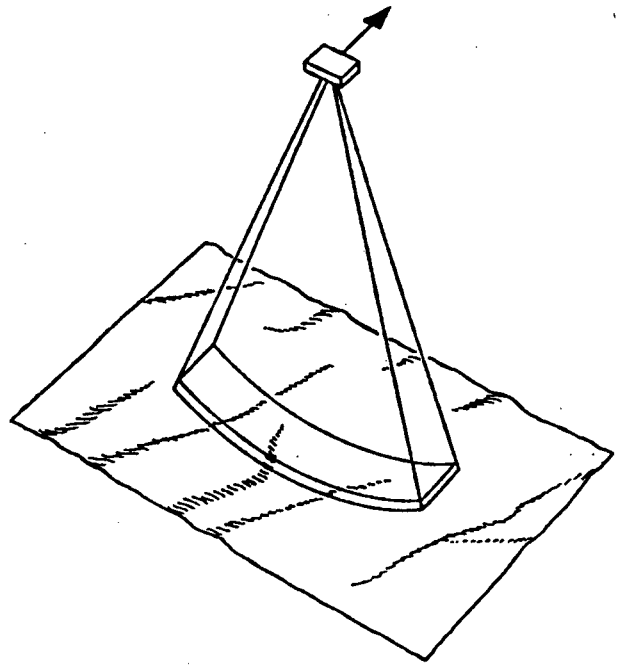

Figure 6.5 Intersection of synthesized fan beam with the sea bed.

Fig. 6.6(a) repreents a vertical cross-section of the beam corresponding to Fig. 6.5 and shows the resolution cell. Directly beneath the transducer, in the centre of the physical beam, the sensitivity is maximum. However, the attenuation of the sediment reduces the return echo. To the side of the transducer, in the skirts of the physical beam, the sensitivity is lower but the penetration into the sediment is less, so that the return echo is less attenuated. Although sub-bottom strata may still be imaged satisfactorily due to their specularity, small objects are likely to appear stronger when they are located to the side of the transducer than when they are beneath it. Bearing in mind that the intention of a high resolution sub-bottom profiler is to image small targets, it is apparent that the image will be very difficult to interpret.

6.3 SIDESCAN MODE

Because of the foregoing problems, the mode of operation was altered to use the system as a short-range sidescan sonar in which the use of low frequencies enables bottom penetration.

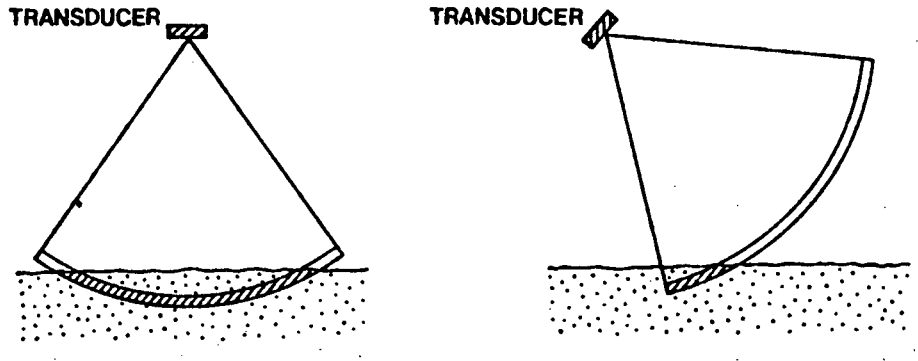

Figure 6.6 Intersection of synthesized fan beam with sea bed (a) echo sounding mode; (b) sidescan mode.

After synthetic aperture processing,the resolution cell is as shown in Fig. 6.6(b). Essentially, the geometry is the same as in Fig. 6.6(a) except that, because the transducer is now tilted sideways, the sensitivity to targets directly beneath the transducer is greatly diminished. The dominant echoes may be expected to come in from the side and, because of the sediment attenuation, they may be expected to rise in the top metre or so of the sediment. The volume making a significant contribution to the return signal at any instant now becomes relatively small and, because of this, the reconstructed image becomes much more amenable to interpretation. As mentioned in Chapter 4, this mode of operation has a further big advantage, in that a greater mapping rate is achievable.

The effect of this sidescan mode of operation on the transmission coefficient and refraction at the sediment boundary needs to be considered. Figure 6.7 illustrates the ray paths followed by signals arrriving from a number of different buried targets.

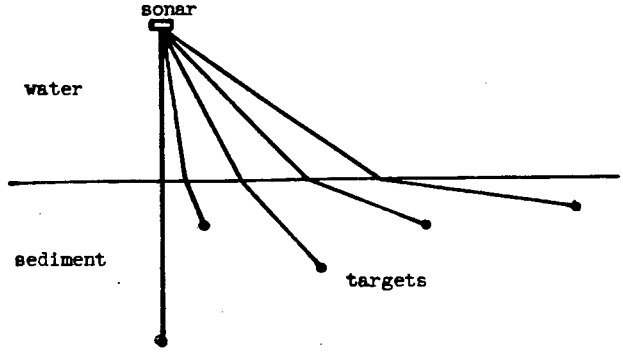

Figure 6.7 Ray paths from buried targets.

The most important point to note is that if the target is at a large slant angle, the path length through the sediment is long even when the target is at a shallow depth. Thus deeply buried targets and targets at large slant angles will be difficult to detect. It is thus likely that the area which may be mapped will be limited to aperture-target angles of approximately 45^{o} for typical sediments(see p. 5.4), and modest penetration depths. Both these limitations will depend upon sediment type, but need not be a serious limitation on the usefulness of the technique. For this range of slant angles, the restriction on aperture length caused by refraction (Section 5.2) will remain largely unchanged. The mapping rate will be improved by using the transducer close to the surface, as this will increase the useful sub-bottom area insonified. The attenuation of the signal within the water will be small compared to that within the sediment, so this mode of operation will not degrade the signals. Considering a typical operating depth of 20m, the maximum horizontal range is then also 20m. It will be very difficult to infer the horizontal range of targets beneath the sonar at very large declination angles and a useful image swath might therefore extend from perhaps 5m to 20m of horizontal range. The realisation of a 7m synthetic aperture will be sufficient to achieve a resolution equal to 1m at the greatest slant range. It should be noted that refraction will lead to an uncertainty about the depth of the object. This discrepancy will be no more serious than the uncertainty caused by the lack of knowledge about the elevation angle of the target.

In spite of the reduced sensitivity and high sediment attenuation in the vertical direction attained by this mode of operation, the large reflections from strata may still dominate the return signal. In order to diminish still further the returns from beneath the transducer, a pressure release reflecting baffle was used beneath the transducer. This was in order to shadow from the transducer that part of the bed of the reservoir directly beneath it. An A/D unit was

obtained which enables 60k of samples to be stored. This enabled 12m of range to be stored with aperture positions spaced 4cm apart.

As an example of the performance of the system Fig. 6.8(a) shows the unprocessed amplitude data collected using the low frequency transducer. Figs. 6.8(b) and 6.8(c) show the reconstructed images obtained over a 4m along-track distance using aperture lengths of 2m and 4m respectively. For the 4m case, the complete aperture data is used for all the points in the image, ie. the beam is focused and steered to each point in the image plane. For the case of a 2m aperture where 4m of data is available, the section of the data used is moved (Fig.6.9). The central 2m of the image is obtained by selecting the appropriate section of the data and using focusing but no beam deflection. The outer 1m parts of the image are obtained by deflecting the beam. A comparison of Figs. 6.8(b) and 6.8(c) clearly shows that the detail of the images is improved as the aperture size is increased.

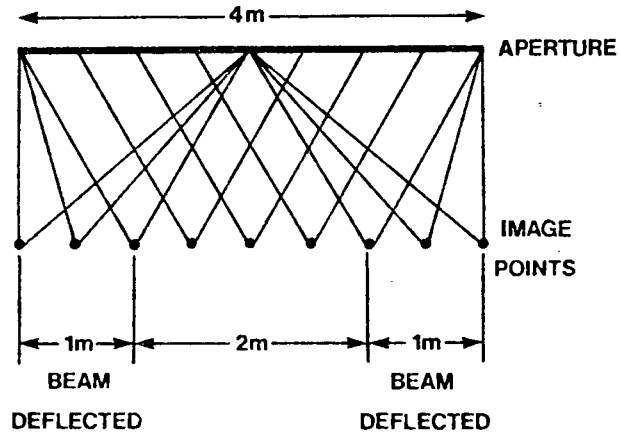

Figure 6.9 Use of data for image reconstruction.

In order to establish whether bottom penetration had been achieved, these images were compared with images obtained using a conventional 300kHz sidescan system where only surface structure can be expected. Such an image is shown in Fig.6.10(a). The transducer was pointing slightly forward of the broadside direction and hence there is a slight displacement of the image compared with that of the 4m

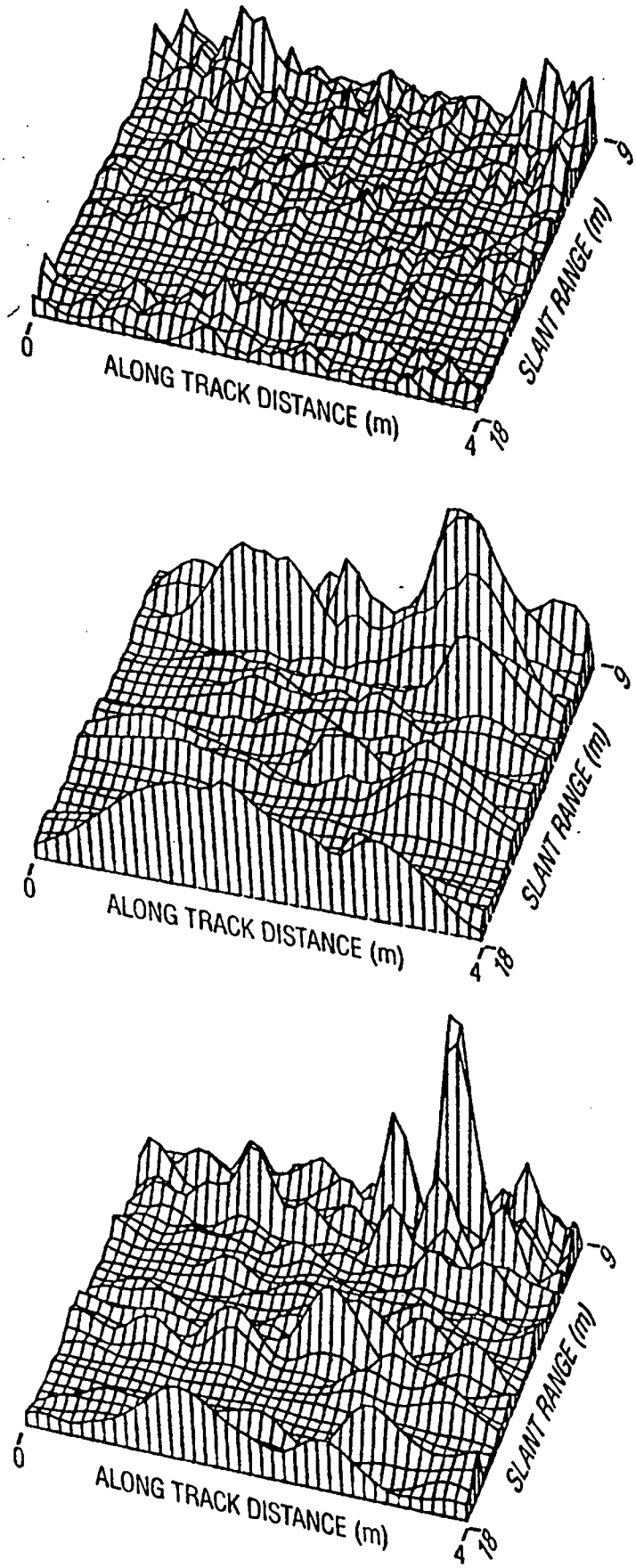

Figure 6.8 Images at reservoir site: (a) unprocessed data; (b) 2m. synthetic aperture; (c) 4m. synthetic aperture.

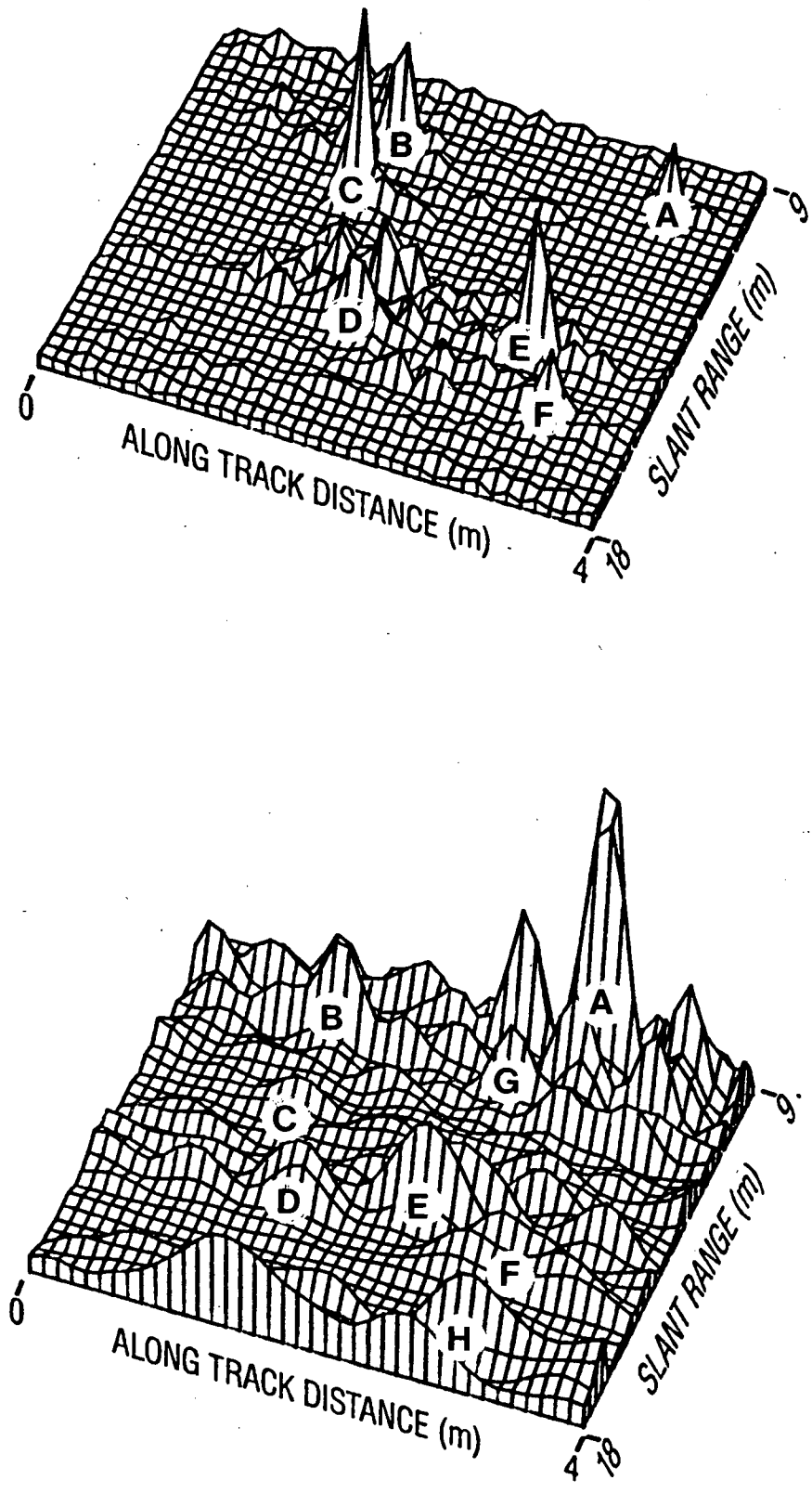

Figure 6.10 Images at reservoir site: (a) 300kHz sidescan; (b) 4.5kHz synthetic aperture.

synthetic aperture image which is repeated in Fig. 6.10(b). Comparison was aided by the marking of six targets A to F, which are common to both images. The differences in the relative strengths of these targets between these two images may be due to the difference in sensitivities at the two frequencies to the submerged parts of these targets. Particularly different in this regard is target C. It is thought that this object is a rock on the bottom, but with no part buried. Hence although it appears as a strong target at high frequencies, its lack of buried volume means that at low frequency it is not as strong a target as others with both buried an unburied parts. The areas marked G and H in Fig. 6.10(b) are not apparent in Fig. 6.10(a), thus suggesting that these targets are completely buried. Unfortunately, it was not possible to back up this conclusion by visual observations of the bed of the reservoir as the water was very dark.

6.4 SUMMARY

The results shown in this chapter have demonstrated how fine resolution images can be achieved using synthetic apertures. Some evidence of penetration has been presented. It was however only possible to generate short apertures, and thus the versatility of synthetic aperture processing has not been fully demonstrated.

CHAPTER 7 SEA TESTS

In order to realise longer apertures and to test the system under realistic operational conditions, tests were carried out at sea. The experiments were conducted from the I.M.T. research vessel the 'Shirley T'.

7.1 EXPERIMENTAL PROCEDURE

The system as used at the reservoir remained essentially unchanged. In order to realise the longest possible apertures, with the storage capacity available, the prf and ship velocity were chosen in order to achieve aperture samples spaced just less than $\lambda/2$ apart. This is the maximum aperture sample spacing that ensures the avoidance of grating sidelobes for broadside beams. 64 samples, 160μs apart were stored at each aperture position. This enabled an 8m range gate to be sampled. Using the full 60k of available storage capacity, 450 aperture positions were stored during each run. Based on an aperture spacing of 15cm. this meant that a track of approximately 70m could be imaged. The prf was chosen as 116ms, thus necessitating a ship velocity of less than 1,3m/s (2,6 knots)in order to avoid under-sampling of the aperture. This is fairly slow, and the achievement of long coherent apertures requires calm sea conditions.

The transducer was mounted rigidly between the two hulls of the boat. Due to water-resistance, the pressure release baffle, as used at the reservoir, was dispensed with. This was not a serious problem, as the sea-bottom was further away from the transducer than in the reservoir case.

Experimental data was collected over two days, and stored on floppy diskettes. Two areas were surveyed.

(1) an area known to contain semi-buried concrete pillars

(2) the semi-buried wreck of the Clan Stuart in Simonstown Bay.

For each experiment the return echoes were observed on an oscilloscope and the range interval of interest selected by means of an adjustable potentiometer. This selected the range interval to be stored. The transmitter power was then adjusted to realise a reasonable signal on the in-phase and quadrature outputs of the demodulator. The boat velocity was determined by the boat's taffrail log. This was maintained constant whilst signals were being recorded. Data storage was contolled by HP 86 computer, and was started by depressing a key on the computer. Data storage continued until the full aperture had been traversed. The data was then stored on floppy disk for later use in reconstructions. The storage was in the form of one byte per number, as read in from the A/D, for optimum transfer speed and storage usage.

Back at U.C.T. the data was read off the disk, and converted into amplitude and phase information ready for transfer to the UNIVAC computer. This conversion and transfer procedure was lengthy, and took approximately seven hours per data set. Once on the UNIVAC computer, the generation of synthetic apertures could be carried out.

7.2 RESULTS

The concrete pillars, mentioned in the previous section showed as the stongest echoes on the raw data, hence these were imaged first. With little knowledge of the true detail being imaged, it was necessary to develop techniques of deciding whether the image was genuine or not. If the image is genuine, two factors should demonstrate this. Firstly the image should improve in quality as the aperture length is increased. Theoretically this should proceed until the maximum aperture length for which the target is insonified is reached(Chapter 2), but in practise it will be limited by transducer path irregularities. Secondly the image generated by using beams steered to different squint angles should be similar. They may not be identical because faceted targets may be present, and these will be more visible from certain angles.

When processing, using the velocity as determined from the boat's log, it was found that the image quality did not improve with increase in aperture length. This indicated that the coherence length of the signals was very short. There was poor correlation between images obtained by viewing the same area from different angles(Figure 7.2a). The dominant feature appeared to be displaced between two such angles. Also, certain sharp peaks visible from one angle were not visible from another. This might be expected from a large specular type reflector. The extent of these sharp peaks did not however suggest that the targets were large. Careful consideration of the focusing procedure, showed that this type of behaviour was consistent with that which may be expected when the processing assumes an incorrect boat velocity.

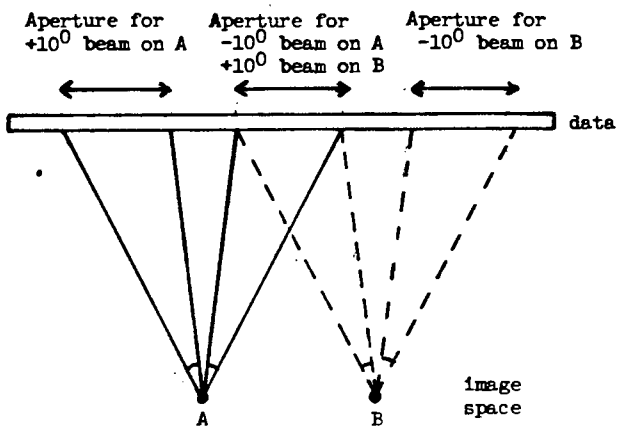

Figure 7.1 Use of data to realise different squint beams.

The use of the data to achieve beams at different squint angles is illustrated in Figure 7.1. Figure 7.2 shows images realised by using beams at squint angles fore and aft of the broadside direction. In this manner the same image point in each picture is imaged using entirely different data. The effect of an incorrect boat velocity is that the two images are dissimilar. An iterative procedure was adopted in which the assumed velocity was changed until the best correlation between images was obtained. By considering the best comparison, a boat velocity of 1.6 m/s was arrived at. This is 45% greater than the measured velocity of 1.1m/s. This discrepancy is thought to be due to one or both of two

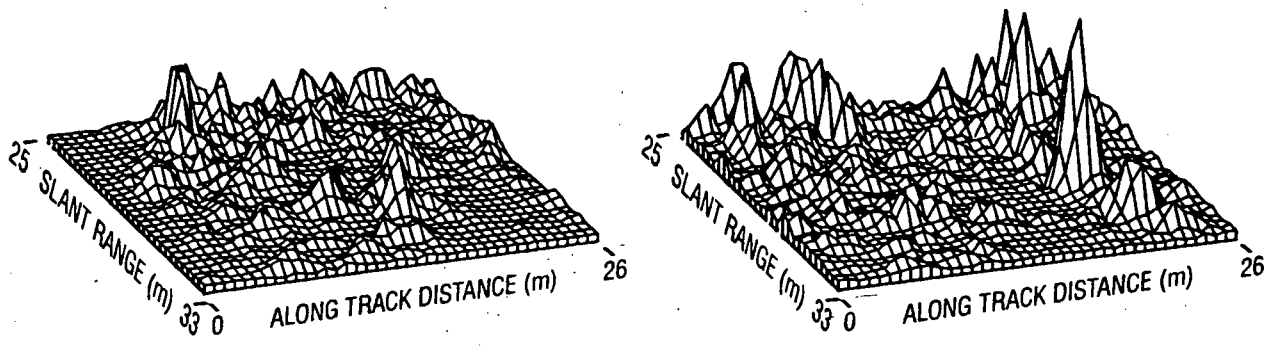

(a) (i) (ii)

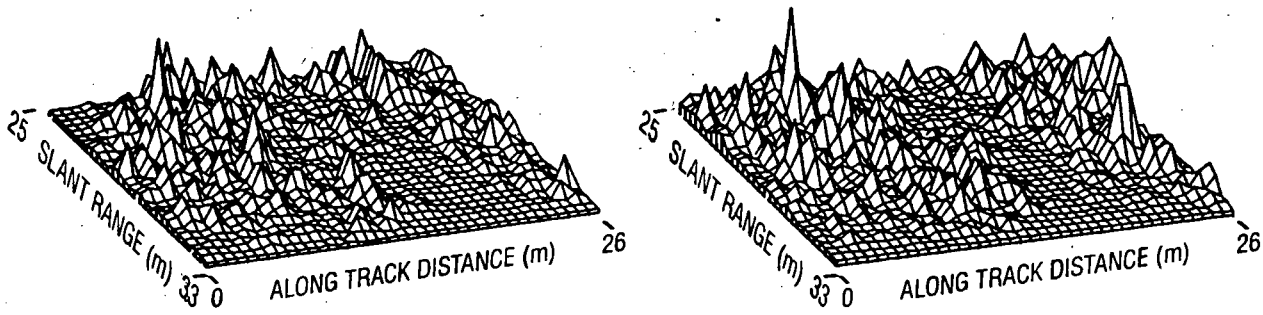

(b) (i) (ii)

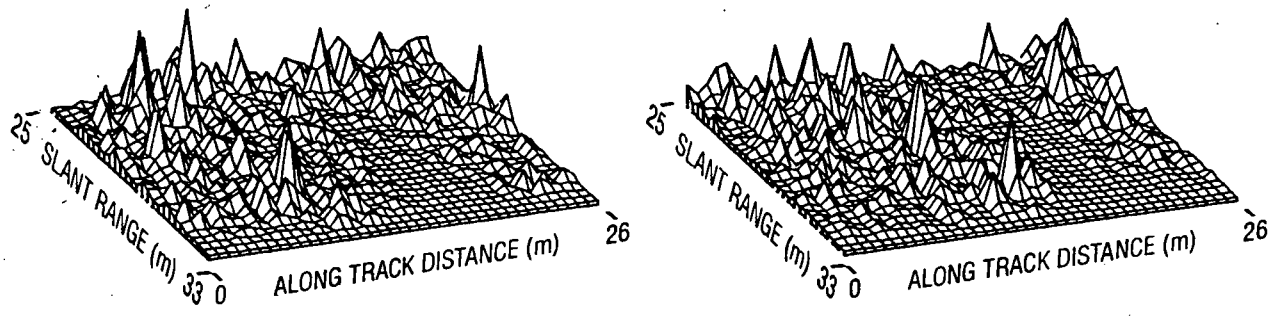

(c) (i) (ii)

Figure 7.2 Views of same area, using synthesized beam steered fore and aft of the boat, for various assumed boat velocities. (a) 1.1m/s (as measured by boat's log); (b) 1.6m/s (best comparison of images); (c) 2.0m/s

effects:

(1) low reading of the instrument due to boundary layer or turbulence effects that are more pronounced at low velocities.

(2) The ground-speed may have been different to the water speed due to the presence of a current.

Based upon this value of 1,6m/s, it followed that the received signals were recorded every 19cm. over total track lengths of 85m. The 19cm. corresponded to a theoretical prediction of grating sidelobes at 60^{o} for a broadside beam. The sensitivity of the physical transducer was well down at this angle. The grating sidelobe levels for large angles of steer may however be high.

One of the practical problems encountered in these sea trials was a very strong acoustic interference signal, attributed to the transmit signal undergoing multiple reflections between the hulls of the boat and returning to the transducer to overlap the wanted echoes. This acoustic interference was therefore confined to the broadside direction. The problem was overcome by forming a squint beam in the reconstruction processing which was insensitive to the broadside interference.

Unprocessed data corresponding to the area near the semi-buried pillars is shown in Fig.7.3a. No meaningful feature can be seen. The remaining images of Fig.7.3 are reconstructions of the same area using different lengths of apertures and a beam which is steered 10^{o} ahead of broadside. Considerable feature is now apparent, with the image quality being improved by increasing the aperture length from 4m to 8m but not when going from 8m to 12m. The processing incorporated a Hamming amplitude shading function as given by $W(z) = 0.54 + 0.46 \cos(2\pi z/L_e)$. This was done because the natural shading of the targets as discussed in Chapter 6, was no longer effective at the increased ranges.

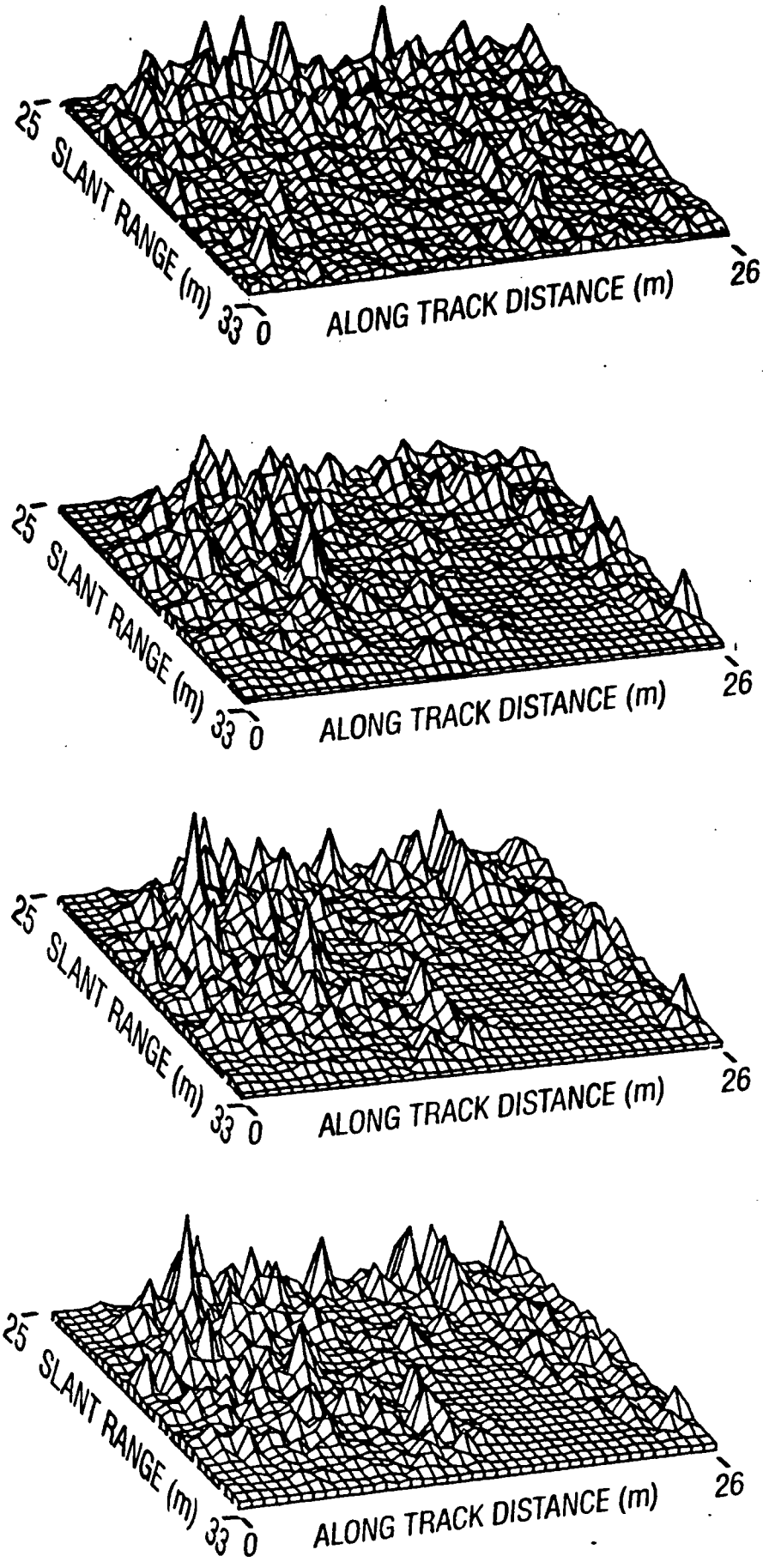

Figure 7.3 Images of sea bed at 10° squint angle:
(a) unprocessed; (b) 4m. synthetic aperture;
(c) 8m. synthetic aperture; (d) 12m. synthetic aperture.

The resolution achieved by the aperture may be found by measuring the half power width of the peaks in the reconstructions. This width is difficult to determine in Figures 7.3, as the grid spacing is too large. Thus Figure 7.4 shows reconstructions of a blown up portion of the area depicted in Figures 7.3 for different lengths of aperture. It would appear as though the sharpness of some peaks (eg. the peak labelled A in figure 7.4d) improves for aperture lengths of up to 18m. For the 18m aperture, the resolution as measured from peak A is 40cm which compares favourably with the theoretical prediction of 30cm (Eq 2.3). It is however noticeable that certain peaks (eg. the one marked B on Figure 7.4a) do not improve in sharpness as the aperture size is increased, and in fact are narrower than expected for short apertures. A plausible explanation for this is suggested later in this chapter.

A similar analysis to that undertaken for data obtained at the concrete pillar site, was carried out on a set of data collected viewing the wreck of the Clan Stuart. Firstly images were obtained using two different beams (steered fore and aft). The assumed boat velocity was varied to find the best comparison between the two images. Figure 7.5 shows a collection of such images. The 'best' comparison is obtained for an assumed velocity of 1.4m/s which is 40% greater than the measured velocity of 1.1m/s. This is a similar deviation to that determined in the earlier case. It would thus seem likely that the reading on the ships log is inaccurate, probably because of boundary layer or turbulence effects at low velocities. Even these 'best' images have many differences between them. Particularly for the large amplitude peaks at short range, there are inconsistencies between the two images. Reconstructions using different aperture lengths showed a similar effect to that mentioned earlier, in that many peaks were sharper than expected for images reconstructed using short apertures.

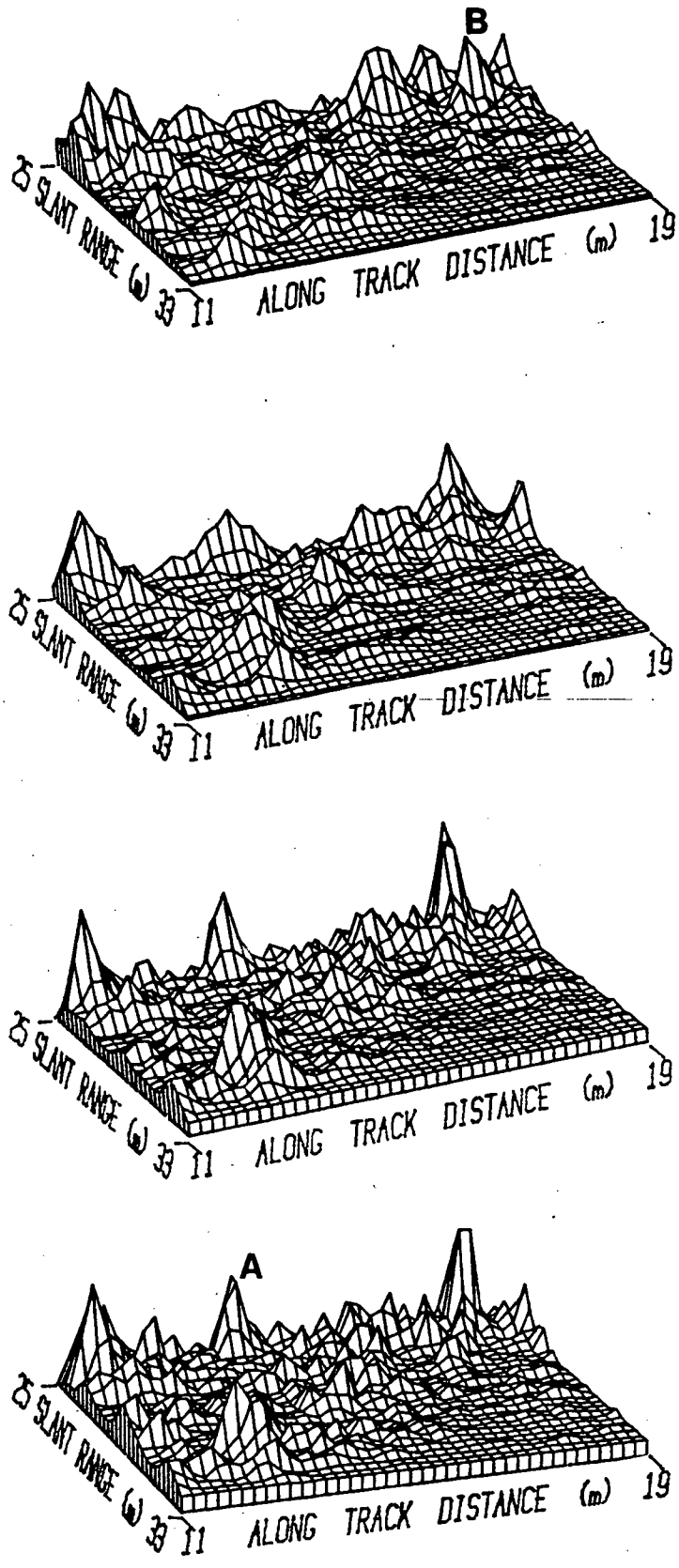

Figure 7.4 Images of sea bed at 10° squint angle (expanded view). (a) 2m aperture; (b) 6m aperture; (c) 12m aperture; (d) 18m aperture.

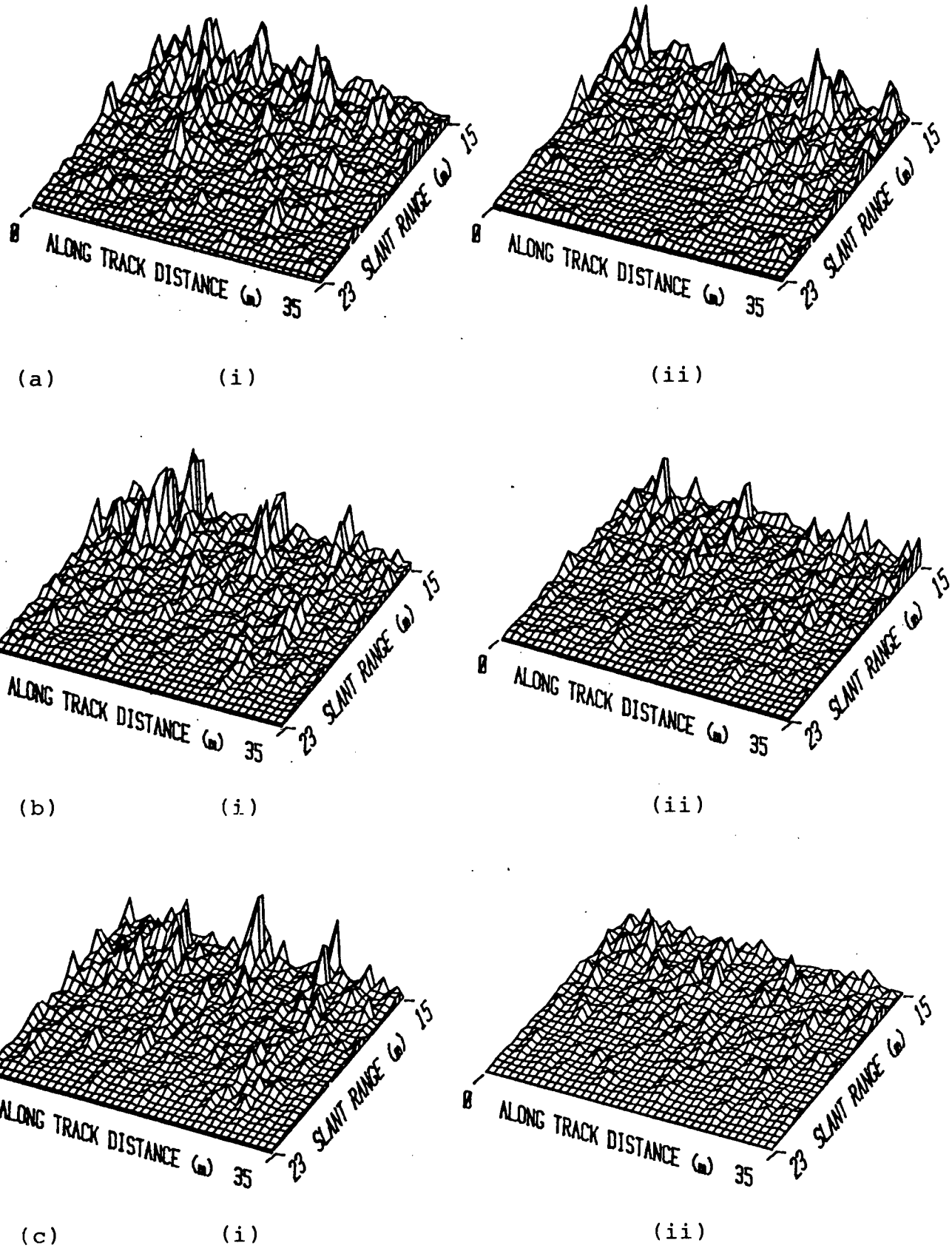

Figure 7.5 Views of same area, using synthesized beams steered fore and aft of broadside, for various assumed boat velocities (a) 1.0m/s (as measured by boat's log); (b) 1.4m/s (best comparison of images); (c) 1.6m/s

7.3 LARGE TARGETS AND IMAGE SPECKLE

These results led to a consideration of the types of targets being imaged. The focusing procedure assumes that any target may be considered as a collection of discrete point targets. This is however often not the case. Real targets will have large dimensions. In particular there are likely to be flat specular type targets present. These targets will appear much stronger when viewed from a particular angle.

Consider again the images presented in Figure 7.2(b). The appearance of two distinct groupings of targets suggests that the dominant reflectors may in fact be two large objects. Knowing that the area contains concrete pillars, it seems likely that the two dominant reflectors are the faces of two such pillars. This interpretation is supported by the observation that the image constructed using a beam steered to an angle of -10^{o} (Figure 7.2b(ii)) has more energy apparent than the image generated using a squint angle of $+10^{o}$ (Figure 7.2b(i)). This may be explained if the pillars are facing at an angle away from the broadside direction (Figure 7.6). Thus an interpretation of the major structure is that there are two large specular type reflectors present.

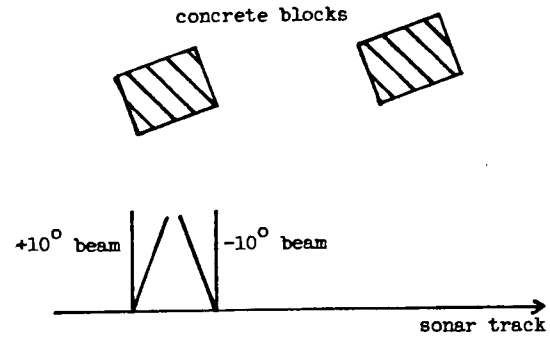

Figure 7.6 Suggested orientation of two concrete blocks.

If the targets were truly specular, it would be expected that the reconstructed image would be regular in appearance (Figure 7.7a). This is however not the case, as there are rapid fluctuations in strength of the returned signal across the pillars. If a large, flat, homogenous target is considered as

a rough surface, it may be treated as a dense collection of equal amplitude point targets at slightly different ranges from the aperture. This will be called a distributed target. The signal received by a beam insonifying such a target will be a complex combination of the returns from those point targets within the beamwidth (Figure 7.7b). Depending upon whether the individual echoes interfere constructively or destructively there will be fluctuations in the signal strength, as was observed. These fluctuations will be more severe for narrower beams, because fewer point targets are within the beam width, and hence the fraction of targets changing as the beam is moved is greater than is the case for a wider beam. There will however be variability for all beams, as the relative positions of these point targets to the sonar will change as the sonar is moved.

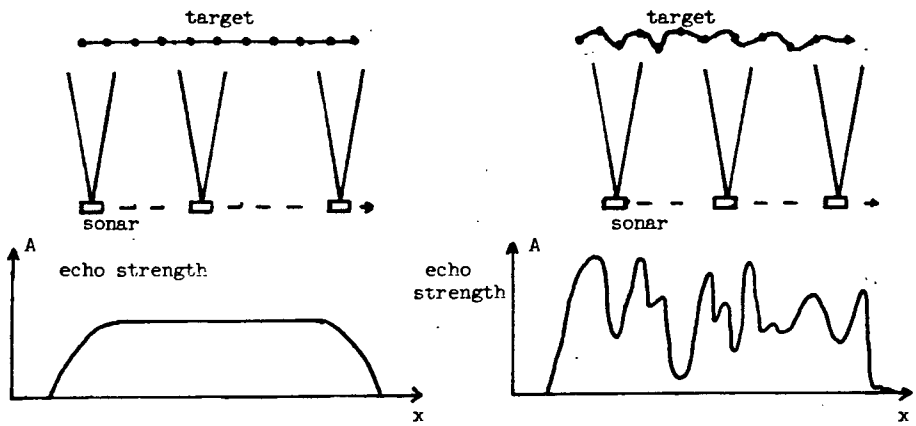

Figure 7.7 (a) specular target; (b) distributed target. Physical picture and sonar returns.

This effect is well known in radar[1,2] as 'image break-up' or 'image speckle'. A particularly graphic illustration of image speckle may be found in a treatment by computer simulation[1]. It is suggested that not all targets present in Figures 7.4 are distributed in nature. There are targets that improve in resolution as the aperture length is increased (eg. the one marked A). This suggests that A is a point like target. Point targets,because of their size, generally give a weaker return echo than distributed targets. Hence they will be less noticeable than distributed targets, when the latter are present.

The effect of image speckle may be reduced by making use of non-coherent processing. By non-coherently combining the images from different beams directed at the same area, the effect may be smoothed. These 'different' beams may be realised using different frequencies, or different squint angles. In synthetic aperture radar imaging it it is common to split the aperture up into a number of smaller apertures, which are then summed[3]. The criterion for best performance is now not the achievement of the sharpest peaks, but rather the best looking image. Unfortunately the reduction of the individual aperture lengths leads to a degradation in resolution but this is compensated for by an improvement in image quality.

The technique of incoherently summing different squint beam images of the same area is well suited to synthetic aperture sonar use. Preliminary work in this regard has been carried out. Due to knowledge of the targets present, the area containing the concrete pillars was used. Figures 7.8(a) and 7.8(b) show two different views of the same area using 6m apertures. Figure 7.8(c) is the image realised by incoherently summing four such images, each overlapping the previous one by 3m (Figure 7.9). Figure 7.8(d) shows the image produced using 11 such beams. The images of the pillars obtained using multiple beams are less 'spiky' in nature than those achieved using single beams. This indicates that the speckle has been been reduced. Comparison of the images using different numbers of short sub-apertures is aided by comparing images of a larger area. These are presented in Figure 7.10. Again, if the spikiness of the pillars is used as a yardstick, the image obtained using eleven sub-apertures is less 'speckled' than that obtained using only four sub-apertures. Further work is necessary in order to determine the optimal trade off between coherent and incoherent use of the aperture.

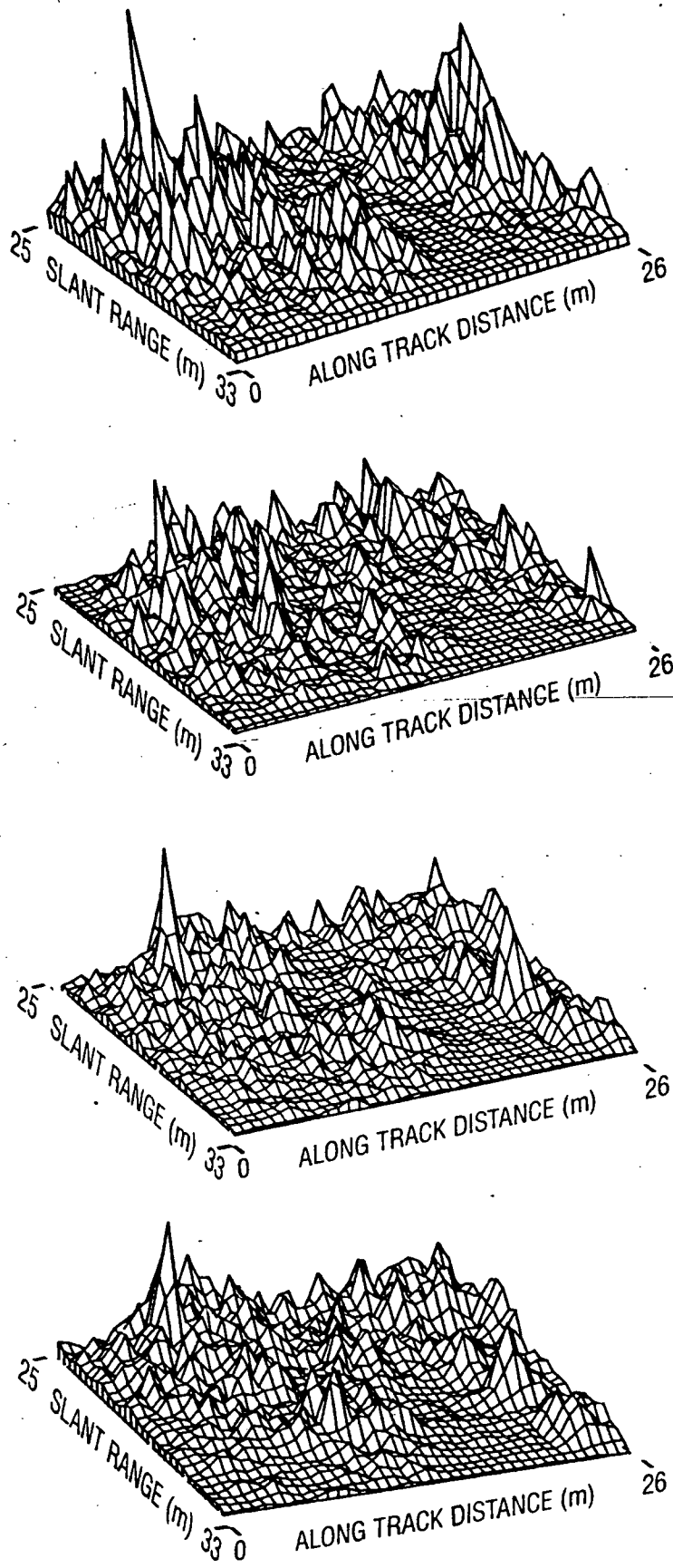

Figure 7.8 Speckle reduction by incoherent summation of apertures. (a) 6m aperture steered -10^{o}; (b) 6m aperture steered $+10^{o}$; (c) sum of four 6m apertures; (d) sum of eleven 6m apertures.

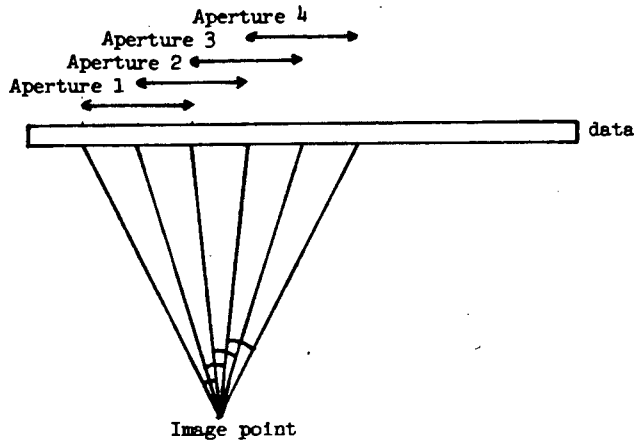

Figure 7.9 Use of aperture to form four sub-apertures, each overlapping the previous one.

It would appear that two options in data usage are available. The first is to realise the longest possible aperture. This will be limited by coherence problems. Incoherent summation of this length of sub-aperture would then be carried out. The second possibility is to select a desired resolution, and use the length of aperture necessary to achieve this as the sub-aperture. It is likely that the optimal aperture usage will depend on the type of objects being imaged, so some form of adaptative processing may be used.

7.4 SUMMARY

Synthetic apertures capable of realising a resolution of less than one metre have been successfully implemented at sea. It has been found that the optimal method of using the full aperture length is likely to be to split it up into a number of small focused sub-apertures, and then non-coherently combine the outputs of several of these sub-apertures.

The achievement of penetration has not been proved. However, based on the frequency being used, and the reservoir results it seems likely that penetration is being achieved. Work using a known buried target in an area free of surface feature is necessary to further investigate the technique.

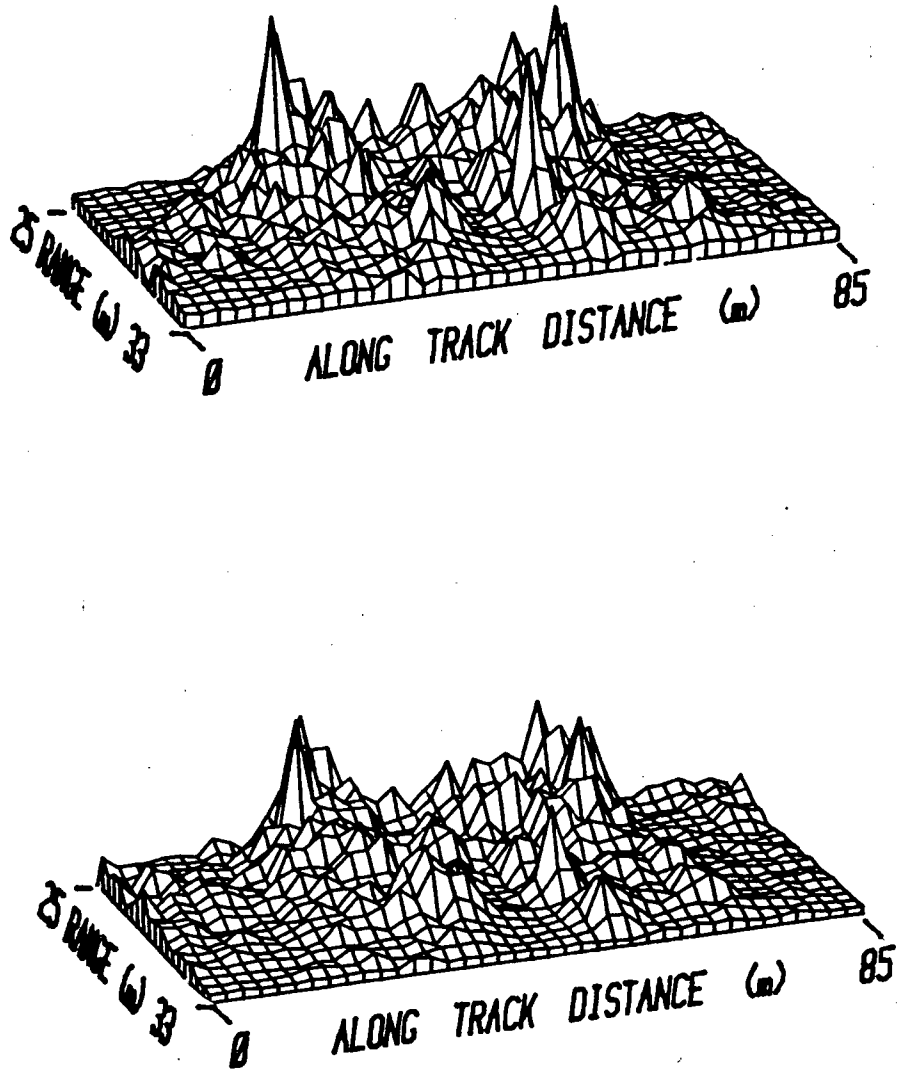

Figure 7.10 Speckle reduction by incoherent summing of many apertures. (a) sum of four 6m apertures;
(b) sum of eleven 6m apertures.

References

1. R.Mitchell, "Models of extended targets and their coherent radar images" , Proceedings of IEEE, Vol. 62 No.6, 754-758(1974).

2. R.K.Moore, "Trade off between picture element dimension and non-coherent averaging in sid-looking airborne radar", IEEE Trans., Vol. AES-15, 697-708(1978).

3. M.I.Skolnik, Introduction to Radar Systems, McGraw-Hill International Student Edition(1981), Chap. 14

CHAPTER 8 CONCLUSIONS

The use of synthetic apertures for sidescan imaging at low frequencies has been demonstrated. Coherent aperture lengths of up to approximately 10m have been achieved under calm conditions at sea. This length of aperture yielded a resolution of less than one metre at 30m range. With less ideal sea conditions, the coherent aperture length is likely to be seriously limited due to tossing and heaving of the mother boat. By mounting the transducer in a towed fish, rather than directly to the boat, longer coherent aperture lengths should be realisable. In practice however, a lack of very long coherence lengths need not be a disadvantage. The non-coherent combination of a number of short apertures has the advantage of reducing the effect of image speckle, which occurs when large, flat targets are imaged. Further work is necessary to determine the optimal trade-off between resolution and speckle reduction. It is likely that this will depend upon the type of targets being detected.

Such a low frequency sidescan sonar system would be suitable for use in sub-bottom imaging, as the use of a low frequency aids sediment penetration. A theoretical examination of wavefront distortion at the sediment-water interface indicated that this effect may limit the coherent aperture length that may be realised. By computer simulation it has been established that for targets that are not too deeply buried, the limitation on the aperture length is no more severe than that which is likely to be caused by unwanted transducer motion.

Synthetic apertures generate a narrow fan beam, which may be most effectively used by pointing the transducer sideways. Thus a sidescan mode of operation is employed, as opposed to the depth sounding mode that is usual in sub-bottom profiling. This yields an improved mapping rate, but leads to uncertainty as to whether feature observed is on the bottom or sub-bottom. By using a high frequency sidescan sonar in conjunction with

the low frequency synthetic aperture sonar, bottom feature may be extracted, thus realising sub-bottom detail. Such an arrangement was used at the reservoir site, with indication that feature evident in the low frequency image, but not visible at higher frequency, was sub-bottom feature. Unfortunately this arrangement could not be adopted for the sea tests, and further work is necessary to establish the degree of penetration achievable.

The use of synthetic apertures has a number of significant advantages over the use of parametric arrays for sub-bottom imaging.

1) For an equivalent acoustic power, the power requirements of the source is much lower for the conventional transducer used in the synthetic aperture than for the parametric array sources.

2) Synthetic apertures create narrow fan beams, whereas the beam achieved by a parametric array is a narrow pencil beam. By using a fan beam in a sidescan configuration, it is possible to achieve a significant greater survey rate than by using a pencil beam.

3) Synthetic apertures rely on data storage and processing for the realisation of narrow beams. The storage of information means that a number of different beams may be focused on the same image point, thus easing the interpretation of the images. With a pencil beam, only one view of the same area may be realised.

It seems that a synthetic aperture sidescan sonar system could be used for shallow penetration sub-bottom imaging. System operation would be improved by mounting the transducer in a fish towed close to the surface. A large amount of data storage and processing is required. This requires the use of a mainframe computer, and the realisation of real-time images may be difficult to achieve.

BIBLIOGRAPHY

BERKTRAY, SMITH, BRAITHWAITE, WHITEHOUSE, "Sub-bottom profilers using parametric sources", Proceedings of the conference 'Underwater applications of non-linear acoustics', Bath University, Sept. 1979.

BOLUS, SIVAPRASAD, FROST, "A theoretical vertical and lateral model for the analysis of acoustic sub-bottom data through simulation.", J.Acoust. Soc. Am., 67(5), 1512-1522(1980).

BONFIELD D.J, "Synthetic aperture radar real-time processing", IEE Proc., Vol 127(2), 155-162(1980).

BROWN W.M, "Synthetic aperture radar", IEEE Trans. Vol AES-3 No 2, 217-229(1967).

CEEN, PACE, "Acoustic signals in marine sediments due to waterborne parametric arrays.", Proceedings of the conference 'Underwater applications of non-linear acoustics', Bath University, Sept. 1979.

CLAY, MEDWIN, Acoustical Oceanography: principles and applications. ,Wiley(1977).

CUTRONA, LEITH, PORCELLO, VIVIAN, "On the application of coherent optical processing techniques to synthetic aperture radar", IEEE Proc. Vol 54(8), 1026-1032(1966).

CUTRONA L.J, Synthetic Aperture Radar, Chap. 23 of "Radar Handbook", M.I.Skolnik(ed.) McGraw-Hill, New York, 1970.

CUTRONA L.J, "Comparison of sonar system performance achievable using synthetic aperture techniques with the performance achievable by more conventional means.", J.Acoust. Soc. Am., 58(2), 336-348(1975).

CUTRONA L.J, "Additional characteristics of synthetic aperture sonar systems and a further comparison with nonsynthetic aperture sonar systems.", J.Acoust. Soc. Am., 61(5), 1213-1217(1977).

DOBRIN M.B, Introduction to geophysical prospecting., 3rd. Edition, McGraw-Hill(1976).

DODDS D.J, "Attenuation estimates from high resolution sub-bottom profiler echoes", Saclant ASW research conference on ocean acoustics influenced by the sea floor, La Spezia, Italy, June 1980.

DUCK, JOHNSON, GREENLEAF, SAMAYOA, "Digital image focussing in the near field of a sampled acoustic aperture.", Ultrasonics, March 1977.

GOUGH P.T, "Side looking sonar or radar using phase difference monopulse techniques, coherent and non-coherent applications.", IEE Proc., 130(5), 392-398(1983).

HAMILTON E.L, "Compressional wave attenuation in marine sediments.", Geophysics, 37, 620-646(1972).

IKEDA, SATO, "Further examination of synthetic-aperture sonar in a turbulent medium.", J.Acoust. Soc. Am., 68(2),56-522(1980).

IKEDA, SATO, MINAWIDO, FUKUSHIMA, "Image reconstruction for disturbed synthetic aperture sonar data using aperture division.", J.Acoust. Soc. Am. 78(1), 112-119(1985).

JOHNSON, BARNA, "The effects of surface mapping corrections with synthetic aperture focusing techniques on ultrasonic imaging.", IEEE Trans., Vol SU-30(5), 283-294(1983).

KIRK J.C, "Motion compensation for synthetic aperture radar.", IEEE Trans., Vol AES-11(3), 338-348(1975).

KONRAD W.C, "Applications of the parametric source.", Proceedings of the conference 'Underwater applications of non-linear acoustics', Bath University, Sept. 1979.

LEE H.E, "Extension of synthetic aperture radar(SAR) techniques to undersea applications.", IEEE Journal Vol OE-4 No 2, 60-63(1979).

LITTLEWORT G.C, "Wavefront distortion and synthetic aperture imaging.", B.Sc(Eng) Thesis, U.C.T.(1982).

LITTLEWORT G.C, "Sub-bottom profiling and synthetic aperture imaging in sonar.", B.Sc(Hons) Project, U.C.T.(1983).

MARCHISO, HODGKISS, "Deconvolution applied to a near-bottom seismic profiler", J.Acoust. Soc. Am., 72(5), 1478-1491(1982).

MITCHELL R.L, "Models of extended targets and their coherent radar images.", Proc. of IEEE, 62(6), 754-758(1974).

MUIR, HORTON, THOMPSON, "The penetration of highly directional acoustic beams into sediments.", Journal of sound and vibration, 64(4), 539-551(1979).

OHGAKI, SHIMIZU, MIYAZAWA, "Acoustical imaging of an object buried in seafloor sediment using a focused ultrasonic transducer.", J.Acoust. Soc. Am., 67(5), 1603-1607(1980).

SATO, UEDA, FUKUDA, "Synthetic aperture sonar.", J.Acoust. Soc. Am., 54(3), 799-802(1973).

SATO, IKEDA, "Sequential synthetic aperture sonar system- a prototype of a synthetic aperture sonar system.", IEE Trans., Vol SU-24(4), 253-259(1977).

SATO, IKEDA, ENDO, "Combined spectral and aperture synthetic ultrasonic imaging system.", IEEE Trans., Vol SU-28, 64-69(1981).

SKOLNIK M.I, Introduction to radar systems, McGraw-Hill International student edition(1981).

SOMERS, STUBBS, "Sidescan sonar.", IEE Proc., Vol 131(3), 243-256(1984).

TYCE, MAYER, SPIESS, "Near bottom seismic profiling: high lateral variability, anomalous amplitudes, and estimates of attenuation.". J.Acoust. Soc. Am., 68(5), 1391-1402(1980).

WILLIAMS R.E, "Creating an acoustic synthetic aperture in the ocean.", J.Acoust. Soc. Am., 60(1), 60-73(1976).

APPENDIX A SONAR SYSTEM DESIGN

In order to make measurements for use in creating synthetic apertures, it was necessary to design and build a sonar system capable of transmitting a tone burst of carrier signal and recording the received signals in a form suitable for later use in synthetic aperture reconstructions. The design of this system is described in this Appendix. It should be noted that the design described is as implemented in the latest reservoir and sea tests. A number of modifications were made to the system used in the early tank tests. In cases of interest details of the earlier design are included.

Figure A1 shows a block diagram of the sonar system. The implementation of the various blocks are described in the sections that follow.

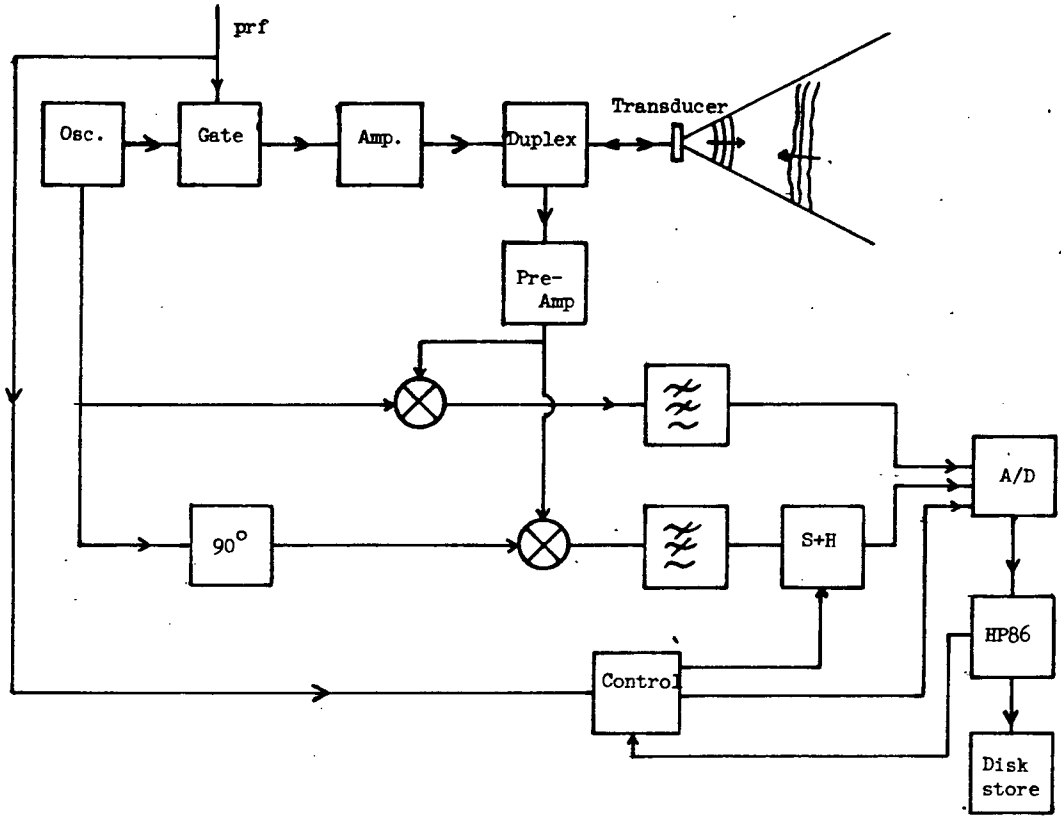

Figure A1 Block diagram of sonar system.

A1 HARDWARE DESIGN

A1.1 TONE BURST GENERATOR

The blocks marked Osc. (Oscillator) and Gate were implemented together. The circuitry used was largely unchanged from that used by Littlewort[1]. A circuit diagram as designed by Littlewort, with a few minor alterations is shown in figure A2. The operation of the tone burst generator will be briefly described. A signal at four times the operating frequency is generated, and then divided down by four to yield the transmit frequency, and divided further by factors of two to yield the prf. The prf may be selected by choosing the relevant output of the counters. The pulse width is controlled by means of an adjustable potentiometer. The design minimizes breakthrough and provides a reference signal for the demodulation into quadrature components as described later. For further details, Littlewort[1] should be consulted.

A1.2 DUPLEXER

The tone burst is amplified by an audio amplifier, and is then applied to the transducer in order to generate the acoustic pulse. Since only one transducer was available, it was used both for transmission and reception of signals. A duplexer was designed in order to apply the transmit pulse to the transducer, and direct the received pulse to the pre-amplifier and then to the demodulator. The design of this duplexer is shown in figure A3.

In order to achieve the maximum received power, it was necessary to match the transducer with an inductance in order to cancel the effect of the clamp capacitance of the transducer. The value of this inductance was calculated from a circle diagram of the transducer, as described in Appendix A2

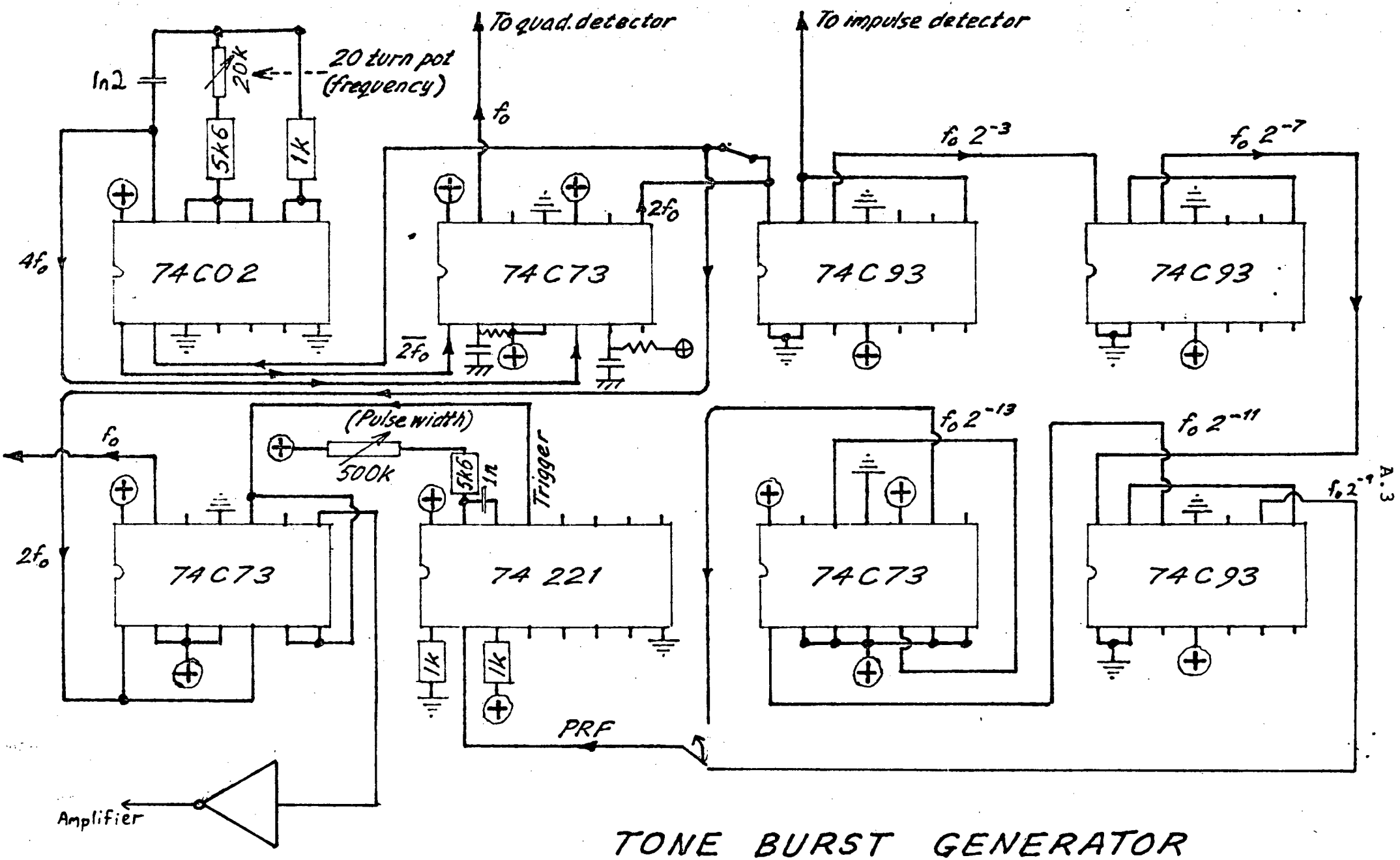

Figure A2: Tone burst generator(Littlewort[1])

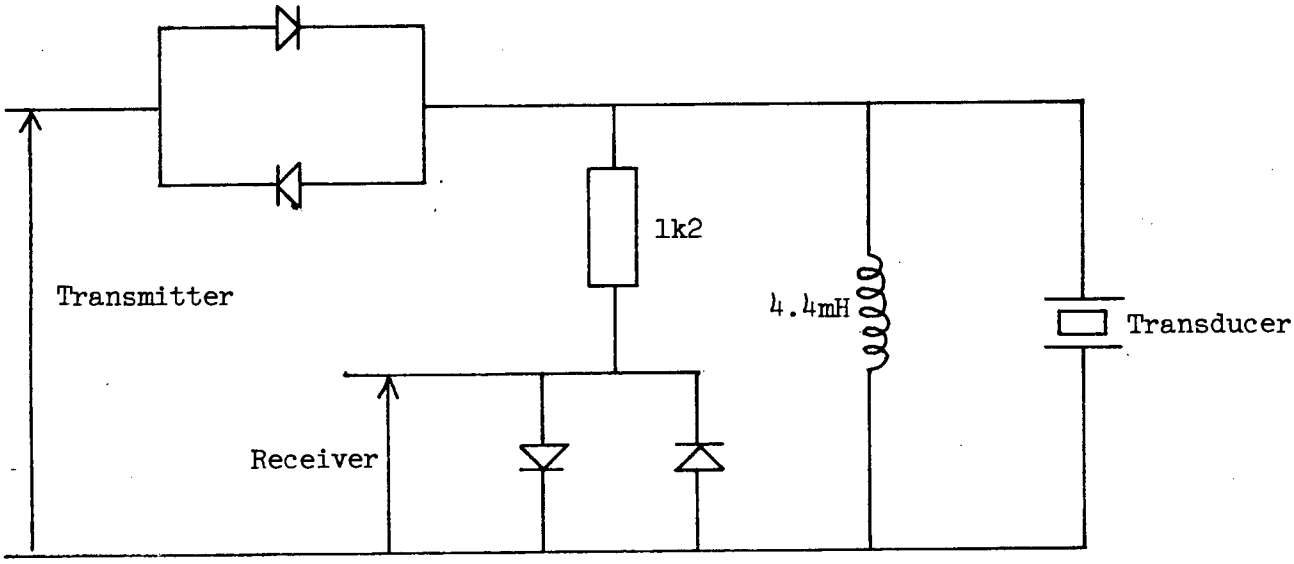

Figure A3 Design of Duplexer.

A1.3 PRE-AMPLIFIER

The received signal was passed through a tuned pre-amplifier with a gain of 60dB. The circuit diagram of this amplifier is shown in figure A4.

A1.4 DEMODULATOR

Demodulation of the received signal produces continuous waveforms of the in-phase(I) and quadrature(Q) components of the signal. These are extracted by multiplying the received signal with the free running oscillator (I component) and a 90^{o} shifted version of the oscillator (Q component). These outputs are then passed through low pass filters in order to remove the sum frequency component which is also produced from such a multiplication.

Again the circuitry is based on the design of Littlewort[1]. The output filters were changed, and the inclusion of a Sample and Hold was necessary because of the recording equipment (See App A1.5). These modifications are included in the circuit of Littlewort as displayed in Figure A5.

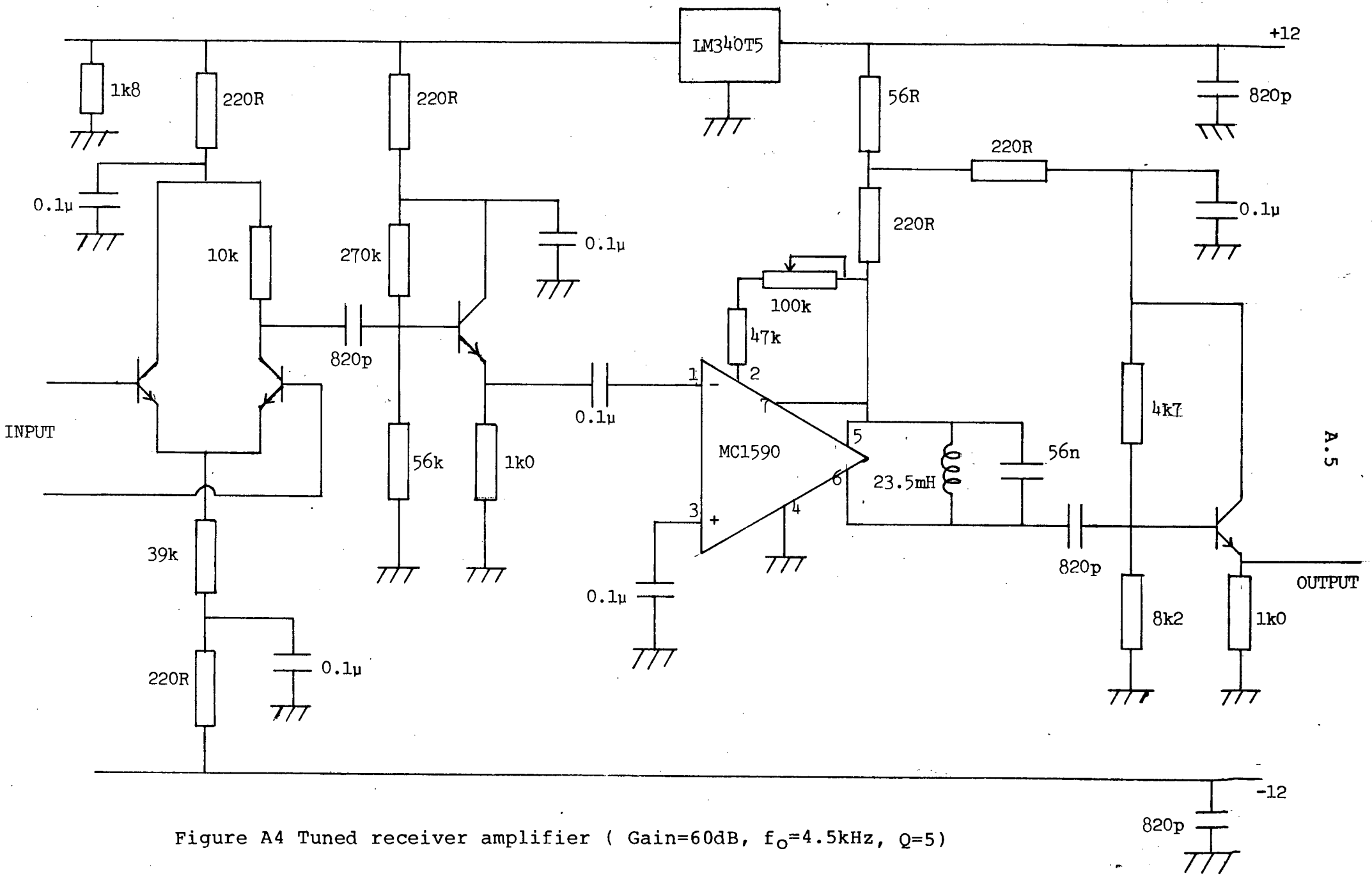

Figure A4 Tuned receiver amplifier (Gain=60dB, f_o=4.5kHz, Q=5)

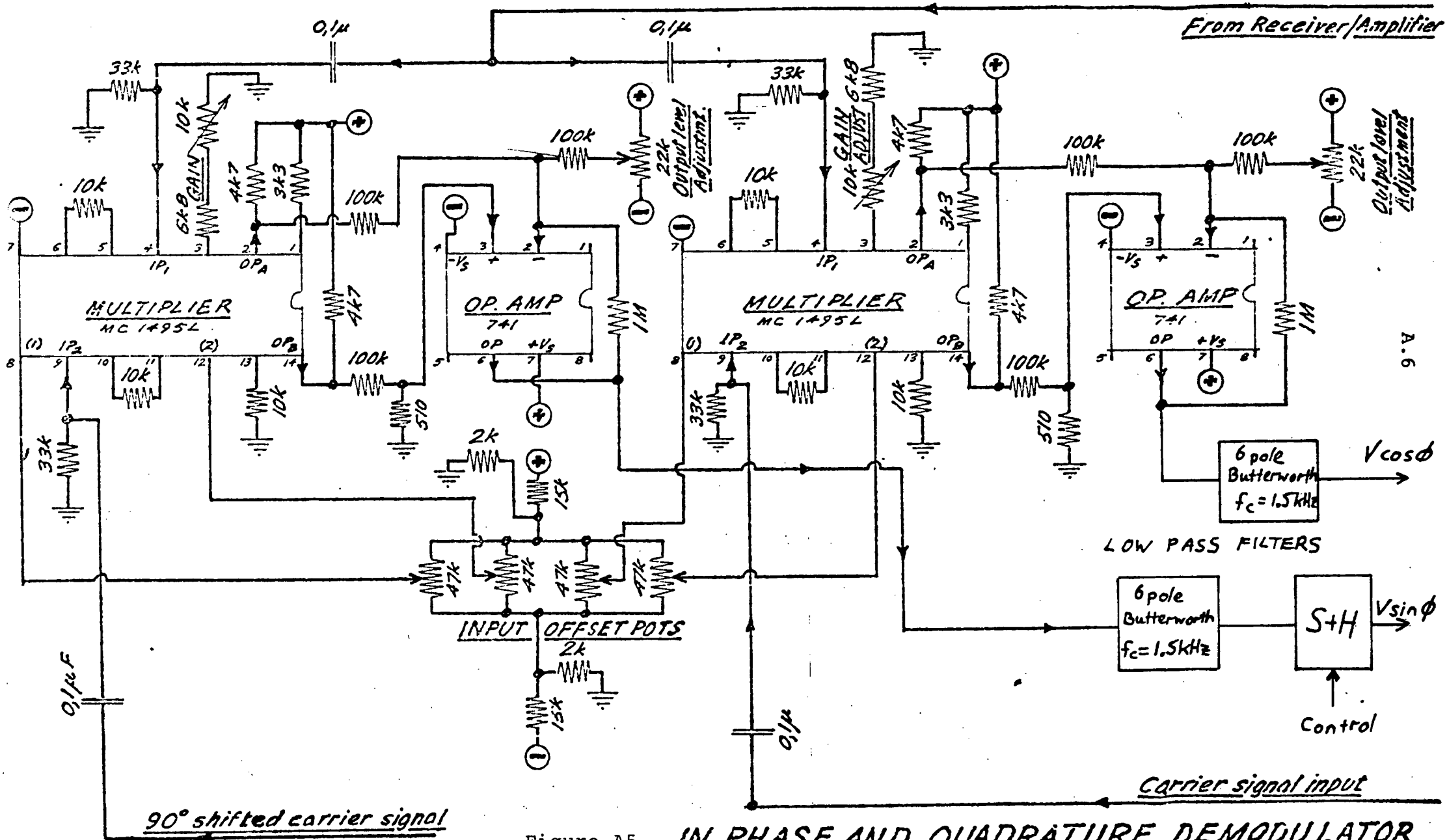

Figure A5 IN PHASE AND QUADRATURE DEMODULATOR CIRCUIT DIAGRAM

G.C.L.

A1.5 CONTROL CIRCUITRY

Because of the limited memory capacity available, and the desire to realise as long an aperture as possible, it was necessary to design clocking circuitry for the A/D. This clocking circuitry enabled a selectable range gate of information to be sampled and stored at each aperture position. The number of samples and sampling rate may be altered, by correct choice of counter outputs. The circuitry detailed is set up to store 128 samples of both I and Q channels at each aperture position. This necessitatesthe generation of 256 clock signals since the A/D sampled each channel alternately. both I and Q components must be stored for each sample. A Sample and Hold is included in the Q channnel in order for the recorded signals to be simultaneous. The control circuit also generates the required signal for the S+H.

The circuit diagram of this procedure is given in figure A6 and timing diagrams of the output signals are shown in Figure A7.

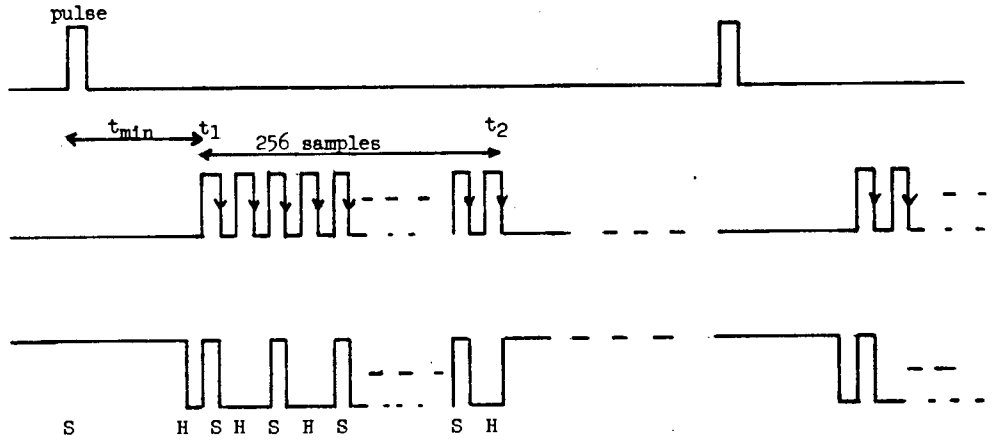

Figure A7 Signal timing (a) pulse at each transmission;
(b) clocking signal;
(c) sample and hold signal.

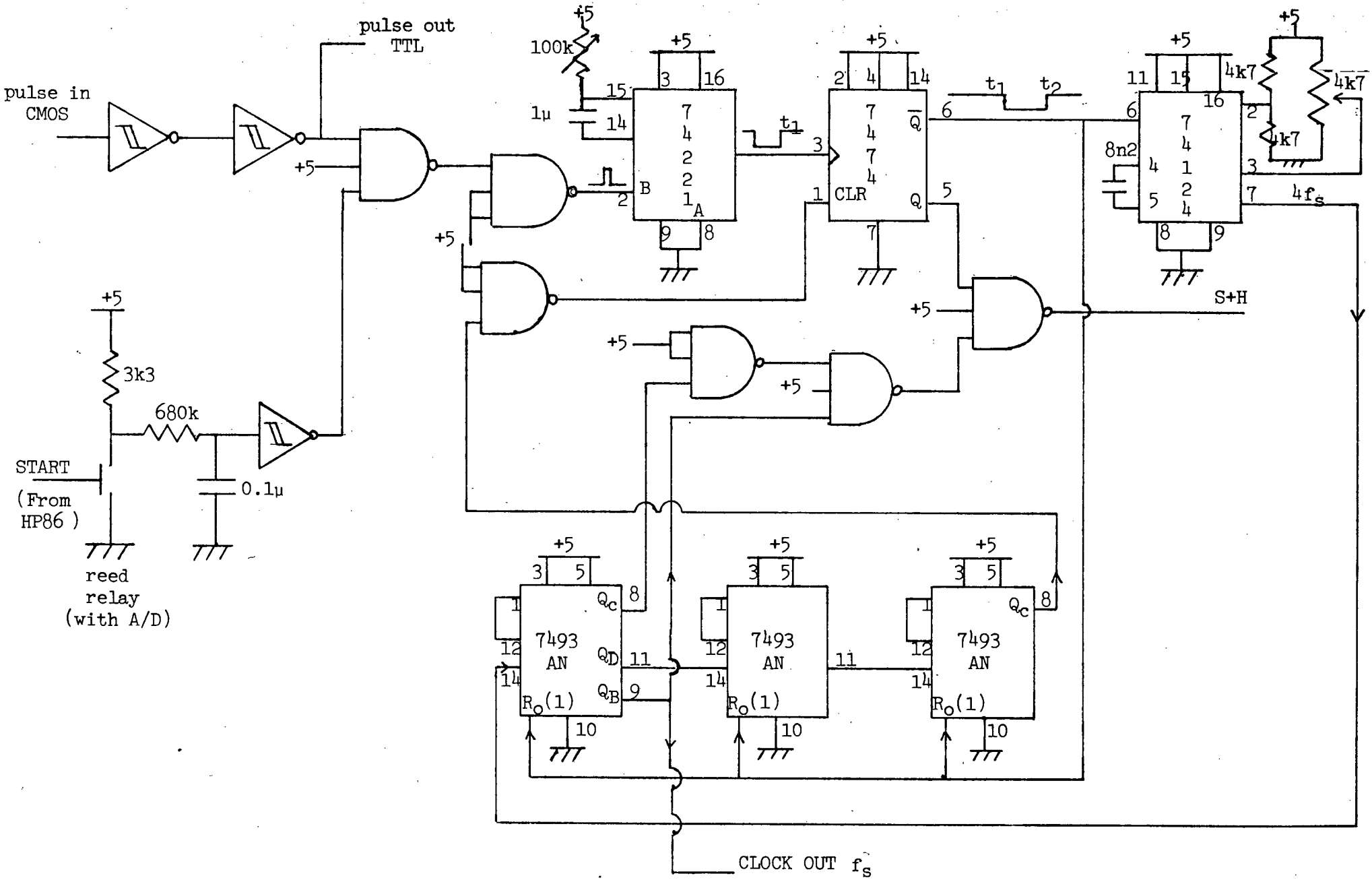

Figure A6 Control Circuitry

A2 DETERMINING TRANSDUCER EQUIVALENT CIRCUIT

A piezo-ceramic transducer may be modelled by the equivalent electrical network shown below:

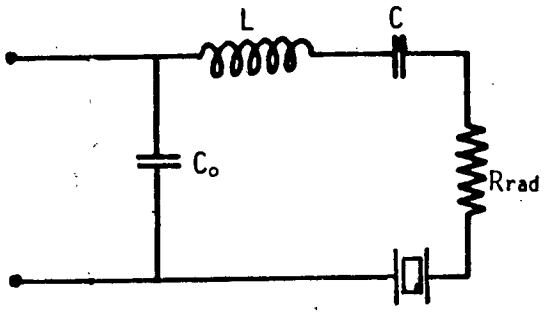

Figure A8 Equivalent circuit of transducer

The values of the various elements may be determined from a 'circle diagram' of the transducer. This diagram is a plot of susceptance against conductance for various frequencies. Such a circle diagram of the 200kHz transducer used for the tank tests is shown below.

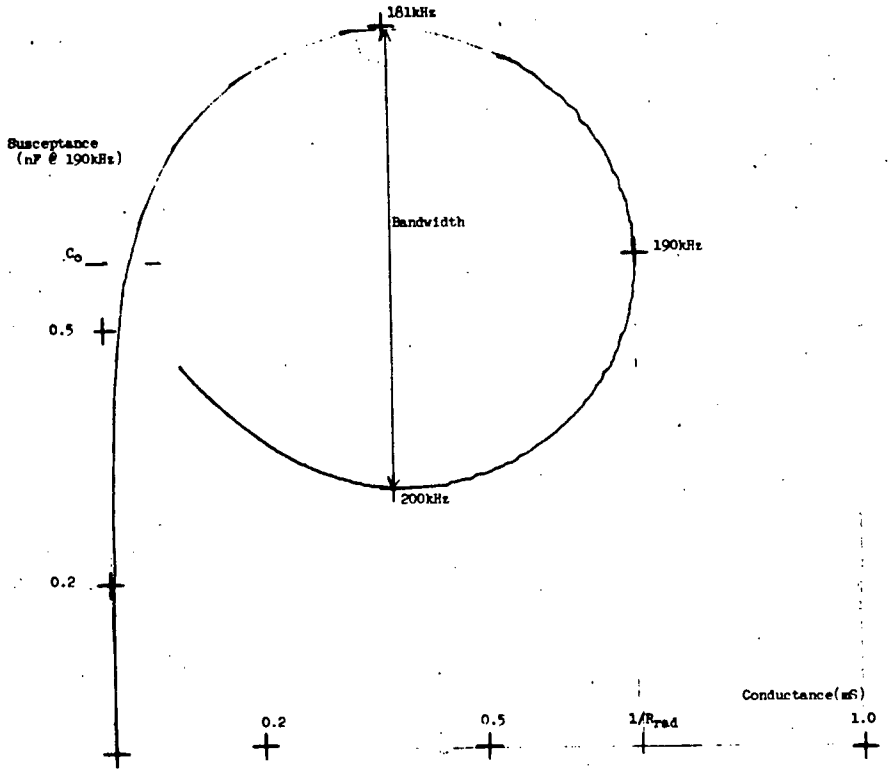

Figure A9 Circle diagram of 200kHz transducer.

The resonant operating frequency is found to be 190kHz. From the circle diagram, the equivalent circuit parameters are found as follows. The radiation resistance is the inverse of the conductance at resonance(1400Ω). The clamp capacitance(C_o) is the susceptance at resonance(0.6nF). The values of C and L are calculated below

$$Q = \frac{\omega_o L}{R} \quad \Rightarrow \quad L = \frac{RQ}{\omega_o}$$

But $Q = \frac{f_o}{B} = \frac{190}{200-181}$ as read from circle diagram

$$= 10$$

$$\Rightarrow \quad L = \frac{1400 \times 10}{2\pi \times 190 \times 10^3}$$

$$= 11.8 \text{ mH}$$

and $\omega_o^2 = 1/LC \quad \Rightarrow \quad C = 59.5 \text{ pF}$

Thus the equivalent circuit parameters are determined.

In order to extract the maximum signal when using the transducer as a receiver, it is usual to match the transducer. Fundamentally this involves the insertion of a shunt inductance to cancel the clamp capacitance at resonance. Often it is beneficial to also design the matching network to match the transducer bandwidth. This improves the signal to noise ratio.

A3 CONTROL SOFTWARE

Experiments were conducted at three different sites during the course of the thesis. The equipment for storage of signals varied from site to site. A listing of a typical program written to control experiments at each site is given in this Appendix. All experiments were controlled by an HP-86 computer, using HP-IB and HP-BCD (tank tests only) interfaces. In each case, a range gate of return signal from each aperture position was quadrature sampled. Then the amplitude and phase of the signal was calculated. This information was then stored in a form suitable for transfer to the UNIVAC computer. This transfer was carried out using the HP Data communications package. The generation of synthetic aperture images was implemented on the UNIVAC computer.

A3.1 LABORATORY TANK

An accurate positioning apparatus was available and the transducer could be kept stationary at each aperture position. Its position could be monitored and controlled by the HP-86 computer. The return signals were digitised and converted at each aperture position separately. Signals were digitised by a Phillips storage oscilloscope, and a range gate of each signal was downloaded to the HP-86 computer. The amplitude and phase of samples within this range gate were stored in a form suitable for transfer to the UNIVAC computer.

A3.2 RESERVOIR SITE

Accurate positioning of the transducer for each aperture position was not possible. Hence external clocking circuitry was designed such that a range gate of the return signals for a full aperture could be stored during one sweep of the oscilloscope (4k samples). The design of this circuitry is detailed in Appendix A1.5. Transmission, reception and storage of signals was carried out whilst the

trolley was moving. Since the prf of the signal was known the spacing of aperture points could be calculated if the velocity of the trolley was known. Audible signals were produced by the computer at the start and finish of transfer, and it was ensured that the trolley travelled the length of the aperture between these signals. Hence, since the distance and time were known, the velocity could be calculated.

A3.3 SEA TESTS

The Phillips oscilloscope had an insufficient memory size for the realisation of long apertures. An A/D unit was loaned from the Dept. of Civil Engineering. This unit when used in conjunction with the HP-86 computer allowed 60k samples to be stored. The aperture spacing was determined from knowledge of the boat's velocity and the transmit signal prf. Calibration and zeroing of the signals on the quadrature outputs of the demodulator could be carried out under program control. The signals were stored on floppy disk in the form of one byte per sample, as measured by the A/D. A program written to convert these measurements into amplitude and phase components suitable for transfer to the UNIVAC is also listed in this Appendix.

```
10 ! ************************************************************
20 ! PROGRAM to control storage of synthetic aperture data
30 ! in CAL laboratory tank. The position of the transducer
40 ! is accurately controlled and monitored using stepper
50 ! motors and Heidenhahn counters under program control.
60 ! Data storage is done on the PHILLIPS scope, with the
70 ! transducer statonary at each aperture postion. A range
80 ! gate of signal is downloaded and stored in a form suitable
90 ! for transfer to the UNIVAC
100 ! ************************************************************
110 !
120 DISP "INPUT FILENAME" @ INPUT FILE$
130 ASSIGN# 1 TO  FILE$&":D701" ! file for data storage
140 !
150 CLEAR
160 OPTION BASE 1
170 DIM VALUE(4120),PHASE(60),AMPL(60),LINE$[100]
180 RESET 3 @ CLEAR 6 @ RESET 6
190 !
200 ! set up PHILLIPS scope for data storage
210 CONTROL 6,16 ; 1,10
220 OUTPUT 608 USING "K" ; "SPR"
230 OUTPUT 608 USING "K" ; "USP /"
240 OUTPUT 608 USING "K" ; "MOD SNG/TIM 2E-03/DOT ON"
250 !
260 ! first determine zero levels of each channel
270 DISP "ZERO CHANNELS @ PRESS CONT" @ PAUSE
280 OUTPUT 608 USING "K" ; "MOD SNG" @ WAIT 1000
290 OUTPUT 608 USING "K" ; "BGN 50/END 172/CNT 1/DAT ALL/DAT ?"
300 !
310 FOR I=1 TO 120
320    ENTER 608 ; VALUE(I)
330 NEXT I
340 !
350 ZERO1=0 @ ZERO2=0
360 FOR I=1 TO 63 STEP 2
370    ZERO1=ZERO1+VALUE(I)
380    ZERO2=ZERO2+VALUE(I+1)
390 NEXT I
400 ZERO1=ZERO1/32 @ ZERO2=ZERO2/32
410 DISP ZERO1,ZERO2
420 !
430 ! now to start sampling
440 DISP "RESET CHANNELS AND PRESS CONT" @ PAUSE
450 OUTPUT 608 USING "K" ; "MOD SNG"
460 DISP "WHEN TRACE IS COMPLETE PRESS CONT" @ PAUSE
465 !
470 CNT=0
475 ! Set up BCD interface to control trolley
480 CONTROL 3,4 ; 0@ CONTROL 3,5 ; 0@ CONTROL 3,3 ; 85
485 !
486 ! Now store data for 70 aperture positions
490 FOR C=1 TO 70
500    D=C*5*100 ! desired transducer position
510    ENTER 301 ; X@ GOSUB 690 ! present transducer position
520    M=X-D
530    IF M<0 THEN D1=2 ! move backwards
540    IF M>0 THEN D1=8 ! move forwards
545 ! Now move
550    FOR I=1 TO ABS (M)
560       ASSERT 3;D1
```

```
570        ASSERT 3;1
580        WAIT 1
590     NEXT I
600     ASSERT 3;1 @ ASSERT 3;8
610     ASSERT 3;0 @ WAIT 50
615 !
620 ! Check if in correct position
630     ENTER 301 ; X@ GOSUB 690
640     IF ABS (X-D)>2 THEN GOTO 500 ! if not, then move
645 !
650     DISP C
655 ! now sample signal
660     GOSUB TRNSFR
665 !
670 NEXT C
680 END
685 !
686 ! ***********************************
687 ! SUBROUTINE to correct for error in
688 !              measuring interface
689 ! ***********************************
690 IF X>29999 THEN GOTO 710
700 IF X<10000 THEN GOTO 710
710 RETURN
711 !
712 ! ************************************************************
713 ! SUBROUTINE to sample signal, and convert I and Q components
714 !              to AMP and PHASE. The latter values are stored
715 !              in a form suitable for UNIVAC transfer
716 ! ************************************************************
717 !
720 TRNSFR:
725 !       sample part of the signals(2 channels)
730         OUTPUT 608 USING "K" ; "BGN 20/END 142/CNT 1/DAT ALL/DAT ?"
740         FOR I=1 TO 120
750            ENTER 608 ; VALUE(I)
760         NEXT I
765 !
766 !      convert to AMP and PHASE storing as strings for UNIVAC
770         FOR J=1 TO 5
780         LINE$=""
785 !
790         FOR K=1 TO 24 STEP 2
800            I=J*24-24+K ! position in array
810            VALUE(I)=VALUE(I)-ZERO1 @ VALUE(I+1)=VALUE(I+1)-ZERO2
820            AMPL((I+1)/2)=IP (SQR (VALUE(I)^2+VALUE(I+1)^2))
830            PHASE((I+1)/2)=IP (ATN2 (VALUE(I),VALUE(I+1))*360/2/3.14159)
840            IF PHASE((I+1)/2)<0 THEN PHASE((I+1)/2)=PHASE((I+1)/2)+360
850            LINE$=LINE$&FNCA$(AMPL((I+1)/2))&FNCA$(PHASE((I+1)/2))
860         NEXT K
865 !
870         DISP LINE$
880         CNT=CNT+1 @ PRINT# 1,CNT ; LINE$
890         NEXT J
895 !
900         OUTPUT 608 USING "K" ; "MOD SNG" ! reset scope
910         GOSUB DISPLY  ! display amplitude vs. time
920 RETURN
```

```
921 !
922 ! ****************************************
923 ! SUBROUTINE to convert number to a 3
924 !          digit string
925 ! ****************************************
926 !
930 DEF FNCA$(DUMMY)
940                 X$=VAL$ (DUMMY)
950                 IF LEN (X$)=1 THEN X$="00"&X$
960                 IF LEN (X$)=2 THEN X$="0"&X$
970                 FNCA$=X$
980 FN END
981 !
982 ! ****************************************
983 ! SUBROUTINE to display amplitude versus
984 !             time on the screen
985 ! ****************************************
986 !
990 DISPLY:
1000        MOVE 0,0
1010        SCALE 0,60,0,100
1020        FOR I=1 TO 60
1030        PLOT I,AMPL(I)
1040        NEXT I
1050 RETURN
```

```
1 ! ************************************************************
2 ! Program to control storage of information at reservoir site.
3 ! Data is stored on PHILLIPS scope. Clocking of scope is done
4 ! by hardware circuitry. Oscilloscope is downloaded to HP-86
5 ! by HP-IB cable, and stored on floppy diskette, in a form
6 ! suitable for immediate transfer to UNIVAC
7 ! This program is designed for 120 aperture positions, with the
8 ! storage of 16 samples at each aperture position
9 ! ************************************************************
10 !
20 CLEAR @ OPTION BASE 1@ DEG
30 DIM A(70),X(70),S(70),VALUE(4000),AMPL(120,16),PHASE(120,16)
35 DIM LINE$[80]
36 !
40 ! Set up PHILLIPS scope for transfer
50 CLEAR 6
60 CONTROL 6,16 ; 1,10
70 OUTPUT 608 USING "K" ; "SPR"
80 OUTPUT 608 USING "K" ; "USP /"
90 OUTPUT 608 USING "K" ; "MOD SNG"
100 !
110 GOSUB ZEROES  ! Work out zeroes for channels
141 !
142 ! Now ready to sample
143 DISP "PRESS CONT AND MOVE " @ PAUSE
145 WAIT 5000 @ BEEP @ WAIT 1000 ! Wait for ready,give beep then go
146                               ! allow time for start up
148 OUTPUT 608 USING "K" ; "MOD SNG" ! Start scope off
150 WAIT 13000 @ BEEP @ PAUSE ! Beep when track should finish
160 !
196 GOSUB TRPHIL  ! Download
197 DISP "FINISHED" @ BEEP @ PAUSE ! Operator decides whether to store
198 GOSUB STRIT
200 END
210 !
220 ! ************************************
230 ! SUBROUTINE to download oscilloscope
240 ! ************************************
250 !
400 TRPHIL: OUTPUT 608 USING "K" ; "BGN 4/END 3999/CNT 1/DAT ALL/DAT ?"
410         FOR I=1 TO 3994
420            ENTER 608 ; VALUE(I)
430         NEXT I
435         GOSUB AMPPHA  ! Calculate components
440 RETURN
442 !
443 ! ************************************
444 ! SUBROUTINE to determine zero level
445 !             of each channel
446 ! ************************************
447 !
450 ZEROES:
460         DISP "ZERO CHANNELS AND PRESS CONT" @ PAUSE
470         OUTPUT 608 USING "K" ; "MOD SNG" @ WAIT 10000
480         OUTPUT 608 USING "K" ; "BGN 4/END 69/CNT 1/DAT ALL/DAT ?"
485 !
490         FOR I=1 TO 64
500            ENTER 608 ; VALUE(I)
510         NEXT I
515 !
```

```
120         ZERO1=0 @ ZERO2=0
130         FOR I=1 TO 63 STEP 2
140            ZERO1=ZERO1+VALUE(I)
150            ZERO2=ZERO2+VALUE(I+1)
160         NEXT I
170         ZERO1=ZERO1/32 @ ZERO2=ZERO2/32
180         DISP ZERO1,ZERO2
190         DISP "RESET CHANNELS AND PRESS CONT" @ PAUSE
195 !
200         OUTPUT 608 USING "K" ; "MOD SNG" ! reset oscilloscope
210 RETURN
212 !
214 ! ***********************************************
215 ! SUBROUTINE to convert I and Q channels to
216 !              AMP and PHASE
219 ! ***********************************************
220 !
300 AMPPHA:
310         FOR I=1 TO 120
320            FOR J=1 TO 32 STEP 2
321               NUMB=(I-1)*32+J ! Place in string
322 !           remove zeroes
324               VALUE(NUMB)=VALUE(NUMB)-ZERO1
325               VALUE(NUMB+1)=VALUE(NUMB+1)-ZERO2
326 !
330 !           determine AMPL and PHASE
340               AMPL(I,(J+1)/2)=IP (SQR (VALUE(NUMB)^2+VALUE(NUMB+1)^2))
350               PHASE(I,(J+1)/2)=IP (ATN2 (-VALUE(NUMB),-VALUE(NUMB+1)))
360               IF PHASE(I,(J+1)/2)<0 THEN PHASE(I,(J+1)/2)=PHASE(I,(J+1)/2)+3
)
370            NEXT J
380         NEXT I
390 RETURN
391 !
392 ! ***********************************************
393 ! SUBROUTINE to store data in form suitable for
394 !              UNIVAC tansfer (strings of <80 ASCII
395 !              characters)
396 ! ***********************************************
397 !
800 STRIT:
802       DISP "ENTER FILE NAME" @ INPUT FILE$
805       CREATE FILE$,240,60
810       ASSIGN# 1 TO  FILE$
820       CNT=0
910      ! Now store amplitude and phase info
920       FOR I=1 TO 120
925          LINE$=""
930          FOR J=1 TO 8
940             LINE$=LINE$&FNCA$(AMPL(I,J))&FNCA$(PHASE(I,J))
950          NEXT J
960          CNT=CNT+1 @ PRINT# 1,CNT ; LINE$
962          DISP LINE$
965          LINE$=""
970          FOR J=9 TO 16
980             LINE$=LINE$&FNCA$(AMPL(I,J))&FNCA$(PHASE(I,J))
990          NEXT J
1000         CNT=CNT+1 @ PRINT# 1,CNT ; LINE$
1005         DISP LINE$
1010      NEXT I
1020 RETURN
```

```
5 ! ******************************************************
10 ! Program to control sea tests using A/D converter
20 ! Needs: 1. HP-IB interface
30 !        2. One reed relay connection
32 ! User is prompted through varous stages of operation
33 ! Note needs to be made of zero readings as displayed by
34 ! program. Data is stored on floppy diskette in a form
35 ! of one byte per number, and needs to be run through
36 ! TRANSFER program before transfer to UNIVAC
39 ! ******************************************************
40 !
50 OPTION BASE 1
55 !
60 P1=2 @ S1=30 @ S2=16 ! Addresses for A/D
65 !
66 ! First the two channels are calibrated using a test signal;
67 ! then the strength of the returned signals (using transmitter)
68 ! must be set so as not to saturate the demodulator
69 ! This is set by the transmitter power.
70 !
75 GOSUB SETUP  ! Set up A/D in order to calibrate channels
80 GOSUB TRNSFR  ! Read in the values
90 GOSUB CNVRT  ! Display average, max and min values
95 !
100 DISP "Do you wish to adjust further?";
110 INPUT A$@ IF A$[1,1]="Y" THEN 70
115 !
120 ! Now check zeroes with the transmitter off
125 !
130 DISP "Connnect transmitter ,but leave off"
135 !
140 GOSUB SETUP
150 GOSUB TRNSFR
160 GOSUB CNVRT
165 !
166 ! If unhappy, calibration/zero adjustment may be repeated
170 DISP "Further calibration";@ INPUT A$
180 IF A$[1,1]="Y" THEN 140
181 !
185 ! Now ready to sample
190 DISP "Turn transmitter on; ";
195 !
200 GOSUB SETUP2  ! set up A/D for 60k of data storage
201 !
202 SEND 6 ; LISTEN P1 SCG S2 MTA ! ready to sample
203 A=TIME
204 OUTPUT 6 USING "#,B" ; 1 ! close reed relay
206 SEND 6 ; UNL TALK P1 SCG 0 MLA
208 TRIGGER 6 ! start transfer
210 TRANSFER 6 TO  Y$ FHS ! transfer direct to IOBUFFER Y$
211 BEEP ! finished
212 STATUS Y$,0 ; Q0,Q1,Q2,Q3
214 IF Q3#0 THEN 212
215 BEEP @ DISP "TRANSFER COMPLETE";TIME -A;"Seconds"
216 WAIT 500
217 !
218 RESET 6
220 SEND 6 ; UNT
```

```
225 !
230 ! Now recheck zeroes
235 !
240 DISP "switch transmitter off; ";
242 GOSUB SETUP
244 GOSUB TRNSFR
246 GOSUB CNVRT
247 !
248 GOSUB STRIT  ! store signals
249 !
250 DISP "Do you wish to display echoes";@ INPUT A$
252 IF A$[1,1]="Y" THEN GOSUB DISPLY
255 !
260 END
262 !
265 ! ********************************************
266 ! SUBROUTINE to configure system for transfer
267 !             of 1000 bytes of information
268 !             Used in calibration/zeroing
269 !             procedure
270 ! ********************************************
271 !
290 SETUP:
300       DIM Z$[1000]
310       IOBUFFER Z$ ! for data input
350       DISP "press ENDLINE when ready",@ INPUT A$
370       SEND 6 ; LISTEN P1 SCG S1 MTA DATA 31,400 ! set up clock(EXT)
390       SEND 6 ; UNL
410       SEND 6 ; LISTEN P1 SCG 1 MTA DATA 2 ! listen on two channels
430       SEND 6 ; UNL
450 RETURN
451 !
452 ! ********************************************
453 ! SUBROUTINE to read in 400 values from A/D
454 !             used in zero/calibrate procedure
455 ! ********************************************
456 !
470 TRNSFR:
490       SEND 6 ; LISTEN P1 SCG S2 MTA
510       OUTPUT 6 USING "#,B" ; 1 ! close reed relay
530       SEND 6 ; UNL TALK P1 SCG 0 MLA
550       TRIGGER 6 ! start transfer
570       TRANSFER 6 TO  Z$ FHS ; COUNT 400
590       STATUS Z$,0 ; Q0,Q1,Q2,Q3
610       IF Q3#0 THEN 590
630       WAIT 500
650       RESET 6
670       SEND 6 ; UNT
690 RETURN
691 !
692 ! ************************************************
693 ! SUBROUTINE to convert bytes to numbers,displaying
694 !             the average, maximum and minimum values.
695 !             Used in zero/calibrate routines
696 ! ************************************************
697 !
710 CNVRT:
730       ZERO1=0 @ ZERO2=0
750       MAX1=NUM (Z$[1,1]) @ MAX2=NUM (Z$[2,2])
770       MIN1=NUM (Z$[1,1]) @ MIN2=NUM (Z$[2,2])
```

```
790       FOR I=1 TO 400 STEP 2
810          ZERO1=ZERO1+NUM (Z$[I,I])
830          ZERO2=ZERO2+NUM (Z$[I+1,I+1])
850          IF NUM (Z$[I,I])>MAX1 THEN MAX1=NUM (Z$[I,I])
870          IF NUM (Z$[I+1,I+1])>MAX2 THEN MAX2=NUM (Z$[I+1,I+1])
890          IF NUM (Z$[I+1,I+1])<MIN2 THEN MIN2=NUM (Z$[I+1,I+1])
910          IF NUM (Z$[I,I])<MIN1 THEN MIN1=NUM (Z$[I,I])
930       NEXT I
950       ZERO1=ZERO1/200 @ ZERO2=ZERO2/200
970       DISP "Zeroes are ",ZERO1,ZERO2
990       DISP "Maxes are ",MAX1,MAX2
1010       DISP "Mins are  ",MIN1,MIN2
1030 RETURN
1031 !
1032 ! ************************************************
1033 ! SUBROUTINE to store IOBUFFER on floppy diskette
1034 !             Used for signal storage
1035 !************************************************
1036 !
1040 STRIT:
1050       DISP "Enter filename";@ INPUT FILE$
1060       ASSIGN# 1 TO  FILE$
1070       PRINT# 1 ; Y$
1075       ASSIGN# 1 TO  *
1080 RETURN
1081 !
1082 ! ****************************************
1083 ! SUBROUTINE to display records in vector
1084 !             representation.
1085 ! ****************************************
1086 !
1090 DISPLY:
1092        DISP "Which records (1-468)";@ INPUT A,B
1110        GCLEAR
1115        SCALE 0,B-A,0,64
1120        FOR I=A TO B
1130           FOR J=1 TO 64
1135              MOVE I-A,J
1140              S=NUM (Y$[(I-1)*128+J*2-1,(I-1)*128+J*2-1])-ZERO1
1150              C=NUM (Y$[(I-1)*128+J*2,(I-1)*128+J*2])-ZERO2
1160              IDRAW C/60,S/60
1170           NEXT J
1180        NEXT I
1190 RETURN
1191 !
1192 ! ************************************************
1193 ! SUBROUTINE to set up A/D and IOBUFFER for
1194 !             sampling and storage of 60k samples.
1195 !             Used for signal storage.
1196 ! ************************************************
1197 !
1290 SETUP2:
1300       DIM Y$[60000]
1310       IOBUFFER Y$ ! for data input
1330       ! DISP "place zeroes on each channel";
1350      DISP "press ENDLINE when ready",@ INPUT A$
1370      SEND 6 ; LISTEN P1 SCG S1 MTA DATA 31,400 ! set up clock(EXT)
1390      SEND 6 ; UNL
1410      SEND 6 ; LISTEN P1 SCG 1 MTA DATA 2 ! listen on two channels
1430      SEND 6 ; UNL
1450 RETURN
```

```
10 ! ************************************************************
20 ! Program to convert numerical data as recorded in sea tests
30 ! into Amplitude and Phase data suitable for transfer to the
40 ! UNIVAC. Input of the zeroes on each channel at storage time
50 ! is required. Output is to a file of 80 character records
60 ! as required by the UNIVAC. This file must contain at least
65 ! 2803 records
70 ! ************************************************************
80 !
100 OPTION BASE 1@ DEG
105 !
110 DISP "INPUT filename" @ INPUT FILE$
120 DISP "Input zeroes ";@ INPUT ZERO1,ZERO2
121 !
125 ! INPUT on unit 1; output on unit 2
130 ASSIGN# 1 TO  FILE$ @ ASSIGN# 2 TO  "UNIVAC:D701"
135 !
136 ! Z$ is buffer used for data storage
137 ! LINE$ is string for output
140 DIM Z$[60000],LINE$[80]
145 !
150 READ# 1 ; Z$ ! read in measurements
152 !
155 ! SAT1 and SAT2 determine number of occasions
156 ! on which channels were saturated
160 SAT1=0 @ SAT2=0 @ CNT=0
162 !
163 ! Total storage consists of 467 aperture positions
170 FOR I=0 TO 467
171 !
172 ! Five lines of 12 samples, then 1 of 4 samples
180    FOR J=0 TO 4
190       LINE$=""
191 !
200       FOR K=0 TO 11
210          POSN=I*128+J*24+K*2 ! position of sample in string
220          GOSUB CONVRT  ! determine AMP and PHASE
230          LINE$=LINE$&FNCA$(AMP)&FNCA$(PHASE)
240       NEXT K
250       CNT=CNT+1 @ PRINT# 2,CNT ; LINE$
260    NEXT J
261 !
270    LINE$=""
280    FOR K=0 TO 3
290       POSN=I*128+5*24+K*2
300       GOSUB CONVRT
310       LINE$=LINE$&FNCA$(AMP)&FNCA$(PHASE)
320    NEXT K
330    CNT=CNT+1 @ PRINT# 2,CNT ; LINE$
331 !
340 NEXT I
341 !
350 CNT=CNT+1 @ PRINT# 2,CNT ; "@END" ! last record in file
360 DISP SAT1,SAT2
370 END
```

```
371 !
372 ! ****************************************************
373 ! SUBROUTINE to calculate AMP and PHASE given the I
374 !             and Q components.
375 ! ****************************************************
376 !
380 CONVRT:
390       IPHASE=NUM (Z$[POSN+1,POSN+1])
400       QUAD=NUM (Z$[POSN+2,POSN+2])
405 ! see if saturation had occurred
410       IF IPHASE=255 THEN SAT1=SAT1+1
420       IF IPHASE=0 THEN SAT2=SAT2+1
430       IF QUAD=255 THEN SAT2=SAT2+1
440       IF QUAD=0 THEN SAT2=SAT2+1
445 !
446 ! remove zeroes
450       IPHASE=IPHASE-ZERO1
460       QUAD=QUAD-ZERO2
461 ! convert
470       AMP=IP (SQR (IPHASE^2+QUAD^2))
480       IF IPHASE=0 AND QUAD=0 THEN 510
490       PHASE=IP (ATN2 (QUAD,IPHASE))
500       IF PHASE<0 THEN PHASE=PHASE+360
510 RETURN
511 !
512 ! ****************************************
513 ! FUNCTION to convert a number to a 3
514 !           character string
515 ! ****************************************
516 !
520 DEF FNCA$(VALUE)
530       X$=VAL$ (VALUE)
540       IF LEN (X$)=1 THEN X$="00"&X$
550       IF LEN (X$)=2 THEN X$="0"&X$
560       FNCA$=X$
570 FN END
```

A4 VERIFICATION OF SYSTEM OPERATION

In cases where experiments were carried out in the laboratory tank, it was a simple task to set up a known control target, and image it using the sonar system in order to verify the system operation. In the field however, this was not possible and other methods were necessary to verify the operation of the various elements of the sonar system described earlier in this appendix. A number of such tests will be described.

A4.1 TRANSMITTER AND DUPLEXER

With the transducer matched, and used with the duplexer, the transmit frequency was adjusted until the received signal appeared strongest. Providing a good return signal was received, these elements were regarded as operating correctly. The pulse width was adjusted to achieve the optimal trade-off between received power and resolution. In principle the shortest transmit pulse was desired, but in practice, the shortness of the pulse is limited by the signal bandwidth of the transducer resonance. This may be determined from the circle diagram(Appendix A2).

A4.2 RECEIVER PRE-AMPLIFIER

The pre-amplifier could be tested by feeding a small test signal to the input and monitoring the output. The phase and amplitude response of the amplifier could be verified.

A4.3 DEMODULATOR

Independent testing of the demodulator operation was possible. A continuous signal of frequency close to the transmit frequency was fed to the input of the demodulator. The output signals from the I and Q channels are then at the difference frequency. If all is well, they should be

90 shifted with relation to one another. The linearity of the outputs could be checked by varying the input signal amplitude. It was important that both channels had the same gain, and this could be checked and adjusted using a similar test siganl.

A4.4 STORAGE PROCEDURE

The correct storage of the signals could be checked at the laboratory by feeding known signals into the demodulator(as in previous section) and verifying that the siganls stored on floppy disk were those that were measured.

In the above manner, confidence in the system could be gained before the system was used to carrry out measurements

References

1. G.Littlewort "Sub-bottom profiling and synthetic aperture imaging in sonar", B.Sc(Hons) Project, U.C.T.(1983).

APPENDIX B GENERATING FOCUSED SYNTHETIC APERTURES

The creation of a focused synthetic aperture is a complex process. Once the point to be imaged has been selected, the aperture positions required to realise the desired beam (resolution and squint angle) are decided upon. For each position within this aperture the processing begins by calculating the two way return time to the image point. Consulting the memory map of stored signals, the range bin closest to this return time in the signal recorded at the relevant aperture position is selected (Figure B2). The amplitude and phase associated with this range bin are extracted. The phase is corrected to allow for a spherical wavefront arriving at the aperture(Figure B1). This phase correction is calculated according to the number of extra wavelengths that the signal from the image point has travelled than that travelled to and from an aperture position directly above the image point. This phase is subtracted from the signal phase. Similarly the contributions from all aperture positions are correctly phased. The contributions from all aperture positions are then vectorially summed to yield the target strength for the image point. This aperture may be regarded as being curved to fit a spherical wavefront arriving from the image point(Figure B1).

An example of this process is given in this Appendix. A 50kHz transducer was used to image a point-like target. A phasor representation of the return signals from the aperture positions is shown in Figure B3. The rotation of the phasor indicates the phase of the echo from that point. The reconstruction process for an image point and a typical background point is listed. It will be noticed that the corrected phases for the image point are coherent, whereas for the background point they are random.

A reconstructed image of the target is shown in Figure B4
A program to generate the synthetic aperture is listed.

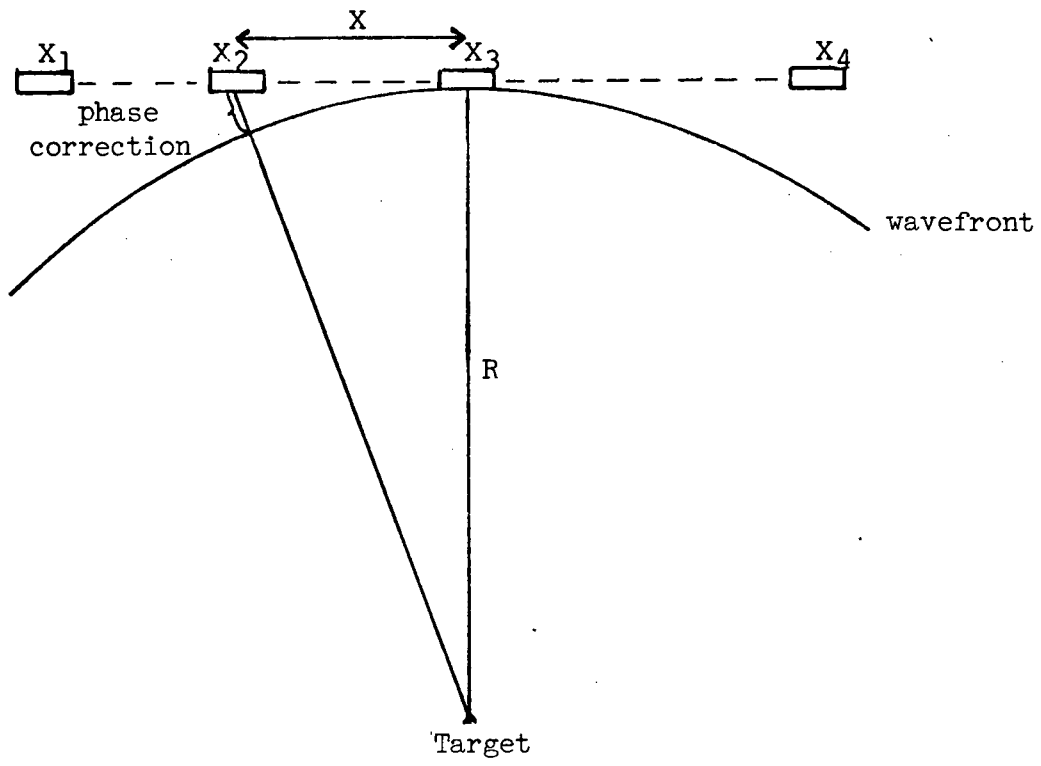

Figure B1 Circular wavefront arriving at the aperture.

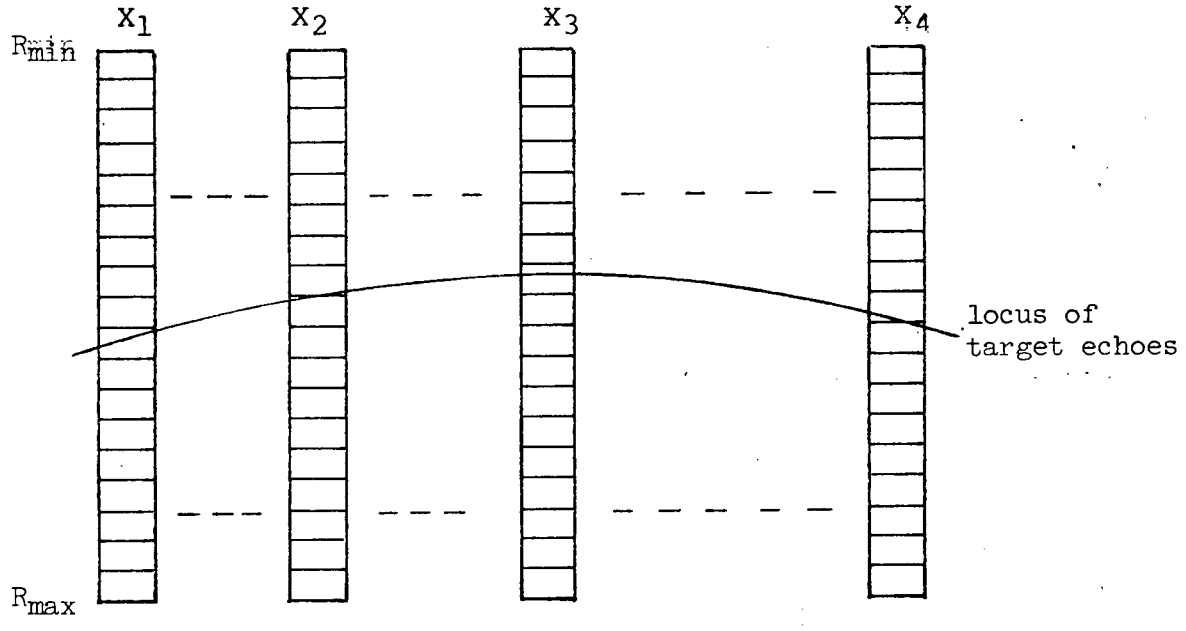

Figure B2 Data stored at each aperture position.

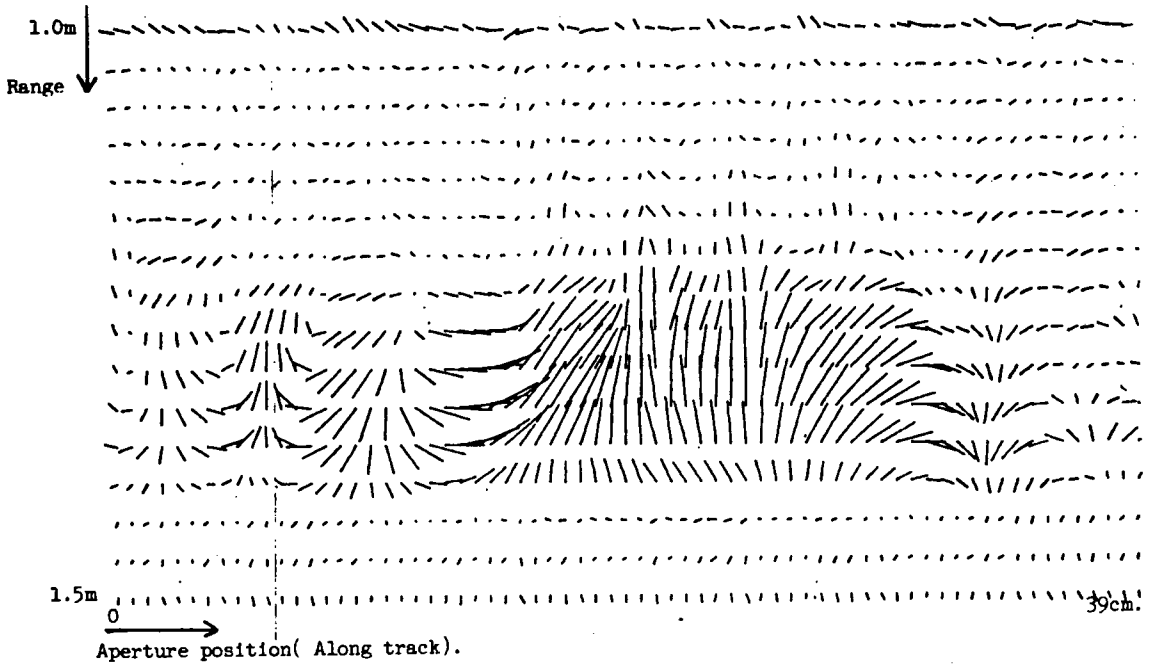

Figure B3 Phasor representation of return signals.

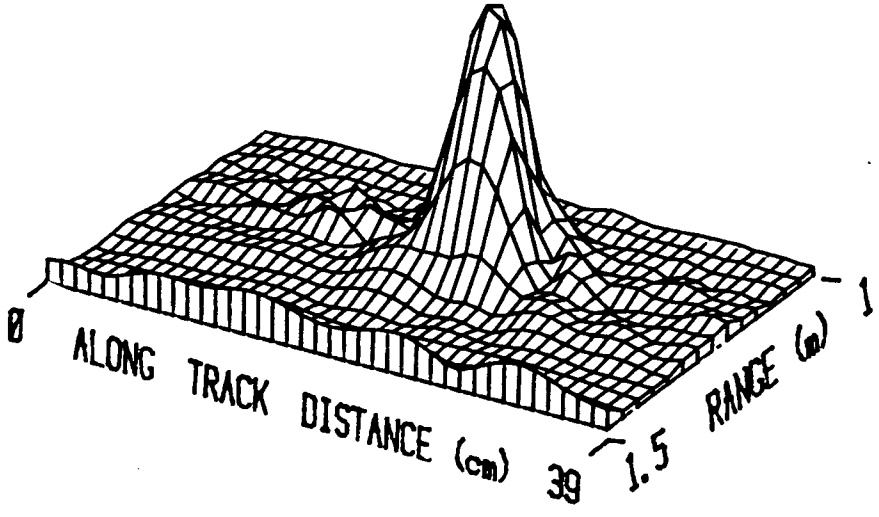

Figure B4 Reconstructed image using 39cm. aperture.

Synthetic aperture example : TARGET point

Aperture position	Signal Amp	Signal Phase	Phase Correction	Corrected Phase
11	73	0	349	11
12	68	344	324	19
13	69	312	300	11
14	69	277	276	0
15	77	244	254	350
16	93	227	232	355
17	100	217	212	4
18	94	199	192	6
19	85	181	173	7
20	82	154	156	358
21	89	124	139	345
22	109	107	123	344
23	123	93	108	345
24	131	84	94	350
25	142	77	81	356
26	141	64	69	355
27	140	57	58	359
28	144	41	48	353
29	143	35	39	356
30	153	33	30	2
31	159	34	23	10
32	148	27	17	9
33	137	18	12	5
34	133	12	7	4
35	132	5	4	0
36	136	2	1	0
37	134	352	0	351
38	142	1	0	0
39	131	354	0	353
40	128	359	1	357
41	126	2	4	358
42	123	1	7	354
43	121	0	12	348
44	123	8	17	351
45	124	14	23	351
46	122	22	30	352
47	131	34	39	355
48	125	34	48	346
49	126	43	58	345
50	123	50	69	341
51	114	56	81	335
52	115	60	94	326
53	106	74	108	326
54	91	90	123	327
55	78	107	139	328
56	67	118	156	322
57	59	134	173	321
58	50	163	192	331
59	53	189	212	337
60	52	210	232	338
61	53	228	254	334
62	51	246	276	330
63	41	264	300	324
64	33	304	324	340
65	21	341	349	352

Reconstructed amplitude = 6158

Synthetic aperture example: BACKGROUND point

Aperture position	Signal Amp	Signal Phase	Phase Correction	Corrected Phase
1	10	296	114	181
2	12	273	102	170
3	19	275	91	183
4	14	284	81	202
5	8	287	71	215
6	19	257	62	194
7	25	251	53	197
8	23	229	45	183
9	6	85	38	46
10	12	45	31	13
11	5	286	25	260
12	18	227	20	206
13	5	148	15	132
14	18	82	11	70
15	11	56	7	48
16	10	262	5	256
17	18	247	2	244
18	5	203	1	201
19	5	104	0	103
20	9	299	0	298
21	15	280	0	279
22	14	288	1	286
23	4	123	2	120
24	5	94	5	88
25	2	355	7	347
26	20	292	11	280
27	12	273	15	257
28	13	225	20	204
29	9	212	25	186
30	13	24	31	353
31	20	22	38	344
32	16	286	45	240
33	13	252	53	198
34	4	213	62	150
35	8	80	71	8
36	11	19	81	298
37	22	318	91	226
38	22	314	102	211
39	11	258	114	143
40	9	229	126	102
41	6	358	139	218
42	18	15	153	222
43	15	341	167	173
44	16	286	182	103
45	17	262	198	63
46	9	212	214	358
47	7	166	230	296
48	8	346	248	97
49	24	4	266	98
50	18	0	284	76
51	7	235	304	291
52	16	196	323	233
53	8	153	344	169
54	11	108	5	103

Reconstructed amplitude = 177

```
10 C ***************************************************************
20 C This program uses amplitude and phase information as recorded
30 C in the field to create synthetic aperture images. A number of
40 C degrees of freedom of choice are realisable in terms of aperture
50 C length, squint angle and amplitude shading
60 C This particular version was written to carry out imaging for
70 C data recorded in the SEA TESTS, but minor changes to the READIN
80 C routine and one or two parameters make it suitable for use
90 C with other sets of data
100 C WRITTEN AND MODIFIED BY: Marek Dutkiewicz 1984-1986
110 C ***************************************************************
120 C
130       COMMON ISMPL,NSTIME,AMPL,PHASE
140       DIMENSION Z(120,64),AMP2(120,64)
150       INTEGER AMPL(500,64),PHASE(500,64),A(16)
160       INTEGER CNT,RTIME
170       CHARACTER*1 DISPAP,DISPZ
180 C
190  1    FORMAT(2A1)
200  3    FORMAT(1X,3(F10.2,3X))
210  4    FORMAT(1X,13(I4,1X))
220  5    FORMAT(1H1)
230 C
240 C Read in whether numeric listing of raw and reconstructed
250 C data is desired
260       READ(5,1)DISPAP,DISPZ
270 C
280 C Read in various operational parameters
290 C       NREC = number of aperture positions
300 C       NSTIME= start time in microseconds of each record
310 C       ISMPL = sampling interval in microseconds
320 C       SSPACE= spacing between aperture positions in metres
330 C
340       READ(5,*)NREC,NSTIME,ISMPL,SSPACE
350       PRINT*,NREC,NSTIME,ISMPL,SSPACE
360 C NPTS = number of samples stored for each position
370       NPTS=64
380 C
390       FREQ=4.5
400       PI=3.14159
410        WRITE(6,5)
420 C
430 C First read in all the amplitudes and phases
440        CALL RDIN(NREC,DISPAP)
450 C
460 C produce an amplitude modulated type display of raw intensity
470 C intensity=amplitude**2
480        DO 25 II=1,NREC,4
490         I=(II+3)/4
500          DO 25 J=1,NPTS
510 25     AMP2(I,J)=AMPL(II,J)**2
520        THRESH=30000.
530        CALL DISPLY(AMP2,THRESH,NREC)
540 C
550 C Now synthetic aperture imaging may commence
560 C major loop is for each range increment
570       DO 200 I=1,NPTS
580 C work out one way range in microseconds
590        R=(I*ISMPL+NSTIME)/2.
600 C
610 C loop for every fourth aperture position. I and J define the
620 C coordinates of the point in the image plane being imaged
```

```
630          DO 150 J=1,NREC,4
640 C
650 C zero the two summing variables
660            TSIN=0
670            TCOS=0
680 C The following steps determine the aperture length and degree
690 C of squint in terms of aperture positions. In this case the
700 C 15 is half the aperture length, and +30 is the degree of squint
710            NFST=J-15+30
720            NLST=J+15+30
730 C limit the aperture if it goes beyond available data
740            IF(NFST.LT.1)THEN
750              NFST=1
760            END IF
770            IF(NLST.GT.NREC)THEN
780              NLST=NREC
790            END IF
800 C
810 C K defines which aperture position is being used
820  370       DO 140 K=NFST,NLST
830 C Work out which record corresponds to correct range
840              RCORR=SQRT(R**2+((K-J)*SSPACE/1500.*10**6)**2)*2
850              RTIME=INT((RCORR-NSTIME)/FLOAT(ISMPL))
860 C
870 C ignore if out of range
880              IF(RTIME.GT.NPTS)GOTO 140
890              IF(RTIME.LT.1)GOTO 140
900 C
910 C calculate required phase correction and apply it
920              PHCORR=(RCORR-R*2)*FREQ/10.**3*2*PI
930              THETA=PHASE(K,RTIME)/360.*2*PI-PHCORR
940 C
950 C calculate required amplitude shading according to HAMMING function
960              ZED=(K-(NLST+NFST)/2.)/((NLST-NFST)/2.)
970              WEIGHT=0.08+0.92*(COS(PI*ZED/2.))**2.
980 C
990 C now sum the contents of the relevant range bin, suitably weighted
1000 C and phased
1010  125          TSIN=TSIN+AMPL(K,RTIME)*SIN(THETA)*WEIGHT
1020               TCOS=TCOS+AMPL(K,RTIME)*COS(THETA)*WEIGHT
1030 140         CONTINUE
1040 C
1050 C Now calculate the image intensity
1060             JJ=(J+3)/4
1070             Z(JJ,I)=(TSIN**2.+TCOS**2.)/1200.
1080 C write in a form suitable for SACLANT package
1090             WRITE(11,3)FLOAT(I),FLOAT(JJ*1.4),Z(JJ,I)
1100 150       CONTINUE
1110 200     CONTINUE
1120 C
1130         IF(DISPZ.EQ.'N')GOTO 500
1140 C Display the results(numerically)
1150         WRITE(6,5)
1160         DO 400 J=1,9
1170           DO 300 I=1,NPTS
1180             WRITE(6,4)(INT(Z(JJ,I)),JJ=J*13-12,J*13)
1190 300       CONTINUE
1200         WRITE(6,5)
1210 400     CONTINUE
1220 C
1230 C Produce amplitude modulated display of intensity
1240 500     THRESH=8000.
1250         CALL DISPLY(Z,THRESH,NREC)
1260 C
1270         STOP
1280         END
```

```
C ***********************************************************
C SUBROUTINE to read in the amplitudes and phases from
C             the relevant UNIVAC file. Also will list the
C             amplitudes and phases if desired
C ***********************************************************
C
      SUBROUTINE RDIN(NREC,DISPAP)
C
      COMMON ISMPL,NSTIME,AMPL,PHASE
      INTEGER AMPL(500,64),PHASE(500,64)
      INTEGER A(128)
      CHARACTER*1 DISPAP
C
C for some experiments, I and Q components were reversed
C this is undone if INVERT=1
      INVERT=0
C
      PI=3.14159
C
      DO 100 I=1,NREC
        READ(5,2)(A(II),II=1,24)
        READ(5,2)(A(II),II=25,48)
        READ(5,2)(A(II),II=49,72)
       READ(5,2)(A(II),II=73,96)
       READ(5,2)(A(II),II=97,120)
       READ(5,3)(A(II),II=121,128)
2      FORMAT(24I3)
3      FORMAT(8I3)
        DO 10 J=1,128,2
          AMPL(I,(J+1)/2)=A(J)
          PHASE(I,(J+1)/2)=A(J+1)
C
        IF(INVERT.EQ.1)THEN
          CPHASE=COS(PHASE(I,(J+1)/2)/180.*PI)
          SPHASE=-SIN(PHASE(I,(J+1)/2)/180.*PI)
          PHASE(I,(J+1)/2)=IFIX(ATAN2(SPHASE,CPHASE)*180/PI)
          IF(PHASE(I,(J+1)/2).LT.0)PHASE(I,(J+1)/2)=PHASE(I,(J+1)/2)
     &+360.
        END IF
C
  10    CONTINUE
100   CONTINUE
C
      IF(DISPAP.EQ.'N')RETURN
C
C Display the amplitudes and phases
      DO 250 I=1,9
        DO 200 J=1,64
        WRITE(6,1)(AMPL(II,J),II=I*52-51,I*52,4)
1       FORMAT(1X,13(I4,1X))
200   CONTINUE
          WRITE(6,5)
5         FORMAT(1H ,10(/))
250     CONTINUE
      DO 350 I=1,7
        DO 300 J=1,64
        WRITE(6,1)(PHASE(II,J),II=I*52-51,I*52,4)
300   CONTINUE
        WRITE(6,5)
350   CONTINUE
      RETURN
      END
```

APPENDIX C SIMULATION OF A BURIED TARGET

In order to simulate a buried target, it was necessary to devise an algorithm to calculate the path followed from the transmitter to a buried target and back. This is dependent upon the relative refractive index of the sediment to water. Once the path lengths in water and sediment are known, it is a simple matter to compute the return time of the signal, the phase of the return signal and the amount of attenuation undergone in the sediment.

Consider a transducer at some position relative to the target(Figure C1)

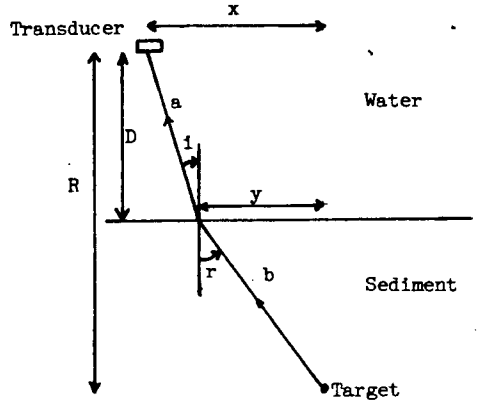

Figure C1 Ray paths from transducer to buried target.

We are interested in determining a and b in terms of the known quantities D,x,R.

$$\text{By Snell's law} \quad \frac{\sin i}{\sin r} = \eta$$

$$\sin i = \frac{x-y}{a} = \frac{x-y}{((x-y)^2+D^2)^{0.5}}$$

$$\sin r = \frac{y}{b} = \frac{y}{((R-D)^2+y^2)^{0.5}}$$

$$\text{Setting} \quad \frac{x-y}{((x-y)^2+D^2)^{0.5}} = \eta \frac{y}{((R-D)^2+y^2)^{0.5}}$$

we may solve iteratively for the only unknown y.

$$\text{Then} \quad a = ((x-y)^2+D^2)^{0.5}$$

$$\text{and} \quad b = (y^2+(R-D)^2)^{0.5}$$

Then the relative timing, phase and amplitude of the return signal may be calculated.

The program to generate the simulated data is listed on the next few pages. The identical algorithm is used when creating synthetic apertures which allow for refraction at the interface.

```
10 C
20 C ***************************************************************
30 C SIMULATION program. This program calculates simulated
40 C returns from a buried target. Refraction at the
50 C interface,attenuation within the sand and spherical
60 C spreading loss is modelled.
70 C The simulated object is a point reflector buried 5cm
80 C beneath the sand surface which is 30cm below the transducer
90 C The sand attenuates the signal at 1 dB/cm at an operating
100 C frequency of 200 kHz. The refractive index of water relative
110 C to the sand is 0.8.
120 C The amplitude and phase of the signals relative to the
130 C directly overhead signal are stored in a form suitable
140 C for use in the synthetic aperture programs.
150 C The received signal is modelled as a cos**2 shaped pulse
160 C ***************************************************************
170 C
180 C set up constants
190       ETA=0.8
200       PI=3.14159
210       R=0.35
220 C
230 C 78 aperture positions are modelled
240       DO 200 K=1,78
250 C
260 C zero all amplitude and phases
270 C AMPL is used for both
280         DO 20 I=1,92
290 20      AMPL(I)=0
300 C
310 C distance to sand
320         D=0.3
330 C
340 C determine amount of refraction
350         CALL FINDY(I,J,K,ETA,Y)
360 C
370 C P is path length in water, Q that in sand
380         P=SQRT((X-Y)**2+D**2)
390         Q=SQRT(Y**2+(R-D)**2)
400 C RCORR is two way path in microseconds
410         RCORR=(Q*ETA+P)/1500.*10**6*2
420 C work out phase diff from overhead signal
430         PHCORR=(Q*ETA+P)/1500.-(((R-D)*ETA+D)/1500.)
440 C IPHASE is the phase in degrees
450         IPHASE=PHCORR*192*10**3*360*2
460 40      IF(IPHASE.GT.360)THEN
470           IPHASE=IPHASE-360
480           GOTO 40
490         END IF
500 C
510 C calculate time for start of received signal
520         RTIME=INT((RCORR-300)/10.)
530 C if out of range
540         IF(RTIME.GT.46)RTIME=46
550 C LST is end of pulse (100 microseconds)
560         LST=RTIME+10
570         IF(LST.GT.46)LST=46
580 C
590         DO 100 I=RTIME,LST
600 C
610 C first shape the pulse
620           ZED=I-(RTIME+5)
```

```
530           WEIGHT=(COS(ZED/5.*PI/2.))**2
540 C spherical spreading loss
550           WEIGHT=WEIGHT*((R*10**6/1500)**2/RCORR**2)**2
560 C attenuation loss
570           WEIGHT=WEIGHT*(10**(-5*Q))**2
580 C scale amplitude to reasonable level
590           AMPL(I*2-1)=INT(WEIGHT*12000)
'00 C
'10 C phase
'20            AMPL(I*2)=IPHASE
'30 100      CONTINUE
'40 C
'50 C write to file
'60           DO 150 I=1,5
'70             WRITE(11,1)(AMPL(II),II=(I-1)*16+1,I*16)
'80 150      CONTINUE
'90           WRITE(11,1)(AMPL(II),II=81,92)
400 1        FORMAT(16(I3,','))
410 C
420 200    CONTINUE
430 C
440         STOP
450         END
460 C
470 C ****************************************************
480 C SUBROUTINE uses Snells law to find the ray path of a
490 C             signal travelling to/from a buried target to
500 C             an aperure position. Solution of an equation
510 C             by method of halves is used.
520 C             This subroutine is used both in generating
530 C             simulated data for a buried target and in
540 C             synthetic aperture processing allowing for
541 C             refraction.
542 C             It is a very time consuming program.
543 c ****************************************************
545 C
550         SUBROUTINE FINDY(I,J,K,ETA,Y)
552 C
555 C D is transducer-sand distance
556 C R is shortest distance from aperture to target
557 C X is along track distance from overhead target
558 C   all in metres
560         COMMON D,R,X
570         X=ABS(K-J)*0.005
575 C
576 C special case for unburied targets
580         IF(R.LT.D)THEN
590           Y=0
.000           D=R
.010         ELSE
.012 C
.015 C buried targets
.016 C solve by method of halves
.020           Y1=-X
.030           Y2=X
.040 1000      Y=(Y1+Y2)/2.
.050           A=(X-Y)/SQRT((X-Y)**2+D**2)
.060           B=ETA*Y/SQRT(Y**2+(R-D)**2)
.070           IF(ABS(A-B).LT.0.001)RETURN
.080           IF((A-B).LT.0)Y2=(Y1+Y2)/2.
.090           IF((A-B).GT.0)Y1=(Y1+Y2)/2.
.100           GOTO 1000
.110         END IF
.120         RETURN
```

APPENDIX D

Paper entitled:
"Synthetic Aperture Sonar for Sub-Bottom Imaging."
presented by:

Prof. P.N.Denbigh

at:

15th Symposium on Acoustical Imaging
July 1986
Halifax, Nova Scotia
Canada.

SYNTHETIC APERTURE SONAR FOR SUB-BOTTOM IMAGING

M.K. Dutkiewicz and P.N. Denbigh

Central Acoustics Laboratory
Department of Electrical and Electronic Engineering
University of Cape Town, Rondebosch 7700, R.S.A.

ABSTRACT

Many of the difficulties which arise in a medium range synthetic aperture sidescan sonar are avoided when the synthetic aperture method is applied to sub-bottom imaging. Preliminary results have been obtained and show the technique to be viable.

INTRODUCTION

Outstanding success has been achieved in radar terrain mapping by using synthetic apertures to achieve fine along-track resolution[1]. A wealth of literature exists on the implementation of the technique, which was primarily developed in the 1960's.

Attempts to extend the technique to sonar applications have, however,not met with the same degree of success. Since Cutrona's benchmark paper[2] a number of attempts have been made to build synthetic aperture sonar systems[3,4]. These attempts have met with success under controlled conditions using 'good' targets. Attempts to extend the technique to use in sidescan sea bed mapping applications are believed to have been largely unsuccessful and this is because of two major problems which do not occur in radar

1) In spite of the lesser operating ranges the low propagation velocity of sound causes the two-way propagation times to be much larger for a sideways looking sonar than for an equivalent radar. This is liable to cause a severe undersampling of the synthetic aperture at typical towing speeds.

2) The inertia of a boat or towed body is much less than that of an aircraft or satellite. This together with the influence of swell and waves can result in deviations of the sampling positions from a straight line path. The deviations may constitute an unacceptably large fraction of a wavelength.

It appears from the foregoing, that a large number of difficulties associated with implementing synthetic apertures in sonar would be overcome

if work was carried out at low frequencies and short ranges. Such an application is sub-bottom imaging. It has been shown[5] that it is possible to achieve coherence over long linear arrays in the ocean at low frequencies.

REVIEW OF SUB-BOTTOM IMAGING

Acoustic methods are used to image objects and layers beneath the sea bed and may fall into one of two broad categories, namely seismic profiling and sub-bottom profiling. Seismic profiling usually uses a single explosive or explosive type source and multiple omnidirectional receive hydrophones mounted in a long streamer behind the survey ship. Penetration depths are considerable and the signal processing is aimed particularly at emphasizing strata using reflection or refraction methods[6]. On the other hand sub-bottom profiling usually combines a boomer, air gun, or tone burst source with a single directional hydrophone receiver, both commonly mounted on a "fish" towed close to the sea bed. The maximum penetration is modest compared with seismic systems and, depending upon the type of sediment and the frequency range in which most of the transmit energy is contained, might be between 1m and 100m.

A large amount of research has been carried out into the characteristics of various sediments and a good summary can be found in Hamilton[7]. One of the important features is the largely empirical observation that the attenuation of sound in sediments is proportional to frequency. For sand we have $\alpha = 0.5f(kHz)$ dB/m; for clays we have $\alpha = 0.1f(kHz)$ dB/m. Penetration is clearly increased by a decrease in frequency but the penalty for a given size of receiver is a broadening of the beam. As an example, a typical operating frequency of 4kHz corresponds to a wavelength of 0.375m so that a receiver 0.5m in diameter has very little directionality. For reflecting strata this is not particularly disadvantageous. The first return shows up clearly as a sharp transition between white and black on the chart recording and the only effect of a wide beam is to cause a broadening of the black bands corresponding to strata. For the imaging of buried objects, however, a broad beam is very disadvantageous as the resolution of closely spaced objects is then very poor. At a range of 15m, for example, the lateral resolution corresponding to the 0.5m diameter receiver discussed would be 11.25m.

Clearly there is a need for high lateral resolution sub-bottom imaging. Examples of application are mine detection, treasure hunting, and the checking of buried pipelines. A technique that appears to be suitable for this type of use is that of parametric arrays. These produce narrow, low frequency beams, but a big problem is the conversion efficiency. The source level tends to be insufficient for any great penetration depth although improvements are achievable using pulse compression[8]. Another technique that suggests itself is that of synthetic apertures. This technique has a number of advantages over existing techniques.

(i) Providing a long array can be synthesized, fine resolution can be achieved.

(ii) A large amount of information is stored at the time of measurement, giving a great deal of versatility in the use of the information. The beam can be steered and focused in order to look for details of interest. For example the optimal detection process for a point target may be different to that for a faceted target. For a faceted target it may depend on the angle of the facet. As another example amplitude shading can be applied to reduce sidelobe levels.

(iii) Source level (and thus penetration) is high since a conventional transducer is used.

Problems with synthetic apertures include the degradation of performance due to towing path irregularities, and beam distortion due to refraction at the sediment-water interface. Early work on the project has shown little degradation due to the latter effect and that, if required, corrections may be incorporated into the processing algorithm. The problem of towing path irregularities is alleviated by working at fairly long wavelengths (e.g. 30cm).

THEORY OF SYNTHETIC APERTURES

A synthetic aperture is generated in a similar fashion to a conventional array except that, instead of having a long line array of elements, a single element is traversed across the space and the return echoes at each position are stored (typically in digital or optical form). After the full aperture has been traversed, the array is synthesized. At this stage a variety of different beams can be realized. What follows is a brief development of the theory. For a more detailed treatment see Cutrona[1].

For a conventional physical array the beam pattern is given by

$$D(\theta) = \frac{\sin\left(\frac{\pi N d_e}{\lambda} \sin\theta\right)}{\sin\left(\frac{\pi d_e}{\lambda} \sin\theta\right)}$$

where N = number of points in array, d_e = element spacing.

In the synthetic case the transmitter and receiver both move and are indeed usually the same transducer. The path length to a target changes twice as much with the position of this transducer as it would with the position of an element across the receive physical array for the case of a stationary transmitter.

Hence
$$D(\theta) = \frac{\sin\left(\frac{2\pi N d_e}{\lambda} \sin\theta\right)}{\sin\left(\frac{2\pi d_e}{\lambda} \sin\theta\right)} \qquad (1)$$

This will be termed a two-way pattern. For apertures which are large in wavelengths this gives an angular resolution of $\lambda/2Nd_e$ for synthetic case, as compared to λ/Nd_e for a real array. The sidelobes for the two-way pattern are 13.2dB down on the main beam. This is appreciable but may be reduced by an amplitude shading of the aperture.

Further, by analogy to a real array, grating sidelobes will occur when the denominator in Eq.1 is zero.

i.e. when $\frac{2\pi d_e}{\lambda} \sin\theta = \frac{\pi}{2}$ or $\sin\theta = \frac{\lambda}{2d_e}$

These will disappear providing the aperture samples are spaced closer than $\lambda/2$.

We have $L_e = (N-1)d_e = Nd_e$ for large N. It follows from the angular resolution of $\lambda/2Nd_e$ that the along-track resolution is given by

$$\delta = \frac{R\lambda}{2L_e} \qquad (2)$$

where R is the range of the target and L_e is the length of the synthetic aperture. Depending on whether the aperture is focused or unfocused a variety of different values of L_e can be achieved.

(i) unfocused. In this case the aperture length is limited by requiring the target to be in the far field of the aperture.

i.e. $R \geq \frac{L_e^2}{\lambda}$ giving $L_e \leq (R\lambda)^{0.5}$

Therefore resolution $\delta \geq \frac{(R\lambda)^{0.5}}{2}$

(ii) focused: If the aperture is focused, the aperture may be as long as the distance for which the target is insonified by the physical transducer.

Hence $L_e = \frac{R\lambda}{D}$, where D is the transducer diameter.

Combining this with eq.(2) gives $\delta = D/2$. It will be noted that this is independent of range and wavelength. At times, it may prove advantageous to focus the array but not to use the full aperture. Under these circumstances $\delta = D/2\gamma$ where γ equals the fraction of the maximum possible aperture.

Further degradation of resolution occurs due to phase errors. These are primarily caused by tow path irregularities. A theoretical treatment of this is available[9] . Experimental results illustrating this effect as well as other features mentioned earlier will be shown later.

EXPERIMENTAL WORK

The system built to realise synthetic apertures used a single transducer for both transmission and reception. Data capture was performed in the field on a HP-86 microcomputer, using a single A/D converter with quadrature sampling. This was later transferred to a UNIVAC mainframe computer where the amplitude and phase of the receive signal was calculated for every range bin of each transmision. Each transmission corresponded to a different sampling point along the synthetic aperture. Processing was carried out for each image point in turn and began with a calculation of the two way propagation distances to each of the sampling points on the synthetic aperture. On the basis of this the phase correction needed to make all receive signals co-phasal was calculated. This was then applied to the contents of the range bin which corresponded most closely to the two way propagation distance. The corrected signals for all the aperture positions were then summed vectorially to yield the target strength for that image point. This is equivalent to realising a curved array centred about the image point. The procedure was carried out for each point in the image space in turn and the displays generated used a SACLANT graphics package. These displays show along-track distance versus range with the vertical axis being an indicator of the target strength. The experimental work began with laboratory tests under carefully controlled conditions, and progressed to reservoir tests, and finally to tests at sea. As a point of interest it has not always been found advantageous to apply amplitude shading to the data. This is because targets move in and out of the skirts of the physical beam as the transducer is scanned across the aperture, and this imposes a very effective natural amplitude shading.

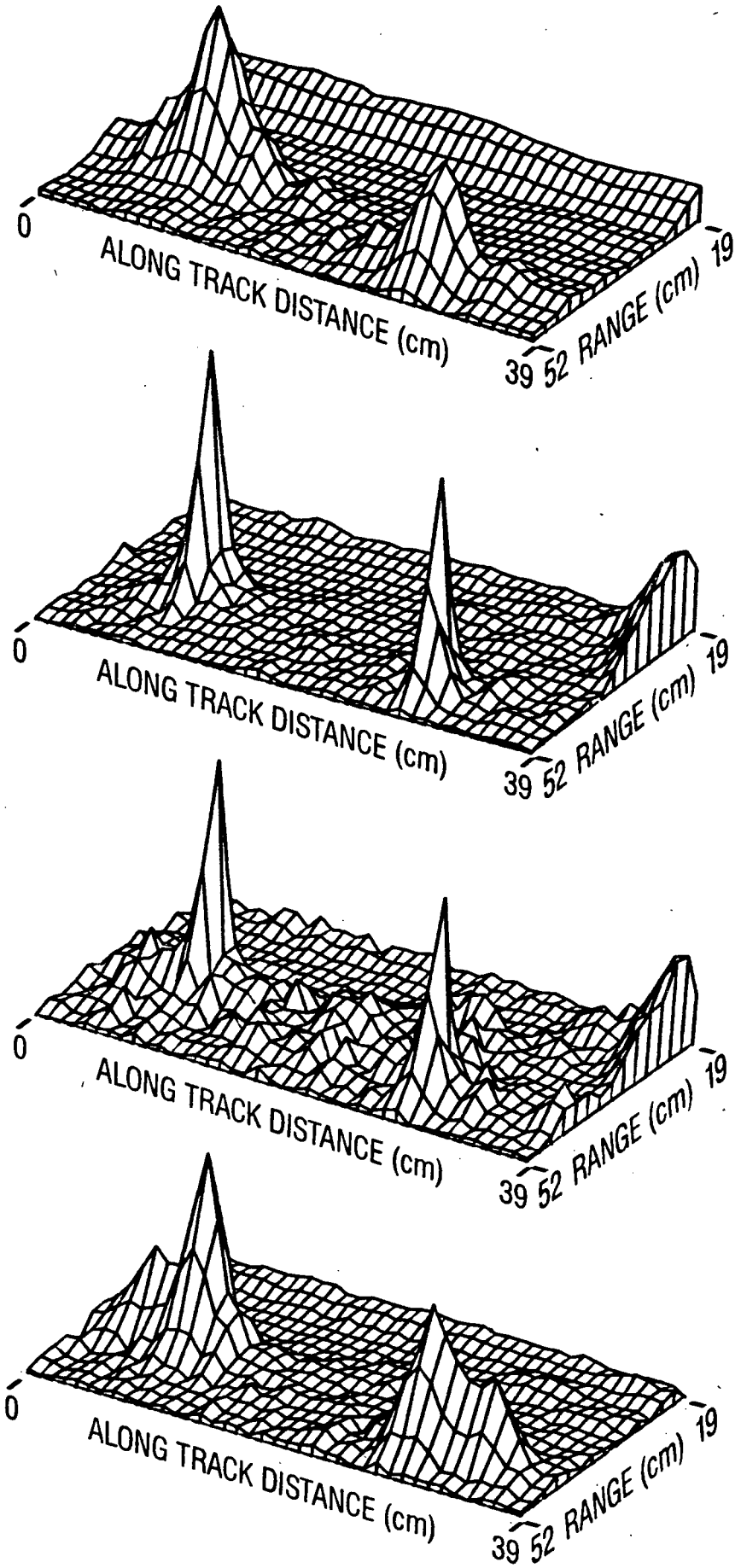

Figure 1. Images of two mid-water targets: (a) 10cm. unfocused aperture; (b) 39cm. focused aperture; (c) focused aperture with random phase errors; (d) focused aperture with 10% velocity error.

200kHz tank tests

Two ping pong balls were used as mid water targets and were imaged using a 200kHz transducer. The size of the transducer used was 8mm square. Transmission and reception were performed with the transducer stationary at each position along the aperture. A total of 78 aperture points spaced 5mm apart were used. The results shown in Fig. 1 are gratifying, showing the expected improvement in resolution as the aperture length is increased. It should be noted, in this and subsequent images, that the vertical displacement represents intensity and not target height.

When making synthetic aperture measurements under less controlled conditions, at sea for example, it is to be expected that the data will contain phase errors due to sideways perturbations of the transducer position; also because an incorrect velocity might be assumed in the processing. Work has been done in which the tank data has been perturbed by random phase errors and by a systematic 10% velocity error. The effect is shown in Fig. 1 and has been to degrade resolution and to increase sidelobes.

Reservoir Tests

Experiments were carried out from a floating laboratory on a fresh water reservoir. The reservoir was known to contain scattered rocks lying in a bed of silt. The laboratory had a 4.5m long rectangular hole cut in the floor. The transducer was suspended in the water from a trolley which ran on rails along the length of the hole. Apertures 4.5m long were created by pulling this trolley by hand at constant velocity along the length of the laboratory.

The transducer used was taken from a conventional sub-bottom profiling array. It operated at a resonant frequency of 4.5kHz and gave a beamwidth of 100 degrees. The transducer bandwidth allowed a pulse of 1ms length to be transmitted, corresponding to a range resolution of 0.75m. At the frequency used, the attenuation in the sediment was approximately 3dB/m which, because of the two-way travel time, gave an attenuation of 6dB per metre of penetration.

The initial experiments were conducted with the transducer looking directly downwards, as is usual in sub-bottom profiling. However, a problem arises that would not, for example, occur with a parametric array. Although the processing of the synthetic aperture leads to a good along-track resolution, the lateral resolution remains unchanged and is poor. A perspective view of the geometry is shown in Fig. 2.

Fig. 3(a) represents a vertical cross-section of the beam corresponding to Fig. 2 and shows the resolution cell. Directly beneath the transducer, in the centre of the physical beam, the sensitivity is maximum. However the attenuation of the sediment reduces the return echo. To the side of the transducer, in the skirts of the physical beam, the sensitivity is lower but the penetration into the sediment is less, so that the return echo is less attenuated. Although sub-bottom strata may still be imaged satisfactorily due to their specularity, small objects are likely to appear stronger when they are located to the side of the transducer than when they are beneath it. Bearing in mind that the intention of a high resolution sub-bottom profiler is to image small targets, it is apparent that the image will be very difficult to interpret.

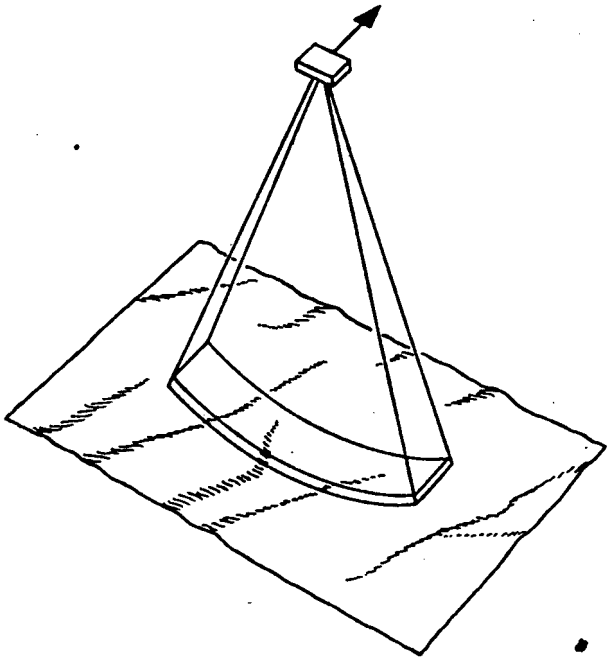

Fig. 2. Intersection of synthesized fan beam with sea bed.

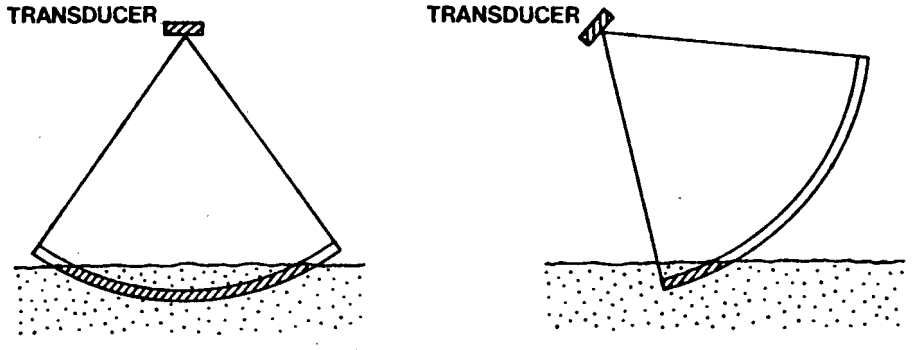

Fig. 3. Intersection of synthesized fan beam with sea bed
a) echo sounding mode b) sidescan mode

Because of the foregoing problems, the preferred mode of operation now is to use the system as a short-range sidescan sonar in which the use of low frequencies enables bottom penetration. After synthetic aperture processing, the resolution cell is as shown in Fig. 3(b). Essentially, the geometry is the same as in Fig. 3(a) except that, because the transducer is now tilted sideways, the sensitivity to targets directly beneath the transducer is greatly diminished. The dominant echoes may be expected to come in from the side and, because of the sediment attenuation, they may be expected to arise in the top metre or so of the sediment. The volume making a significant contribution to the return signal at any instant now becomes relatively small and, because of this, the reconstructed image becomes much more amenable to interpretation. However, in spite of the reduced sensitivity and high sediment attenuation in the vertical direction, the large reflections from strata can still dominate the return signal. In order to diminish still further the returns from beneath the transducer, a pressure release reflecting baffle was used beneath the transducer. This was in order to shadow from the transducer that part of the bed of the reservoir directly beneath it.

As an example of the performance of the system Fig. 4(a) shows the unprocessed amplitude data collected using the low frequency transducer.

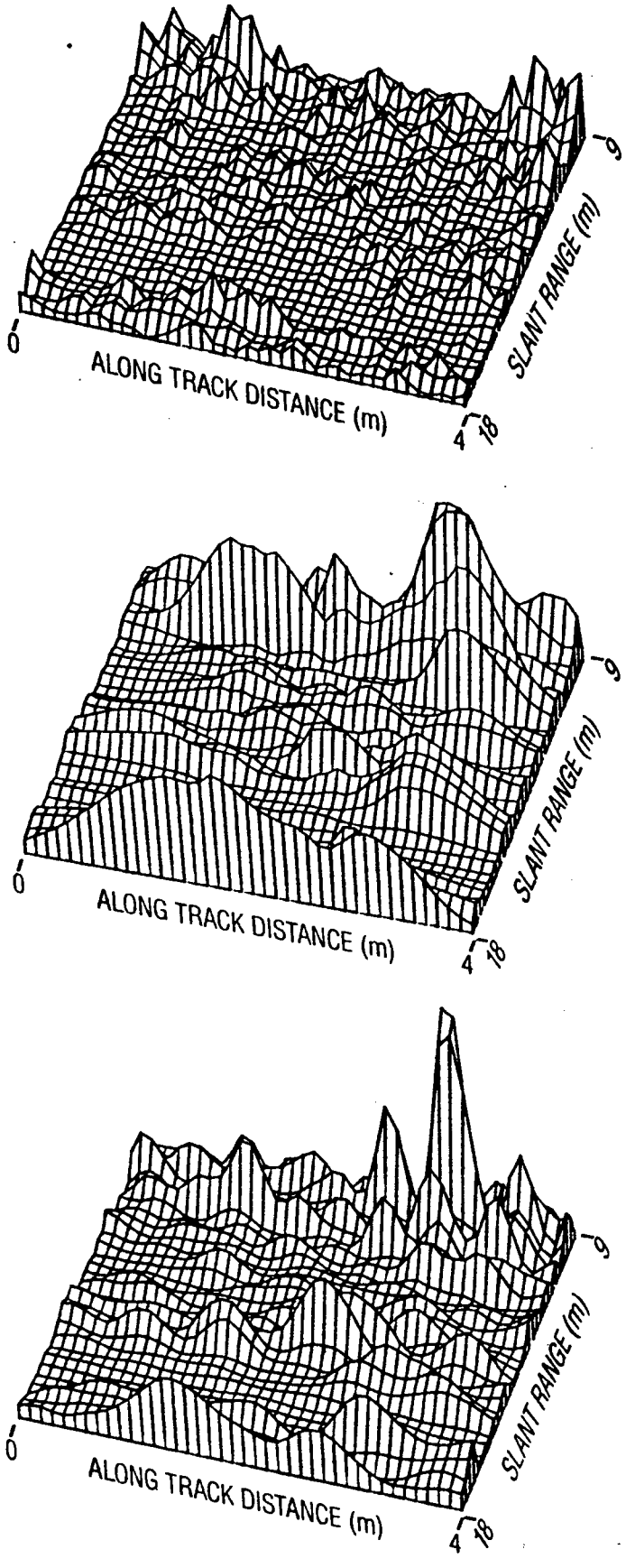

Figure 4. Images at reservoir site: (a) unprocessed data; (b) 2m. synthetic aperture; (c) 4m. synthetic aperture.

Figs. 4(b) and 4(c) show the reconstructed images obtained over a 4m along-track distance using aperture lengths of 2m and 4m respectively. For the 4m case, the complete aperture data is used for all the points in the image, i.e. the beam is focused and steered to each point in the image plane. For the case of a 2m aperture where 4m of data is available, the section of the data used is moved (Fig. 5). The central 2m of the image is obtained by selecting the appropriate section of the data and using focusing but no beam deflection. The outer 1m parts of the image are obtained by deflecting the beam. A comparison of Figs. 4(b) and 4(c) clearly shows that the detail of the images is improved as the aperture size is increased.

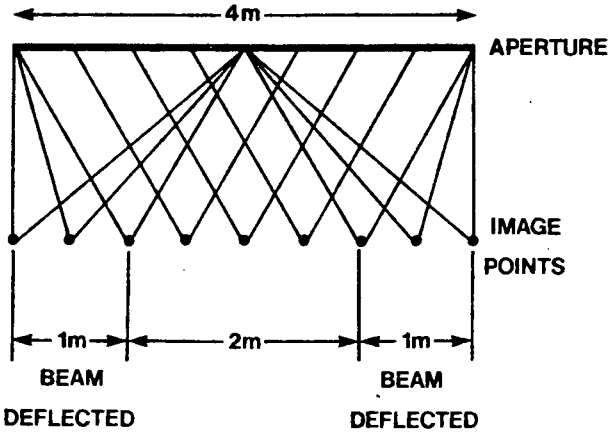

Fig. 5. Use of data for image reconstruction.

It is important to know whether bottom penetration has been achieved and, although not entirely conclusive, it has proved useful to compare the images with those obtained using a conventional 300kHz sidescan system where only surface structure can be expected. Such an image is shown in Fig. 6(a). The transducer was pointing slightly foreward of the broadside direction and hence there is a slight displacement of the image compared with that of the 4m synthetic aperture image which is repeated in Fig. 6(b). Comparison aided by the marking of six targets A to F which are common to both images. The differences in the relative strengths of these targets between these two images may be due to the difference in sensitivities at the two frequencies to the submerged parts of these targets. The areas marked G and H in Fig. 6(b) are not apparent in Fig. 6(a) thus suggesting that these targets are completely submerged. Unfortunately it has not been possible yet to back up this conclusion by visual observations of the bed of the reservoir.

Sea Tests

In order to image a larger area and to test the system under realistic operational conditions, tests were carried out at sea. The same transducer as used previously in the reservoir tests was mounted rigidly between the hulls of a twin engined catamaran. The sideways looking configuration was again adopted but, because of water resistance, the baffle beneath the transducer was discarded. The speed measured by a taffrail log was 1.1 m/s but images produced using this value were found to be totally unsatisfactory. For example images obtained from beams at different squint angles, but directed at the same area of the sea bed by using different blocks of synthetic aperture data, did not give coincident feature. By trial and error the true velocity relative to the sea bed was found to be 1.6 m/s. Based upon this value and the known interpulse period it followed that

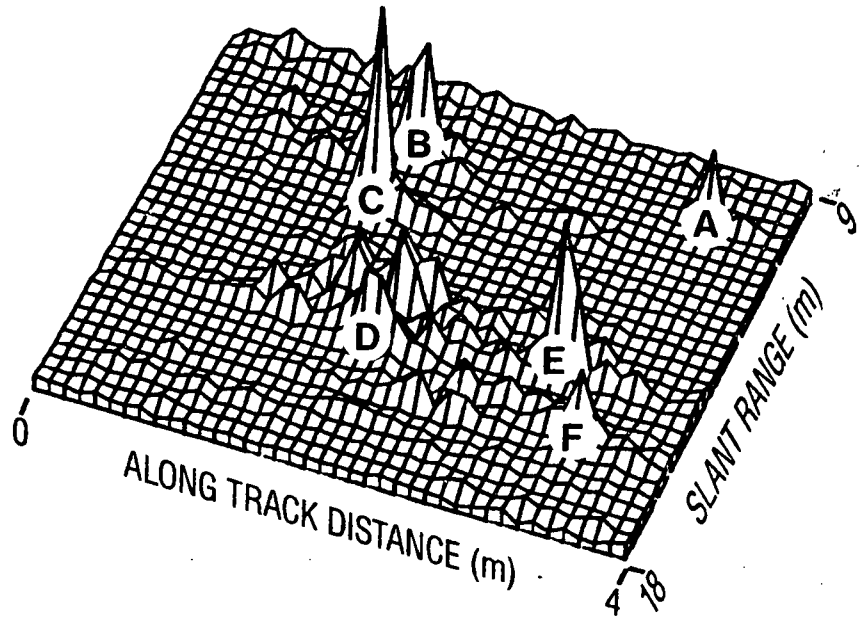

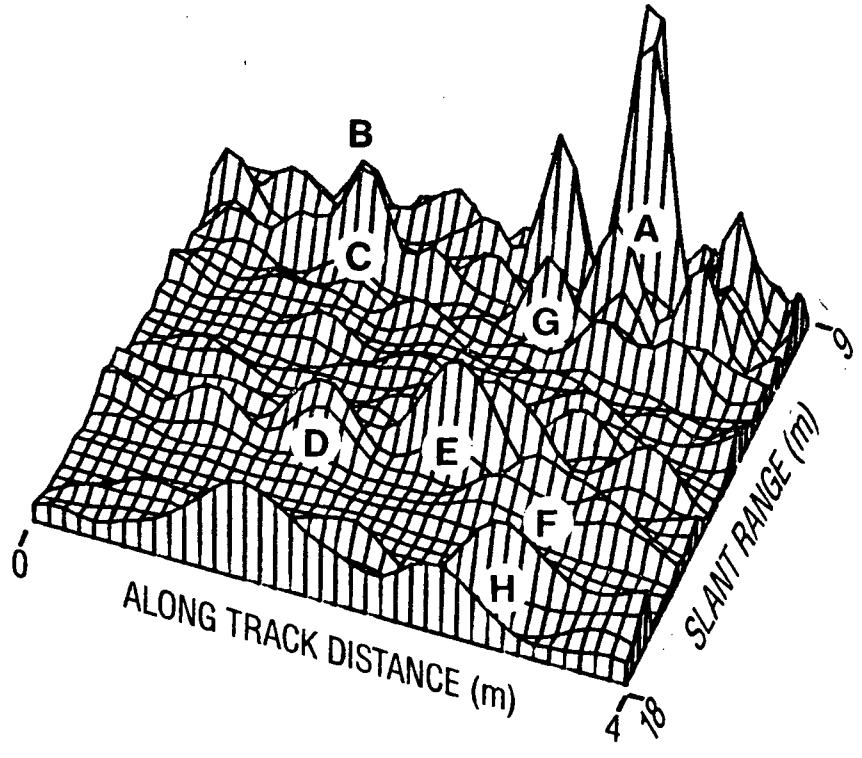

Figure 6. Images at reservoir site: (a) 300kHz sidescan; (b) 4.5kHz synthetic aperture.

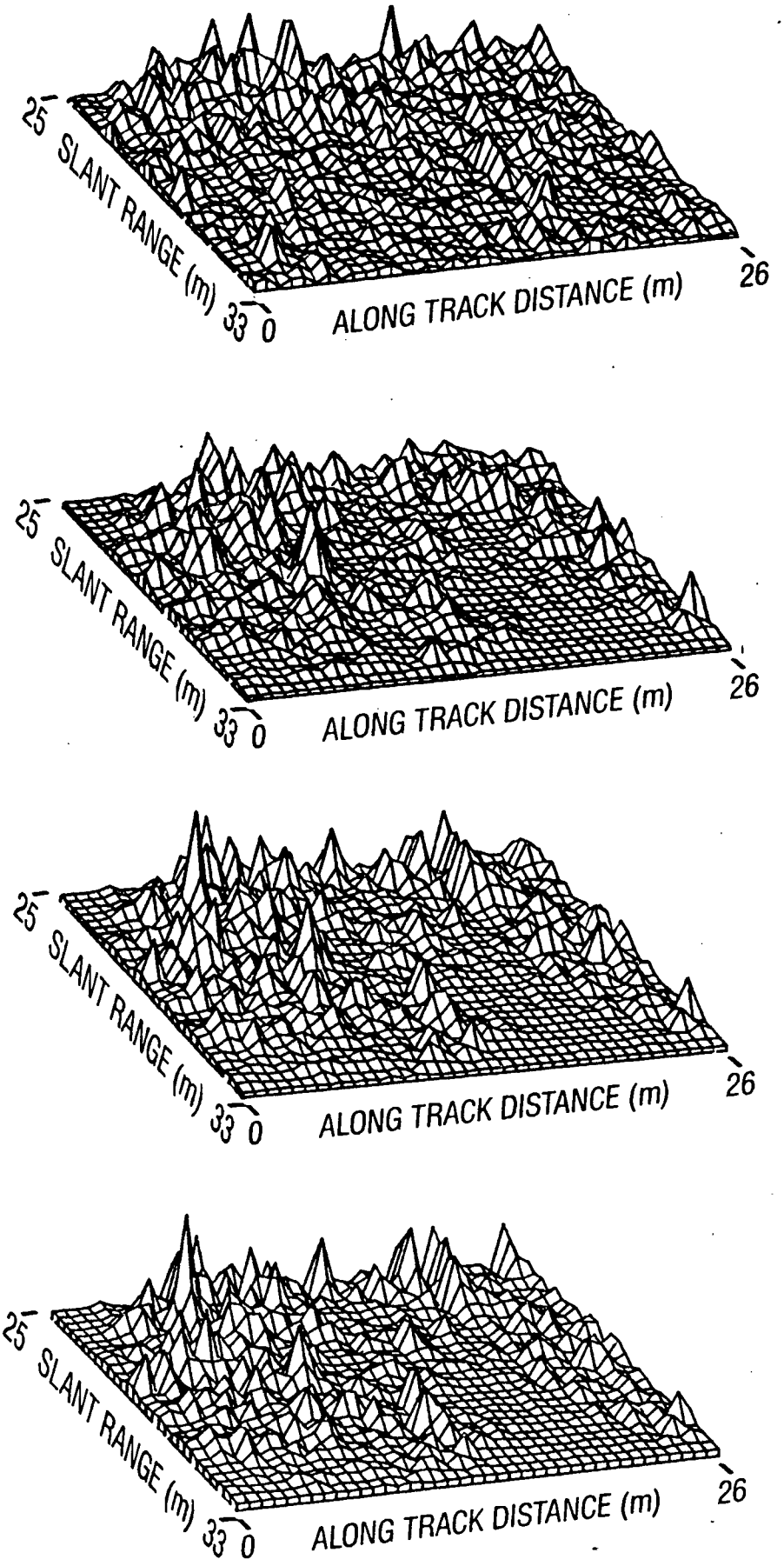

Figure 7. Images of sea bed at 10° squint angle: (a) unprocessed; (b) 4m. synthetic aperture; (c) 8m. synthetic aperture; (d) 12m. synthetic aperture.

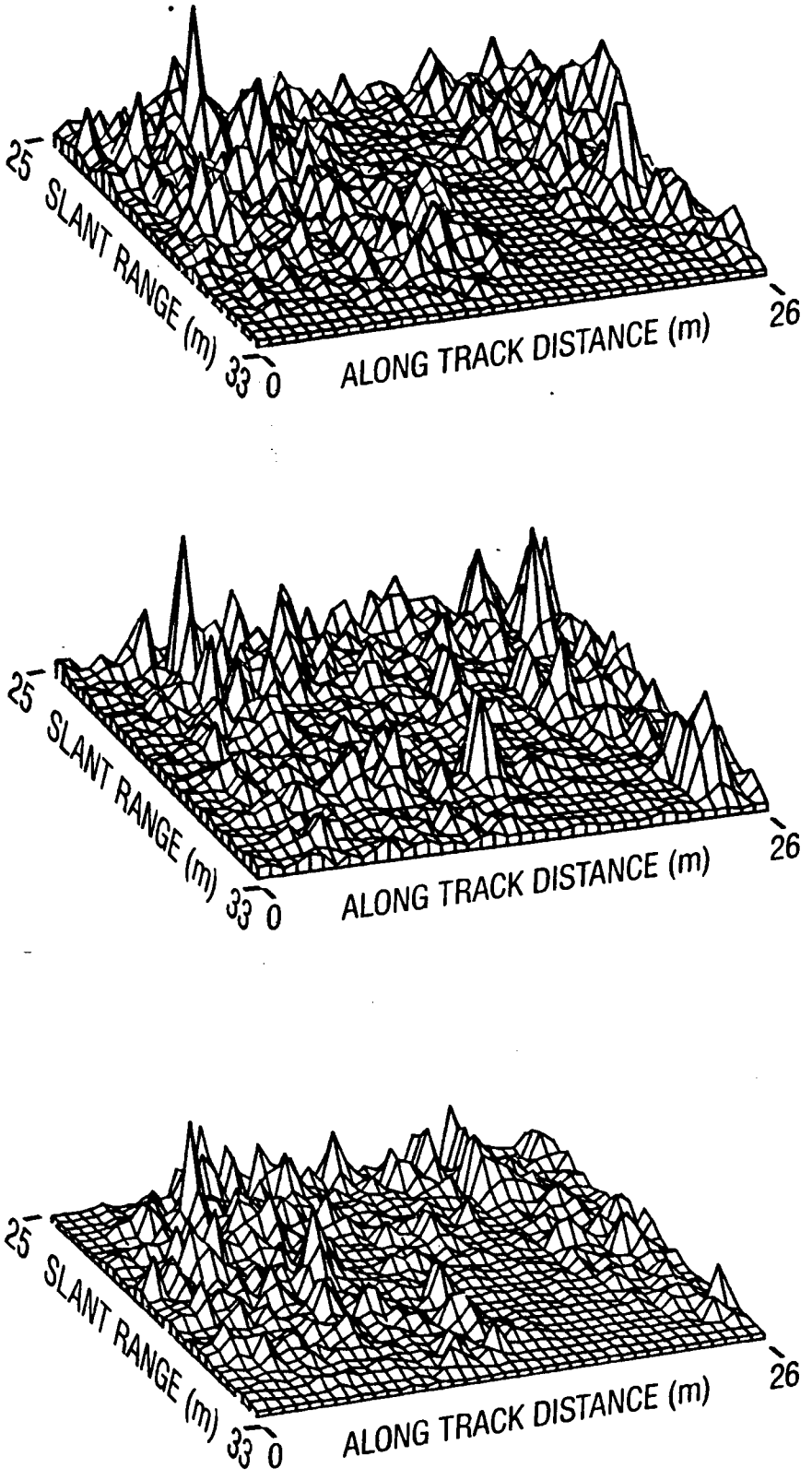

Figure 8. Images of sea bed using 8m. synthetic aperture: (a) -10° squint angle; (b) broadside; (c) +10° squint angle.

receive signals were recorded every 0.19m over total track lengths of 85m. The 0.19m corresponded to a theoretical prediction of grating sidelobes at 60°. The sensitivity of the physical transducer was well down at this angle.

One of the practical problems encountered in the sea trials was a very strong acoustic interfence signal, attributed to the transmit signal undergoing multiple reflections between the hulls of the catamaran and returning to the transducer to overlap the wanted sea bed echoes. This acoustic interference was therefore confined to the broadside direction. The problem was overcome by forming a squint beam in the reconstruction processing which was insensitive to the broadside interference.

Unprocessed data corresponding to an area near some semi-submerged pillars is shown in Fig.7(a). No meaningful feature can be seen. The remaining images of Fig.7 are reconstructions of the same area using different lengths of apertures and a beam which is steered 10° ahead of broadside. Considerable feature is now apparent, with the resolution being improved by increasing the aperture length from 4m to 8m but not significantly when going from 8m to 12m. The processing incorporated a Hamming amplitude shading function as given by $w(z) = 0.54 + 0.46 \cos(2\pi z/L)$. This was done because the natural shading of targets discussed earlier, where targets move in and out of the physical beam, was no longer effective at the increased ranges

Considerable confidence in the images is gained if similar feature is generated when using different blocks of data. This can be tested by imaging the same area with the beam at different squint angles. Fig. 8 shows images for squint angles of -10°, 0°, and +10°. It is seen that there is a strong similarity between them. The broadside image is of degraded quality because of the acoustic interference problem mentioned earlier. The difference between the fore and aft beam images is attributed to the faceted nature of typical targets such as rocks and, in this case, pillars.

DISCUSSION

The tank tests and the reservoir tests have confirmed that, under controlled conditions, the principle of synthetic aperture imaging is viable. There is good evidence, though not yet entirely conclusive, that targets beneath the bed of the reservoir are being imaged. Useful images have been produced applying the synthetic aperture technique at sea, but only after trial and error adjustments have been made to the supposed boat velocity as measured by a taffrail log. The useful aperture length was limited by coherence problems to about 8m. The explanation for this can only be speculative but is probably related to unwanted boat movement. It seems likely that the problem would be reduced if the transducer were mounted in a fish and towed with a cable configuration that provided little coupling to the movements of the mother boat. Based upon the reservoir tests it seems likely that bottom penetration has been achieved but further work needs to be done to establish its extent.

CONCLUSIONS

The feasibility of synthetic aperture techniques for short range low frequency imaging has been demonstrated. In contrast to the parametric array the use of synthetic aperture techniques for sub-bottom imaging does not suffer from a low source level. However the beam resulting from a synthetic aperture is narrow in one direction only and is not a pencil beam.

The disadvantage of a fan beam is greatly reduced by using the system in sideways looking mode. Indeed the fan beam may even be regarded as advantageous as the sidescan mode of operation gives a very much faster rate of survey than the echo-sounder mode of the conventional sub-bottom profiler. Another point in favour of the synthetic aperture may well prove to be the ease with which the surveyed area may be examined from different angles, thus easing the interpretation

REFERENCES

1. L.J. Cutrona, Synthetic Aperture Radar, Chap. 23 of "Radar Handbook", M.I. Skolnik (ed.) McGraw-Hill, New York, 1970.
2. L.J. Cutrona, "Comparison of sonar system performance achievable using synthetic-aperture techniques with the performance achievable by more conventional means", J.Acoust. Soc. Am.,58(2),336-348(1975)
3. T.Sato, O.Ikeda, "Sequential synthetic aperture sonar system-a prototype of a synthetic aperture sonar system", IEEE Trans. on Sonics and Ultrasonics, Vol. SU-24, No.4, July 1977.
4. Loggins et al., "Results from rail synthetic aperture experiments", J. Acoust. Soc. Am., 71(S1), S85(1982).
5. R. Williams, "Creating an acoustic synthetic aperture in the ocean", J. Acoust. Soc. Am., 60(1), 60-73(1976).
6. M. Dobrin, Introduction to Geophysical Prospecting, McGraw-Hill, New York, 1976.
7. E.L. Hamilton, "Compressional wave attenuation in marine sediments", Geophysics, 37, 620-646(1972).
8. H.O. Berktay, et al., "Sub-bottom profiling using parametric sources", Proceedings of the Institute of Acoustics Conference on Underwater Applications of Non-Linear Acoustics, Bath, Sept. 1979.
9. W. Brown, "Synthetic Aperture Radar" , IEEE Trans. on Aerospace and Electronic Systems, Vol. AES-3, No.2, March 1967.